RISK WITH THE COMBINATION WELDMENT AND ELASTIC FOLLOW-UP AT LOW TEMPERATURE CREEP

REPORT 2019:639

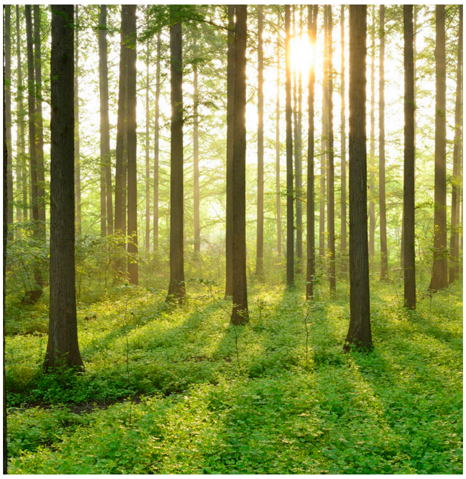

BRÄNSLEBASERAD EL- OCH VÄRMEPRODUKTION

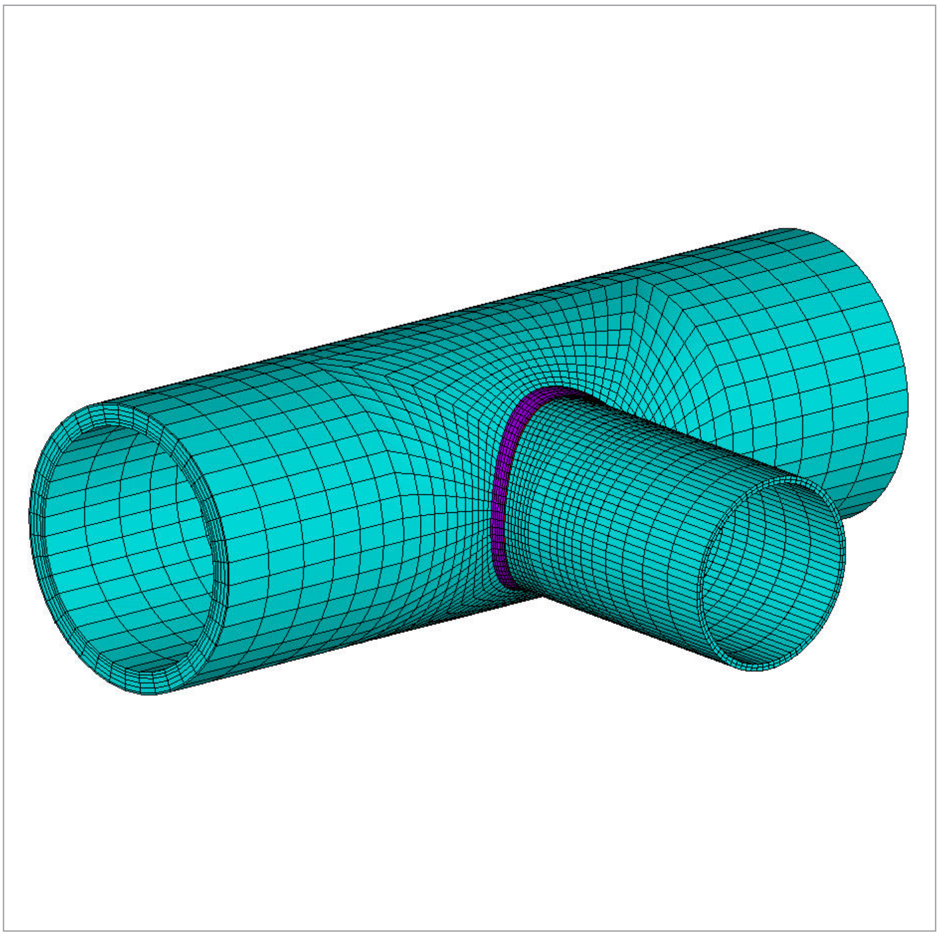

Energiforsk

Risk with the Combination Weldment and Elastic Follow-Up at Low Temperature Creep

PETER SEGLE, YOUSEF ALIPOUR, JAN STORESUND, HENRIK C.M. ANDERSSON-ÖSTLING

ISBN 978-91-7673-639-5 | © Energiforsk February 2020

Energiforsk AB | Phone: 08-677 25 30 | E-mail: kontakt@energiforsk.se | www.energiforsk.se

Foreword

Denna rapport är slutrapportering av projekt M 43447 Risk med kombinationen svetsförband och "elastic followup" vid lågtemperaturkryp (Energimyndighetens projektnummer P 43447) inom SEBRA, samverkansprogrammet för bränslebaserad el- och värmeproduktion.

Programmets övergripande mål är att bidra till långsiktig utveckling av effektiva miljövänliga energisystemlösningar. Syftet är att medverka till framtagning av flexibla bränslebaserade anläggningar som kan anpassas till framtida behov och krav. Programmet är indelat i fyra teknikområden: anläggnings- och förbränningsteknik, processtyrning, material- och kemiteknik samt systemteknik. Programmet är en samverkan mellan Energiforsk och Energimyndigheten. Ingående projekt finansieras alltså av Energimyndigheten och av de parter som Energiforsk samlar i programmet.

Detta projekt har studerat ett T-stycke från ett kraftvärmeverk och som uppvisar oväntade krypskador. Kombinationen svetsförband och ”elastic follow-up” kan begränsa systemets livslängd och arbetet ger ökad förståelse för denna kombination och ett antal rekommendationer för hur skador kan begränsas både i befintliga anläggningar och vid design av nya.

Projektet har genomförts av KIWA Inspecta AB med Jan Storesund och Peter Segle som huvudprojektledare. Projektet har följts av en referensgrupp bestående av:

Rikard Norling, RISE KIMAB
Tommy Larsson, E.ON,
Per-Åke Binett, Iggesund Bruk, Holmen

Stockholm december 2019

Helena Sellerholm
Områdesansvarig
Termisk energiomvandling, Energiforsk AB

These are the results and conclusions of a project, which is part of a research programme run by Energiforsk. The author/authors are responsible for the content.

Sammanfattning

Numeriska analyser och experiment visar att allvarliga krypskador kan utvecklas i rörsystem utsatta för lågtemperaturkryp (≤ 460 °C) vid en kombination av fenomenet ”elastic follow-up” och ett försvagat område i form av en svets. Systemspänningar som relaxerar långsamt tillsammans med reducerad krypduktilitet, orsakad av långa drifttider och en hög grad av treaxlighet lokalt i svetsförbandet, gör detta möjligt.

I kraftvärmeverk som arbetar vid temperaturer kring 460°C eller lägre förväntas inverkan av krypning var liten. För de vanligast använda stålen vid dessa drifttemperaturer blir krypning dimensionerande först vid 470-480°C. Trots detta har betydande krypskador frekvent påträffas i exempelvis T-stycken vid övergången mellan huvudledning och avstickare efter typiskt 25-30 års drift. I många fall är en svets placerad i just övergången vilket torde vara en bidragande orsak till uppkomst av krypskada. Svetsens närvaro kan dock inte ensam förklara skadans uppkomst.

”Elastic follow-up” är ett fenomen som innebär att elastiskt upplagrad energi i ett system driver en inelastisk deformation (plasticering, krypning) i ett försvagat område där påkänningen är förhöjd. Genom att det försvagade området har en liten rumslig utsträckning i förhållande till resterande del av systemet leder inte den lokala inelastiska deformationen till någon märkbar relaxation av påkänningen. En viktig konsekvens av detta är att en last som normalt betraktas som sekundär, exempelvis spänningar orsakade av termisk expansion i en rörledning, istället blir primär.

För ett rörledningssystem som arbetar vid temperaturer kring 460°C eller lägre, där plastisk deformation och krypning förväntas vara liten, torde kombinationen närvaro av svetsförband och ”elastic follow-up” kunna begränsa systemets livslängd. Med ökad kunskap och förståelse för denna livslängdsreducerade kombination bör detta problem kunna hanteras både i existerande anläggningar och på designstadiet.

I detta projekt studeras inverkan av kombinationen närvaro av svetsförband och ”elastic follow-up” på livslängden hos rörledningssystem utsatta för lågtemperturkryp (460°C eller lägre). Arbetet har utgått från kraftvärmeverket i Iggesund där oväntade krypskador påträffats i en svets i ett T-stycke.

Iggesunds kraftvärmeverk togs i drift i slutet på 70-talet. Med materialet 13CrMo4-5 i ångledningarna och en drifttemperatur på 460 °C förväntades det inte att krypning skulle begränsa systemets livslängd. Allvarliga krypskador (3b enligt NT TR 302) upptäcktes dock 2014 i en övergångssvets W2 mellan huvudrör och avstickare i ett T-stycke, se Figur 1.

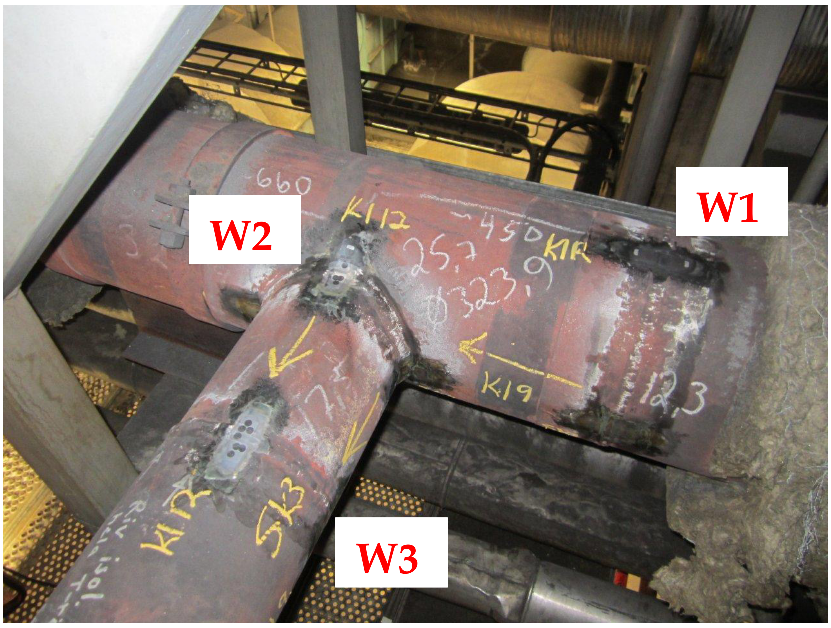

Figur 1: Undersökta svetsar W1, W2 and W3 i T-stycket i Iggesunds kraftvärmeverk.

Inledande krypsimuleringar av Iggesunds rörsystem modellerat med ELBOW31-element i ABAQUS visar att relaxationen av systemkrafter och systemmoment går långsamt. En konsekvens av detta är att systemspänningar kvarstår över tid och att fenomenet ”elastic follow-up” är möjligt vid närvaro av en svagare zon, exempelvis svets W2, där krypdeformation då skulle kunna ackumuleras lokalt.

ELBOW31 är en typ av balkelement som inte medger explicit modellering av övergången mellan huvudrör och avstickare. Inte heller svets W2 kan modelleras med detta element. Genom att solidmodellera T-stycket i Figur 1 och koppla in denna solidmodell i rörmodellen kan responsen hos svets W2 fångas i en krypsimulering, se Figur 2. I solidmodellen modelleras svetsens ingående komponenter; grundmaterial, svetsgods och HAZ, se Figur 3.

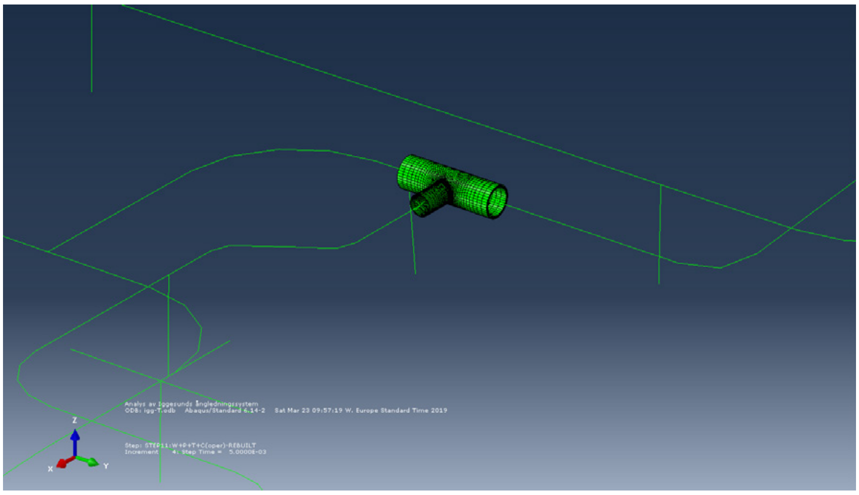

Figur 2: Del av analyserat rörsystem med 3D modell av T-stycket inkopplat.

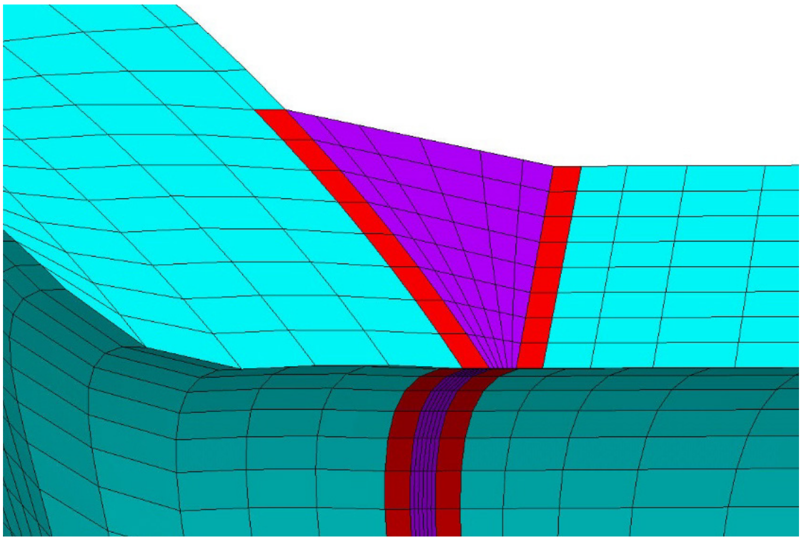

Figur 3: Svets W2 i 3D-modell av T-stycket där elementen för basmaterialet är ljusblå, svetsgodset är lila och HAZ är röda. Bilden visar ett snitt längs med avstickaren.

Driftutsatt grundmaterial och svetsgods uttaget från aktuellt T-stycke har krypprovats vid temperaturen 460 ^{o}C och spänningsnivåer i intervallet 270 till 347 MPa. Resultaten visar att minsta kryptöjningshastighet vid dessa spänningsnivåer är högre för grundmaterialet än för svetsgodset, se Figur 4. Att utgående från detta resultat dra långtgående slutsatser om krypresponsen för grundmaterial och svetsgods vid driftspänningar (40-80 MPa) är svårt. Vid dessa lägre spänningsnivåer kan det omvända gälla vad gäller relationen mellan grundmaterialets och svetsgodsets minsta kryptöjningshastighet. En slutsats som dock kan dras är att kryptöjningshastigheten varierar tvärs svets W2. Effekten av detta studeras numeriskt.

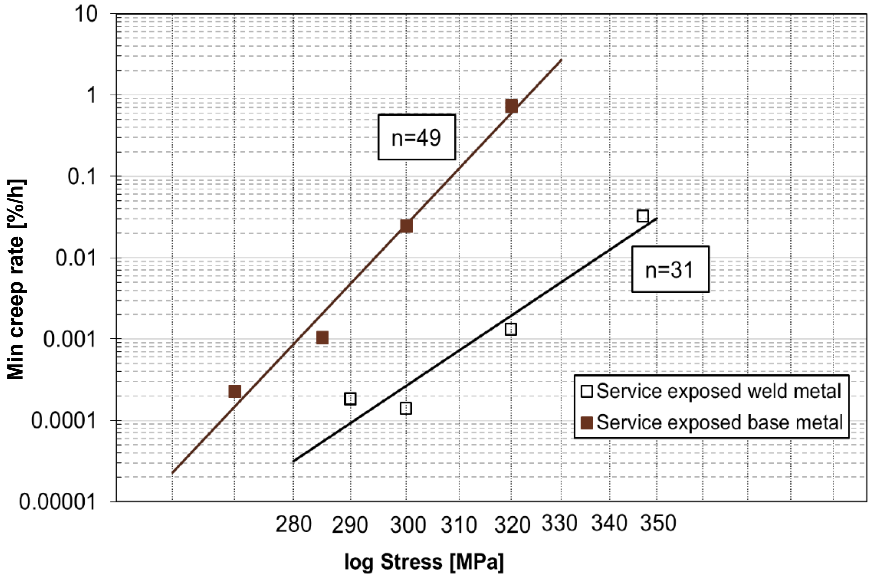

Figur 4: Minsta kryptöjningshastighet som funktion av spänning.

Effekten av olika kombinationer av förhöjd kryptöjningshastighet för materialet i svets och HAZ i svetsen W2 studeras med ABAQUS-modellen i Figur 2 och 3. Jämfört med fallet att samtliga komponenter i svetsen består av grundmaterial fås en ökning av maximal ekvivalent kryptöjning med 60 % om svetsgodsets kryptöjningshastighet ökas en faktor tio. Av totalt nio studerade materialkombinationer (grundmaterial/svetsgods/ HAZ) fås maximal ekvivalent kryptöjning till 0.21 % i svetsförbandet vilket är 166 % mer än om samtliga komponenter i svetsen består av grundmaterial. Även effekten av ej fungerande hängare och rörstöd i T-styckets närhet studeras. Utgående från referensfallet med ett svetsgods som kryper tio gånger snabbare än grundmaterialet fås för det skadligaste fallet (av totalt åtta) en höjning av ekvivalent kryptöjning med 44 % i svets W2. Bidraget från relaxation av svetsegenspänningar till ackumulerad kryptöjning i svets W2 har inte studerats explicit. En förenklad analys ger ett kryptöjningsbidrag på 0.065 %. Bidraget från primärkrypning till ackumulerad kryptöjning bedöms som försumbart i jämförelse med vad sekundärkrypning bidrar med. För drifttider på mer än 300000 timmar dominerar den senare typen av krypning helt. Med beaktande av samtliga orsaker till förhöjd ackumulering av kryptöjning i svets W2 torde denna kunna uppgå till bortåt 0.3 %.

De numeriska simuleringarna av rörsystemet visar sammanfattningsvis att deformationsstyrda krafter och moment i systemet relaxerar långsamt. I kombination med en försvagad sektion i form av svets W2 kan krypskada ackumuleras lokalt, d.v.s. fenomenet ”elastic follow-up” råder. I aktuell anläggning är drifttiden lång (> 300000 timmar) vilket leder till låg krypduktilitet för materialet. Vid närvaro av en svets, med varierande krypegenskaper tvärs svetsen, reduceras krypduktiliteten ytterligare. Orsaken är bl.a. att en hög grad av treaxlighet bildas lokalt i svetsen. Även om simulerad kryptöjning i svets W2 i T-stycket inte överstiger 0.3 % torde oväntade krypskador som påträffats i denna svets kunna förklaras genom den reducerade krypduktiliteten och fenomenet ”elastic follow-up”.

Metallografisk undersökning av krypkaviteter på utsidan av T-stycket verifierar resultaten från tidigare replikprovning. Fördelningen av krypkaviteter tvärs T-styckets svets visar hygglig överensstämmelse med simulerade kryptöjningar, se Figur 5.

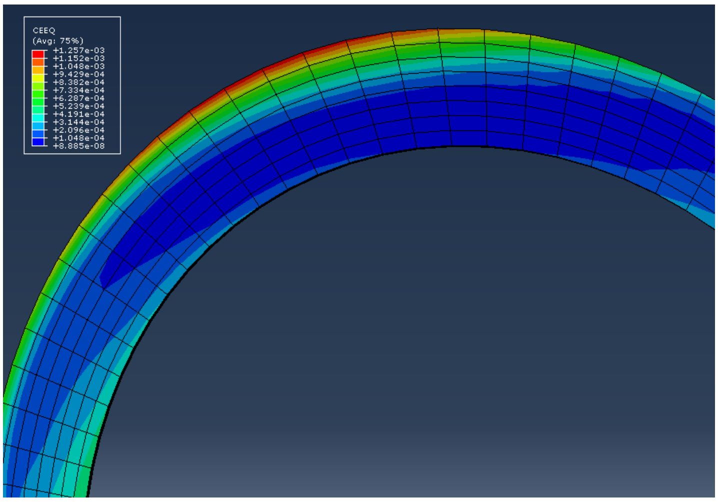

Figur 5: Ekvivalent kryptöjning ε_{eq}^{c} tvärs svets W2 efter 327600 timmars drift. Svetsen ses flödesriktningen där översta punkten motsvarar klockan 12. Rött motsvarar $\varepsilon_{eq}^{c} = 0.126$ %. I simuleringen kryper materialet i svetsen tio gånger fortare än grundmaterialet.

För att minska risken för uppkomst av allvarliga krypskador i rörsystem utsatta för lågtemperaturkryp rekommenderas följande:

- Undvik att placera svetsar i områden med höga spänningsnivåer såsom svets i ett T-styckes övergång mellan huvudrör och avstickare.
- Vid svetsning, använd ett tillsatsmaterial som matchar grundmaterialet.
- Prova regelbundet krypskadeutvecklingen i högt påkända svetsar och rörböjar. Val av provningspositioner görs i början av anläggningens livslängd utgående från elastiska spänningsanalyser. Efter hand som rörsystemet relaxerar väljs provningspositioner utgående från krypanalyser av rörsystemet. Provningsintervallens längd förkortas mot slutet av förväntad livslängd.
- Inspektera regelbundet stöd och hängares funktion.
- Mät kontinuerligt drifttemperaturen vid ett antal positioner i rörsystemet. Utgående ledningen från pannan bör vara en av positionerna.

Summary

The risk with the combination weldment and elastic follow-up at low temperature creep (≤ 460 ^{o}C) is investigated. A piping system in the Iggesund plant where unexpected creep damage was found in a T-piece weldment form basis for the project.

Numerical simulations show the possibility for severe creep damage to develop in the T-piece junction weld W2. The reasons are as follows:

- The effect of elastic follow-up maintains the deformation-controlled system forces and moments for a longer period during operation.
- An operation time of more than 300000 hours is considered as long. One effect of long creep duration is that creep ductility is reduced.
- Differences in creep deformation properties across the weldment result locally in both stress concentrations and a high degree of triaxiality. The latter reduces creep ductility.
- Non-functioning supports in the vicinity of weld W2 might have increased the stresses in the T-piece junction weld.

Considering these factors, it should be possible for sever creep damage to develop in weld W2 even though predicted creep strains do not exceed 0.3 %.

From the metallographic investigation of selected positions of the T-piece welds the following conclusions can be drawn:

- The observed creep damage at on-site replica testing was verified by the metallographic studies. The amount of damage observed at the outer surface agreed well with previous replica test results and a slight damage development could be observed between 2014 and 2017.
- At some positions significant creep damage was formed through the wall where creep cavities were observed almost through the entire wall thickness.
- The creep damage distributions agreed quite well with numerical results at the 12 o´clock position of W2.

Two series of creep tests including base and weld metals from the studied T-piece were conducted. The purpose of the creep testing was to reach the secondary creep region within 100-10 000 hours for the tests of each series. The results could give creep data input for the numerical simulations in comparison to data evaluated from the EN code:

- Relatively high stresses compared to service stresses were required to get into the secondary creep, not only for the short term but also for the long-term testing.
- Higher creep rates were obtained for the base metal than for the weld metal. However, the results indicate the opposite relationship at service stress.
- The creep tested weld metal contained creep cavities before the tests. The amount of cavitation did not increase during the tests.

In order to avoid unexpected creep damage to develop in power plants subjected to low-temperature creep, recommendations are finally given.

List of content

1 Introduction

For power plants operating at a temperature around 460 °C or below, the impact of creep is expected to be small or almost negligible. The yield strength should govern the design of systems. For the most commonly used steels in these plants, creep should need to be considered first when the temperature exceeds 470-480 °C. Despite this, significant creep damage has frequently been found in, for example, T-pieces at the junction between the run pipe and the branch pipe after typically 25-30 years of operation. In many cases, a weld is placed in the junction. The presence of the weld however, does not alone explain the occurrence of the damage.

After a serious accident, the occurrence of so-called low-temperature creep was checked in a number of Swedish plants, mainly forest industry, and the results were compiled within a previous Värmeforsk project [1]. It was found that 17% of the welds surveyed had macro-cracks. In a follow-up project, effects of welding defects on initiation of low temperature creep have been studied since such observations had been made [2]. Recently, however, it has become more frequent that creep damage in the form of creep cavities occurs and develops into cracks without the effect of defects.

Elastic follow-up is a phenomenon that means that elastically stored energy in a system drives an inelastic deformation (plastic, creep) in a weakened region where stresses are enhanced and/or the material properties are weakened [3]. Because the weakened area has a small spatial extent relative to the remaining system, local inelastic deformation does not lead to any noticeable relaxation of the stresses.

For a piping system operating at temperatures around 460 °C, where creep deformations are expected to be almost negligible, the combination of a weld and elastic follow-up might limit the lifetime of the system. An increased knowledge and understanding of how this combination influences the piping system response is therefore of importance.

In this project, the combination of weld and elastic follow-up is investigated for a pipeline system exposed to low-temperature creep. The powerplant at Iggesund Paperboard, where unexpected creep damage was found in a weld at a T-piece, form basis for the project. Results from numerical analyses of the entire system and local weld joints, examination of the microstructure of the damaged component and creep testing of service-exposed material taken out from the weld and base metal in the damaged component lay the foundation for an increased understanding.

2 Concept of elastic follow-up

Elastic follow-up is a phenomenon where the main part of a structural system responds elastically while the remaining part responds inelastically, see Figure 2-1. When inelastic deformation occurs in a region with limited extent, the elastic part of the system "follow-up" with elastic deformation. An important consequence is that a load that normally is considered secondary, for example stresses caused by thermal expansion in a pipeline, instead becomes primary [4]. The potential energy stored in the elastic part can cause extensive inelastic deformation in a local region.

The reason why only a limited part responds inelastically is that this section is weaker compared to the elastic part. In this context, weaker means that the cross section is smaller, resulting in higher stresses, and/or that the material deformation properties are weakened. The latter can be a result of a weldment with lower yield strength or higher deformation rate for one of its constituents or that the temperature is locally enhanced.

In structural systems, inelastic deformation is usually caused by plastic and/or creep deformation. The mechanism considered in this investigation is creep.

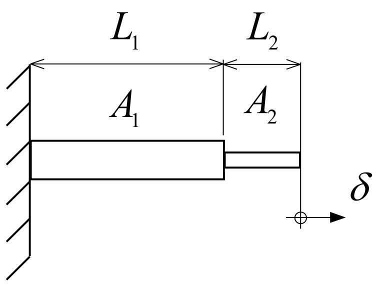

Figure 2-1: Schematic model of a structural system where a deformation controlled load (displacement δ) causes inelastic deformation to occur in part 2 (with limited extent) while part 1 (major part of the system) responds elastically.

3 Standard for design and analysis of piping systems

3.1 SS-EN 13480-3

Part 3 of the European standard SS-EN 13480 [5] contains rules for design and calculation of metallic piping systems. Section 12 in SS-EN 13480-3 addresses the effects of weight and other loadings as well as the effects of thermal expansion/contraction or similar movements imposed by other sources.

For a piping system, a number of different criteria should be fulfilled. According to equation 12.3.1-2 in SS-EN 13480, the sum of primary stresses σ_1 due to sustained loads is calculated as

$$\sigma_1 = \frac{p_c \cdot d_o}{4 \cdot e_n} + \frac{0.75 \cdot i \cdot M_A}{Z} \tag{3-1}$$

where p_c is the calculation pressure, d_0 is the outer dimeter of the pipe, e_n is the nominal thickness, i is the stress intensity factor $(0.75 \cdot i \geq 1)$, M_A is the resultant moment from the sustained mechanical loads and Z is the section modulus of run pipe.

According to equation 12.3.1-4 in SS-EN 13480 the stress range due to thermal expansion and alternating loads can be calculated as

$$\sigma_4 = \frac{p_c \cdot d_o}{4 \cdot e_n} + \frac{0.75 \cdot i \cdot M_A}{Z} + \frac{i \cdot M_C}{Z} \tag{3-2}$$

where M_C is the resultant moment due to thermal expansion and alternating loads.

A comparison with the standards used when the piping system was erected in the late 70s (RN78, TKN73), shows that the equations (3-1) and (3-2) have not been changed.

In validation of the ABAQUS model of the piping system in Iggesund, equations (3-1) and (3-2) are used for comparison of results from ABAQUS [6] and CAEPIPE [7].

4 Pipework at Iggesund

4.1 HISTORY OF PIPING SYSTEM

The investigated piping system was installed 1978 and rebuilt 2011, see Figures 4-1 and 4-2. The pipework consists of the material 13CrMo4-5. The hangers in the initial part of the system were not changed when the system was rebuilt. Hours of operation is shown in Table 4-1.

The purpose with this investigation is to understand why unexpected creep damage could developed in the piping system. Operating temperature is not more than 460 °C and at this temperature the effect of creep should be almost negligible. Focus is on a T-piece and particularly the weld in the junction between the run pipe and the branch pipe where severe creep damage was found, see Figure 4-1.

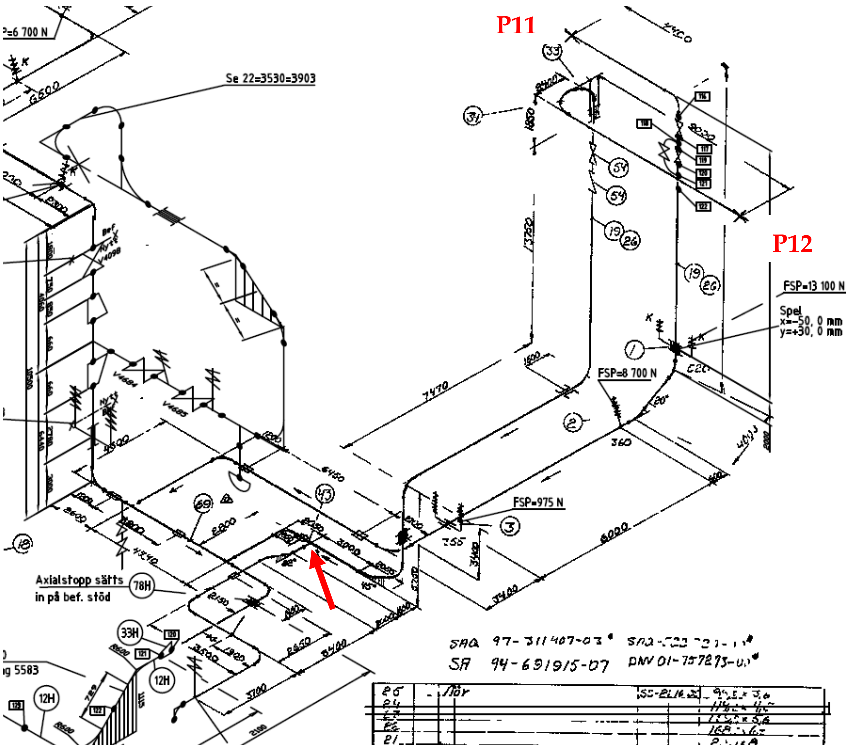

Figure 4-1: Part of pipework in the Iggesund plant. Red arrow points at investigated T-piece. P11 is furnace 11 and P12 is furnace 12. Part of drawing 22-3530-62686 rev 1.

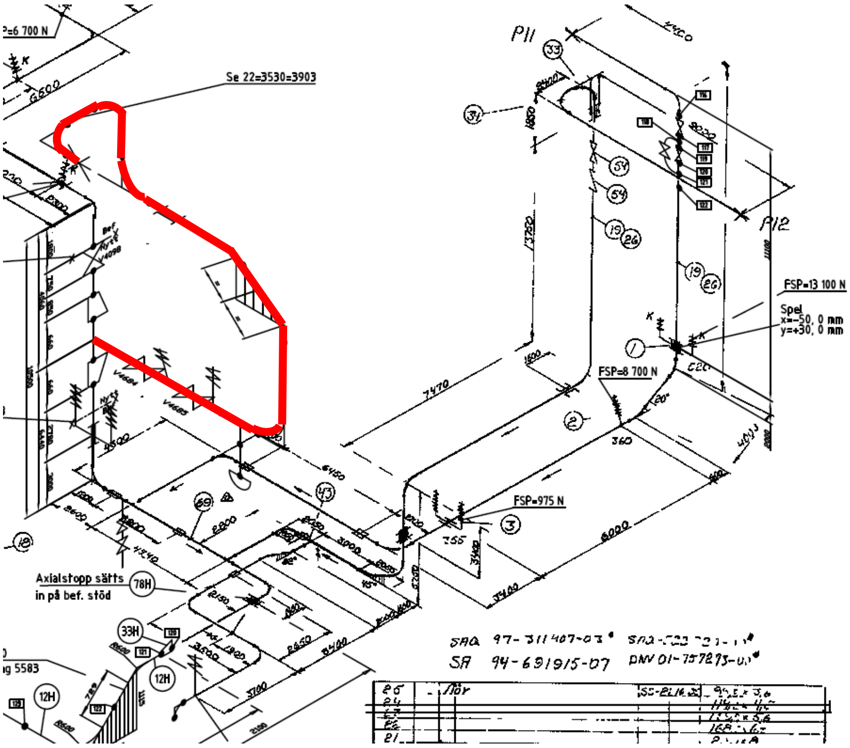

Figure 4-2: Piping marked red was installed 2011. Part of drawing 22-3530-62686 rev 1.

Table 4-1: Hours of operation from installation 1978 to year 2017 when the T-piece was cut out.

Part	Year of installation	Year of T-piece cut out	Years in operation	Hours in operation	Hours of operation per year
Initial	1978	2017	39	327600	8400
Newbuilt	2011	2017	6	50400	8400

4.2 INVESTIGATED WELDS

A specific weld W2 in the T-piece is of interest in this project, see Figure 4-3. The reason is that an unexpected amount of creep damage was detected in this weld. The two other welds, W1 and W3, are also of interest in this investigation, see Figure 4-3.

Results from replica investigations conducted 2014 [8] and 2015 [9] are shown in Tables 4-2 and 4-3. Regarding weld W2, highest creep damage was found at the circumferential position 12, i.e. upper part of the T-piece. Furthermore, an increased creep damage cannot be noticed between 2014 and 2015.

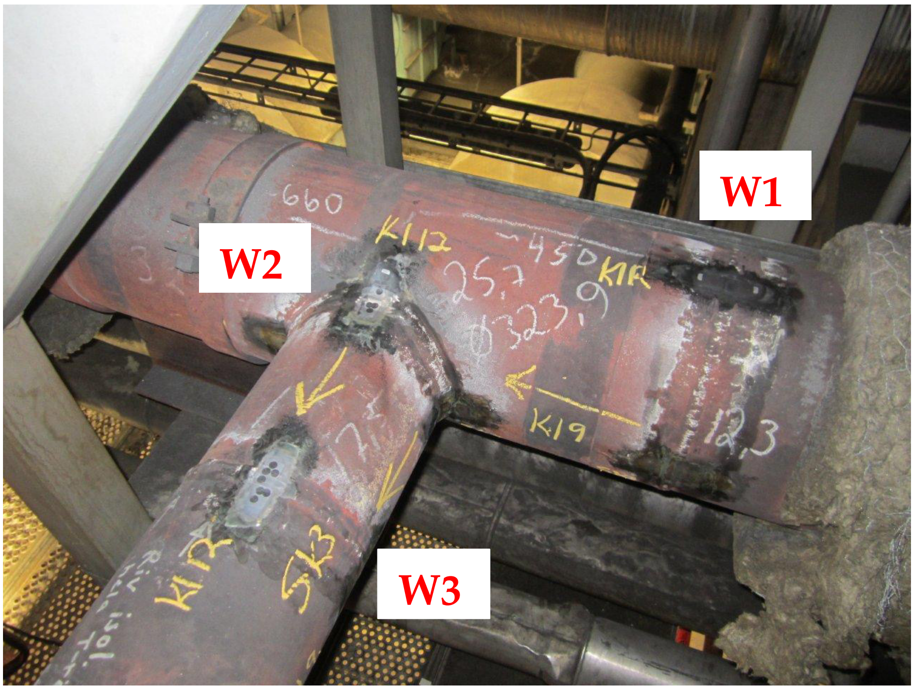

Figure 4-3: Investigated welds W1, W2 and W3 in T-piece.

Table 4-2: Results from replica testing of weld W1, W2 and W3 [8]. Nordtest scale NT TR 302.

Weld	Circum-ferential position	Base mat.	HAZ	Weld mat.	HAZ	Base mat.	Comment
W1	12	1	1	1	1	2a	
	3	1	1	1	1	1	
	6	1	1	1	1	1	
	9	1	1	1	1	1	
W2	12	2b	**3b**	2a	1	1	Cavities approx. 1800 /mm^2
	3	1	1	1	1	1	
	6	1	1	1	1	1	
	9	1	1	1	1	1	
W3	12	1	1	1	1	1	
	3	1	2a	1	2a	1	
	6	1	1	1	1	1	
	9	1	1	1	1	1	

Table 4-3: Results from replica testing of weld W2 [9]. Nordtest scale NT TR 302.

Weld	Circum-ferential position	Base mat.	HAZ	Weld mat.	HAZ	Base mat.	Comment
W2	12	2b	**3b**	2a	1	1	Cavities approx. 1800 /mm^2

5 Numerical analyses

Both linear and non-linear numerical analyses are performed in this investigation. The piping program CAEPIPE is used for the linear analysis and the general-purpose finite element program ABAQUS is used for the non-linear analysis.

5.1 CAEPIPE PIPEWORK MODEL

CAEPIPE is a finite element program for linear elastic analysis of piping systems and consecutive evaluation according to a chosen standard, in Sweden normally SS-EN 13480-3. A piping model of the complete pipework in Iggesund is available. Part of it is shown in Figure 5-1. The T-piece of interest is pointed out in the figure.

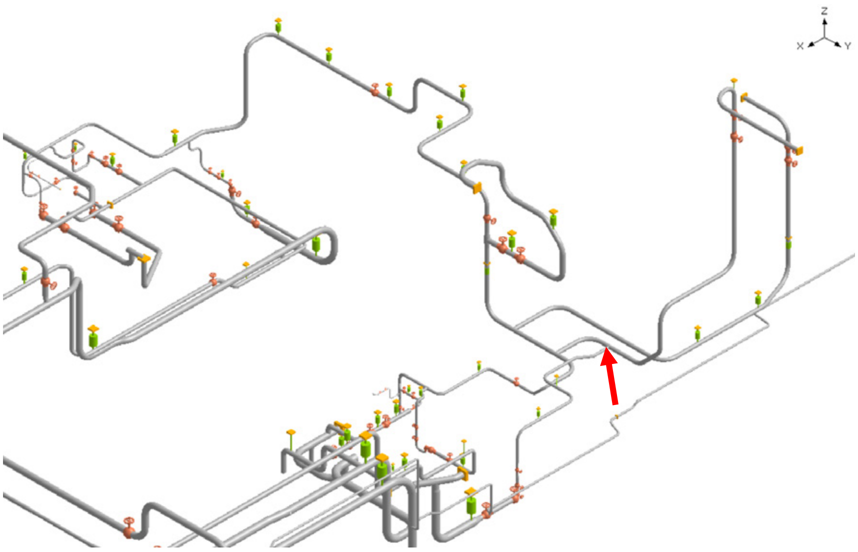

Figure 5-1: CAEPIPE pipework model with T-piece of interest pointed out. Part of the system is shown.

5.2 ABAQUS PIPEWORK MODEL

Part of the CAEPIPE model is modelled in ABAQUS by use of the element ELBOW31, see Figure 5-2. The purpose with this model is to simulate the evolvement of creep strains in the structure. Potential elastic follow-up is also investigated with this model. The location of the weld of interest controls the size of the ABAQUS model, compare Figures 5-1 and 5-2. Sufficiently much of the pipework must be included in the ABAQUS model in order to get a reliable response in the region of interest. At the positions where the ABAQUS model is cut, displacements and rotations from the CAEPIPE analysis are used as boundary conditions.

Building an ABAQUS model with ELBOW31 elements involves a comprehensive amount of manual work. Each element needs information about specific cross section geometry, orientation of cross section, equivalent density considering isolation, material properties and inner radius of pipe element (for application of internal pressure). Available pre-processor is not developed for modelling a pipework with ELBOW31 elements.

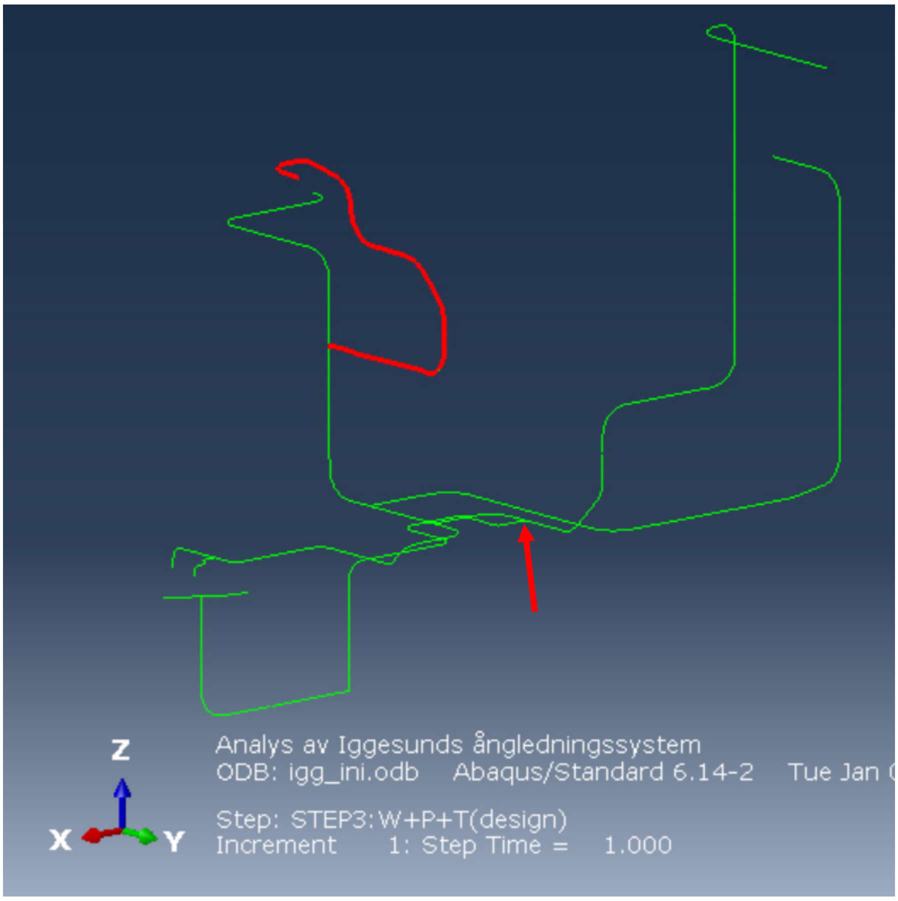

Figure 5-2: ABAQUS model of investigated part of the pipework. Red part of the piping was installed 2011. The red arrow points out the T-piece that was cut out in November 2017.

Figure 5-3 shows the cross section of the finite element ELBOW31. Five integration points through thickness at 20 locations around circumference are used. An element-based co-ordinate system [$\mathbf{a}_1$, $\mathbf{a}_2$, $\mathbf{a}_3$] defines the orientation of the cross section. For bends, $\mathbf{a}_2$ should always point towards the extrados. $\mathbf{a}_3$ points from the start node to the end node of the element.

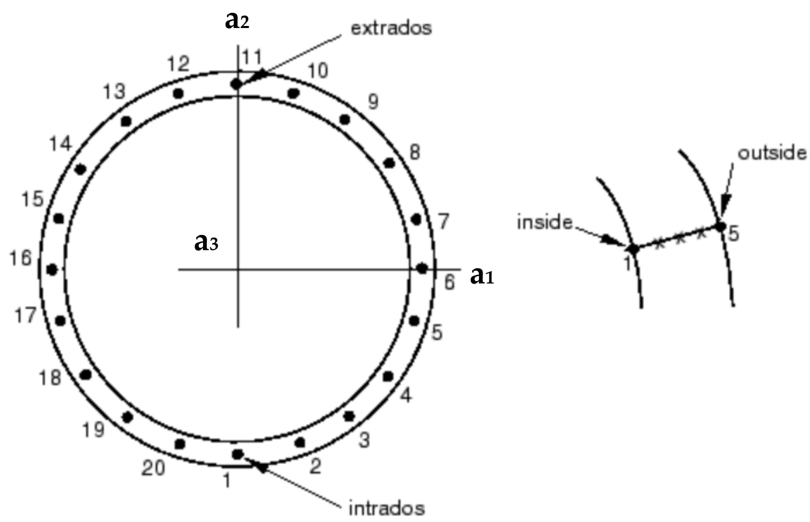

Figure 5-3: Cross section of ELBOW31. Element-based co-ordinate system is given by [$\mathbf{a}_1$, $\mathbf{a}_2$, $\mathbf{a}_3$]. Five integration points through thickness (right figure) are used at 20 locations around the circumference (left figure).

The ELBOW31 element can be used for global modelling of piping systems. With this element, stresses and cross section forces/moments can be calculated for straight pipes and bends. However, local effects at junctions in T-pieces cannot be captured. Simulation of the response in such a component requires a 3D shell or solid model. In this investigation, the T-piece in Figure 4-3 is modelled with a 3D solid model, see section 5-4. With this local model implemented into the piping model, weld W2 in Figure 4-3 can be analysed in more detail.

The present model can be used for creep analysis of the pipework both before and after rebuilt. The former analysis is done by excluding the additional pipework part in the analysis.

Details of the ABAQUS model is shown in Appendix 1.

5.3 VALIDATION OF ABAQUS PIPEWORK MODEL

One way to validate the ABAQUS pipework model is to compare elastic results with those from the CAEPIPE model. Table 5-1 shows a comparison of reaction forces and reaction moments at rigid points of models for the dead weight and pressure load case. A ratio of 1 (ABAQUS result divided by CAEPIPE result) shows perfect agreement. A comparison shows that the agreement between the two models is reasonable and accepted for consecutive creep analyses. The possibility to get the same results from two different piping analyses is difficult for such a complicated structure. Table 5-2 shows a comparison of reaction forces and reaction moments at rigid points of models for the dead weight, pressure and thermal expansion load case. The agreement is judged to be acceptable. The ratio -606.3 emanates from a very small reaction force in the CAEPIPE analysis.

Table 5-1: Reaction forces and reaction moments at rigid points (node 10, 445 and 3930) for dead weight and internal pressure. Ratio equals ABAQUS results divided by CAEPIPE results. Forces in N and moments in Nm.

Node	Component	CAEPIPE	ABAQUS	Ratio
10	F_x	-289	-90	0.3
	F_y	26	47	1.8
	F_z	435	1201	2.8
	M_x	-54	-292	5.4
	M_y	-801	-792	1.0
	M_z	-2260	-633	0.3
445	F_x	-665	-665	1.0
	F_y	-900	-1108	1.2
	F_z	15970	21237	1.3
	M_x	48845	69802	1.4
	M_y	2176	2100	1.0
	M_z	-186	-1445	7.8
3930	F_x	1656	558	0.3
	F_y	3927	2476	0.6
	F_z	19291	17643	0.9
	M_x	-39535	-40263	1.0
	M_y	22672	20968	0.9
	M_z	-14806	-9574	0.6

Table 5-2: Reaction forces and reaction moments at rigid points (node 10, 445 and 3930) for dead weight, internal pressure and thermal expansion. Ratio equals ABAQUS results divided by CAEPIPE results. Forces in N and moments in Nm.

Node	Component	CAEPIPE	ABAQUS	Ratio
10	F_x	-83	-34	0.4
	F_y	-1895	-541	0.3
	F_z	4	-2425	-606.3
	M_x	3428	8392	2.4
	M_y	-9829	-11366	1.2
	M_z	-1127	-3784	3.4
445	F_x	-188	285	-1.5
	F_y	1482	436	0.3
	F_z	-1361	13295	-9.8
	M_x	-5041	47169	-9.4
	M_y	-8177	-9241	1.1
	M_z	-7099	-11328	1.6
3930	F_x	-20758	-22829	1.1
	F_y	7429	886	0.1
	F_z	-11616	-15692	1.4
	M_x	4590	7555	1.6
	M_y	-35238	-42662	1.2
	M_z	-46195	-20334	0.4

Section forces and moments at the location of weld W3 (see Figure 4-3) are also compared. Table 5-3 shows that the agreement is reasonable for the dead weight and internal pressure load case. Corresponding comparison for the dead weight, internal pressure and thermal expansion load case is given in Table 5-4. For this load case the agreement is also reasonable.

Table 5-3: Section forces and moments at the location of weld W3 (see Figure 4-3) for dead weight and internal pressure. Axial force caused by internal pressure is subtracted. Ratio equals ABAQUS results divided by CAEPIPE results. Forces in N and moments in Nm.

Node	Component	CAEPIPE	ABAQUS	Ratio
115	F_{ax}	1783	-234	-0.13
	$M_{torsion}$	1358	1115	0.82
	$M_{bend,tot}$	1330	1375	1.03

Table 5-4: Section forces and moments at the location of weld W3 (see Figure 4-3) for dead weight, internal pressure and thermal expansion. Axial force caused by internal pressure is subtracted. Ratio equals ABAQUS results divided by CAEPIPE results. Forces in N and moments in Nm.

Node	Component	CAEPIPE	ABAQUS	Ratio
115	F_{ax}	-12830	-14694	1.15
	$M_{torsion}$	5852	5337	0.91
	$M_{bend,tot}$	6443	11993	1.86

A comparison of the axial stress at the location of weld W3 (see Figure 4-3) is also done. This stress is a combination of a membrane stress and a bending stress. For the dead weight and internal pressure load case ABAQUS gives

$$\sigma_{ax,max} = \sigma_{ax,membrane} + \sigma_{ax,bend} = 39.1 + 4.6 = 43.7 \text{ MPa}$$

and for the dead weight, internal pressure and thermal expansion load case ABAQUS gives

$$\sigma_{ax,max} = \sigma_{ax,membrane} + \sigma_{ax,bend} = 36.6 + 46.0 = 82.6 \text{ MPa}$$

Corresponding maximum stresses in CAEPIPE are calculated as 51.2 and 83.8 MPa, respectively. The second stress corresponds rather well with that calculated with ABAQUS. The deviation of the first stress is explained by the way CAEPIPE calculates the stress. According to equation 3-1, the sum of primary stresses due to sustained loads is calculated as

$$\sigma_1 = \frac{p_c \cdot d_o}{4 \cdot e_n} + \frac{0.75 \cdot i \cdot M_A}{Z} = 43.8 + 7.4 = 51.2 \text{ MPa}$$

where $i = 1.4$.

σ_1 is conservatively calculated for consecutive evaluation according to the standard SS-EN 13480-3. The stress calculated ABAQUS is most physically correct of the two. Thus, a direct comparison of stresses calculated with CAEPIPE and ABAQUS cannot always be done.

One of the purposes of using the CAEPIPE model is to get the geometry of the piping system when building the model in ABAQUS. A comparison of ABAQUS and CAEPIPE results also helps in avoiding obvious mistakes in the ABAQUS model. The discrepancy in elastic results from the two programs is therefore accepted.

5.4 CREEP ANALYSIS OF PIPING SYSTEM

5.4.1 Constitutive model based on DIN EN 100028-2

A visco-elastic material model is assumed for the creep analysis. For the uniaxial case, the constitutive model is written as

$$\frac{d\varepsilon}{dt} = \frac{1}{E} \cdot \frac{d\sigma}{dt} + B \cdot \sigma^n \qquad (5\text{-}1)$$

where the first term is the elastic strain rate and the second term is the secondary creep strain rate according to Norton.

The creep rupture strength R_{km} and the creep deformation strength R_{A1} for 13CrMo4-5 are given according to the standard DIN EN 100028-2 [10] for 10.000 and 100.000 hours, see Table 5-5. $R_{A1,10000}$ and $R_{A1,100000}$ are the uniaxial stresses at which 1% creep strain is developed after 10000 and 100000 hours, respectively.

Table 5-5: Creep rupture strength R_{km} and creep deformation strength R_{A1} according to the standard DIN EN 100028-2 for 10.000 and 100.000 hours.

Temperature [C]	$R_{km,10.000}$ [MPa]	$R_{km,100.000}$ [MPa]	$R_{A1,10.000}$ [MPa]	$R_{A1,100.000}$ [MPa]
450	370	285	245	191
460	348	251	228	172
470	328	220	210	152
480	304	190	193	133
490	273	163	173	116
500	239	137	157	98
510	209	116	139	83
520	179	94	122	70
530	154	78	106	57
540	129	61	90	46
550	109	49	76	36

With data in Table 5-5, B and n are determined according to

$$n = \frac{1}{\log\left(R_{A1,10.000}/R_{A1,100.000}\right)} \qquad (5\text{-}2)$$

and

$$B = \frac{10^{-7}}{\left(R_{A1,100.000}\right)^n} \qquad (5\text{-}3)$$

and presented in Table 5-6.

Table 5-6: Creep constant *B* and creep exponent *n* for 13CrMo4-5 at different temperatures.

Temperature [C]	*B* $[\mathrm{h} \cdot \mathrm{MPa}^{\mathrm{n}}]^{-1}$	*n* [-]
450	8.04E-29	9.25
460	5.46E-26	8.17
470	2.86E-23	7.12
480	7.34E-21	6.18
490	1.28E-19	5.76
500	1.87E-17	4.89
510	2.69E-16	4.47
520	2.25E-15	4.14
530	3.04E-14	3.71
540	1.97E-13	3.43
550	1.60E-12	3.08

The constitutive model (uniaxial case) for 13CrMo4-5 at 460 °C is now written as

$$\frac{d\varepsilon}{dt} = \frac{1}{169000} \cdot \frac{d\sigma}{dt} + 5.46 \cdot 10^{-26} \cdot \sigma^{8.17} \qquad (5\text{-}4)$$

where E and σ are given in MPa and t is given in hours.

5.4.2 Creep analysis

A creep analysis is performed with the ABAQUS piping model shown in Figure 5-2. The constitutive model based on material properties in the standard 13CrMo4-5 is used, see equation (5-4). The rebuilt of the system 2011 (red part of piping in Figure 5-2) is considered in the analysis. This is done by changing the elastic modulus of an element connecting the original pipework with the additional piping part. Table 5-7 shows the conditions for analysed steps.

Table 5-7: Conditions for steps in analysis of pipework. *W, P,* T_{design}, T_{oper} *and C* denote dead weight, internal pressure, design temperature, operating temperature and creep, respectively.

STEP	Loading condition	Temp [C]	Pressure [bar]	Final time of step [hours/years]	Comments
1	*W*	20	0	0	
2	*W+P*	20	64	0	
3	$W+P+T_{design}$	495	64	0	
4	$W+P+T_{oper}$	460	64	0	Start of operation
5	$W+P+T_{oper}+C$	460	64	100000 / 11.9	
6	$W+P+T_{oper}+C$	460	64	200000 / 23.8	
7	$W+P+T_{oper}+C$	460	64	277200 / 33	
8	*W*	20	0	277200 / 33	Rebuilt of system
9	$W+P+T_{oper}$	460	64	277200 / 33	
10	$W+P+T_{oper}+C$	460	64	327600 / 39	

Figure 5-4 shows bending moments about local axes and twisting moment about elbow axis at the location of weld W3 (see Figure 4-3) for analysed steps described in Table 5-7. Results show that all moments relax with time. Corresponding local axial force at the location of weld W3 is almost constant and is completely controlled by the internal pressure. Comparing bending moments for step 7 and step 9 in Figure 5-4 reveals that rebuilt of the system has a negligible impact on the location of weld W3. Comparing results for step 1 and step 8 shows that creep relaxation of the system during operation, from start to rebuilding, has pre-strained the system.

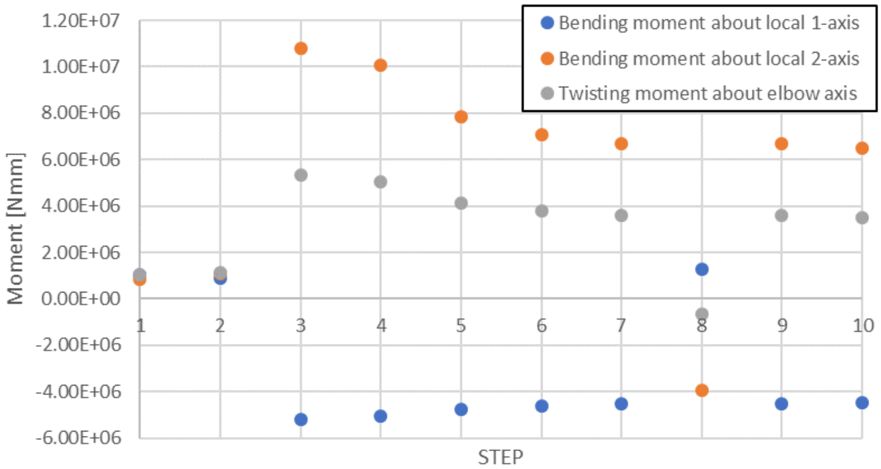

Figure 5-4: Bending and twisting moments at the location of weld W3 as a function of step. Conditions for analysed steps are given in Table 5-7.

Axial stresses and hoop stresses at the location of weld W3 are shown in Figure 5-5 and Figure 5-6, respectively. Stresses are shown as a function of location around the circumference for different loads where *W* denotes dead weight, *P* denotes internal pressure, *T* denotes thermal expansion and *C* denotes creep. Regarding creep, stresses are shown for different number of hours in operation starting from year zero. 277200 hours correspond to 33 years from start to rebuilt of the system. 327600 hours correspond to 33+6=39 years when the T-piece was cut out from the system.

Axial stresses at start of operation (W+P+T_{oper}) show that bending stresses caused by thermal expansion are extensive, see Figure 5-5. As the system starts to creep, these bending stresses relax. Maximum axial stress is reduced with 16 % from 82.5 to 69 MPa after 39 years of operation. The first 12 years of operation result in a reduction of 10 %. Figure 5-5 also shows that the position for maximum axial stress moves during operation from somewhere between integration point 17 and 18 to integration point 18. This is because of creep induced stress redistribution.

Highest stresses in Figures 5-5 and 5-6 are found at integration point 18 (see Figure 5-3 for definition). The way the actual element in the model is oriented gives that this position corresponds to a position between 12 and 3 in Table 4-2. The analysis thus predicts the location where highest creep damage is found in weld W3.

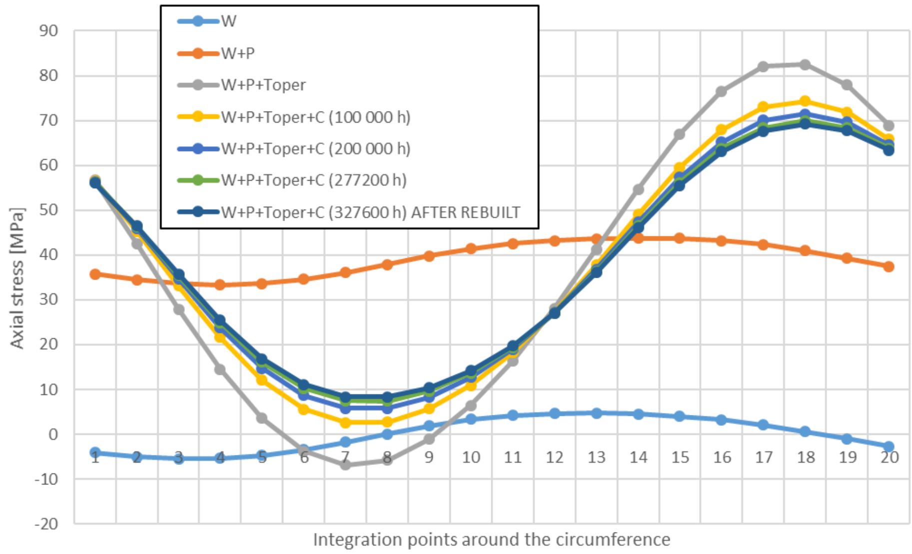

Figure 5-5: Axial stress around the circumference at the location of weld W3 for different loads and different time of operation. Stresses are caused by dead weight *W*, internal pressure *P* and thermal expansion *T*. Number of hours shown within brackets gives time of operation and *C* denotes creep.

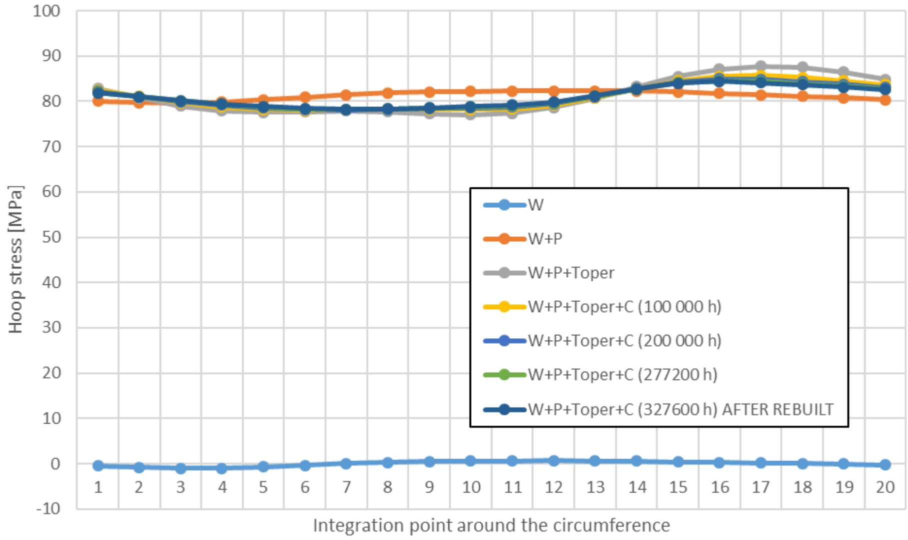

Figure 5-6: Hoop stress around the circumference at the location of weld W3 for different loads and different time of operation. Stresses are caused by dead weight *W*, internal pressure *P* and thermal expansion *T*. Number of hours shown within brackets gives time of operation and *C* denotes creep.

Equivalent creep strain ε_{eq}^{c} in the most strained point around the circumference of the location of weld W3 is shown in Figure 5-7. After 39 years of operation (327600 h) $\varepsilon_{eq}^{c} = 0.0069$ %. This amount of creep strain is regarded as very small and does not explain the creep damage found in weld W3, see Table 4-2. With weld W3 explicitly included (as a solid model) in the ABAQUS model, it is expected that calculated creep strains would increase. The reason is that creep deformation properties vary across the weldment. As weld W2 shows the largest amount of creep damage, the effect of solid modelling the weldment is only investigated for weld W2.

Results from the creep analysis of the piping system show that system forces and moments relax with operation time. But it also shows that these forces and moments remain at a relatively high level. This means that elastic follow-up is possible if a weaker zone is introduced into the system. An explicitly modelled weld with its different constituents could be such a weak zone.

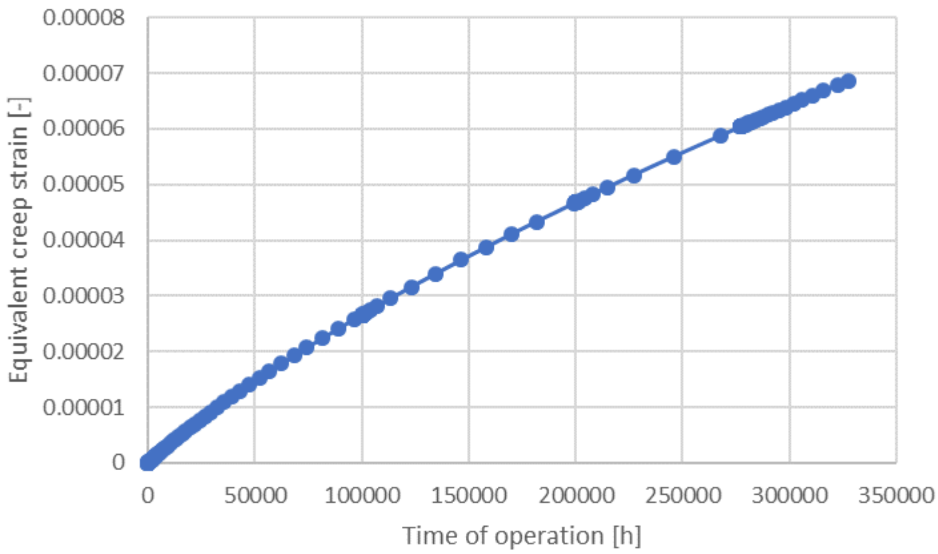

Figure 5-7: Equivalent creep strain ε_{eq}^{c} in most strained integration point around the circumference at the location of weld W3 (element 64 in ABAQUS model).

Stresses and strains at the location of weld W2 (see Figure 4-3) cannot be captured with the present model. The reason is that stresses and strains at the junction of the T-piece cannot be resolved with the ELBOW31 element. The remedy is to introduce a 3D model of the T-piece and connect this model to the piping model. Analysis of weld W2 is reported below.

5.5 CREEP ANALYSIS OF WELD W2 WITH A SOLID T-PIECE MODEL

5.5.1 Solid model of T-piece and weld W2

The stress and strain state at the location of weld W2 is not possible to determine by use of the piping element ELBOW31. Therefore, a solid model of the T-piece and its weld W2 is modelled in ABAQUS by use of the solid element C3D8. The three materials base, weld and HAZ are represented in the model. This gives the possibility to investigate the impact of different creep rate combinations in the weldment region. Figures 5-8, 5-9 and 5-10 show the T-piece model.

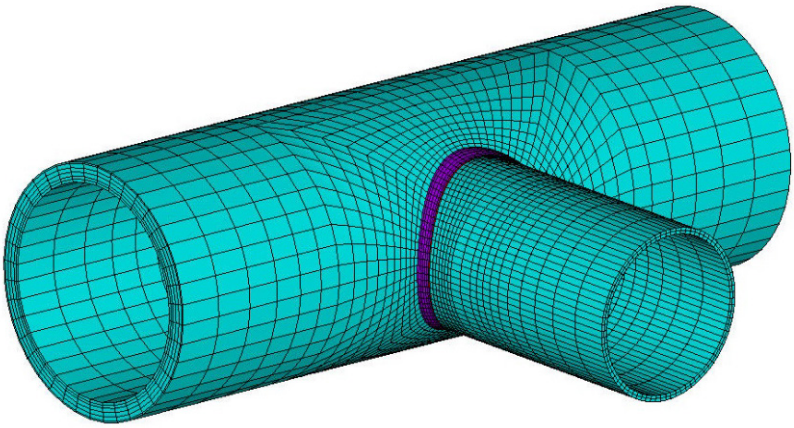

Figure 5-8: 3D solid model of the T-piece.

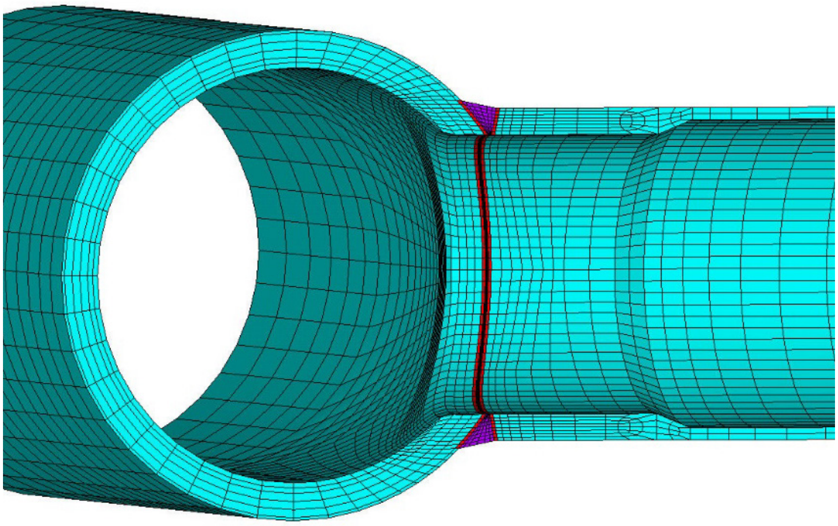

Figure 5-9: Nozzle and weld in 3D solid model of the T-piece. Half model.

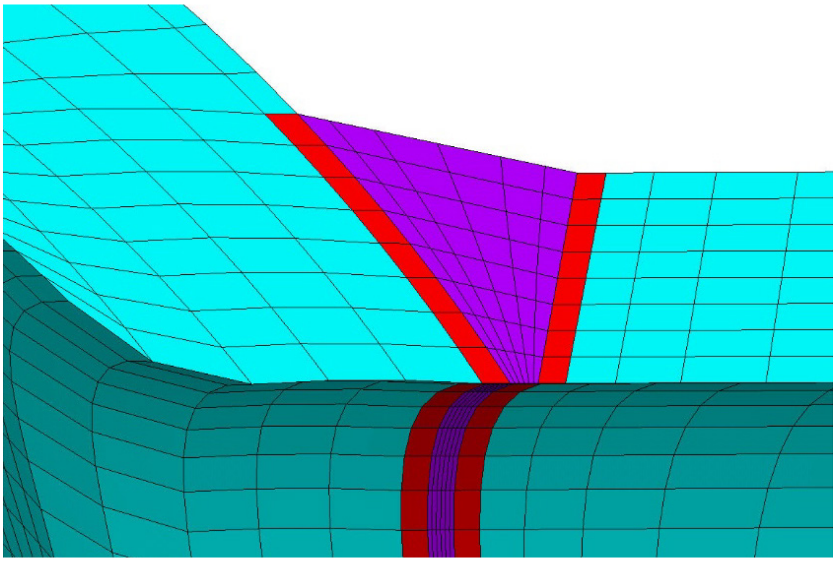

Figure 5-10: Weld W2 in 3D solid model of the T-piece where base material is blue, weld is purple and HAZ is red.

The solid model of the T-piece is connected to the piping model shown in Figure 5-2 by use of rigid bodies at the end sections of the solid model, see Figure 5-11. Introduction of the rigid bodies influences the results locally at about $2.5\sqrt{R \cdot t}$ away from the free ends. For the run pipe and the branch pipe this distance is 159 mm and 74 mm, respectively. As the weld W2, connecting the run pipe with the branch pipe, is of main interest in this analysis, this way of connecting the piping model with the T-piece model can be accepted. Figure 5-12 shows the piping model with the connected 3D model of the T-piece.

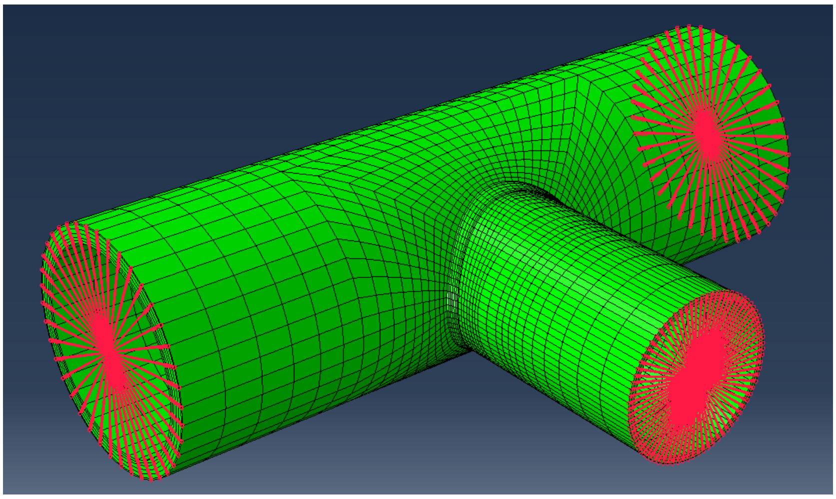

Figure 5-11: Rigid bodies at end sections of the T-piece.

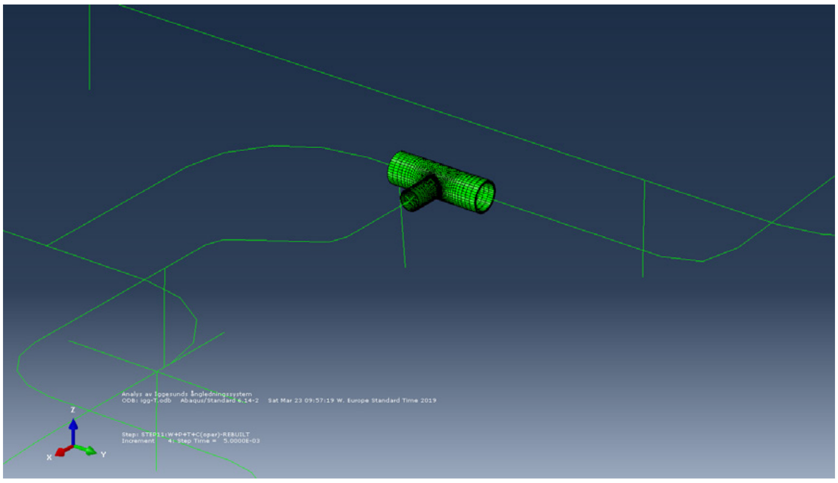

Figure 5-12: Part of piping system model with connected 3D model of the T-piece.

5.5.2 Creep analysis

The weld and HAZ regions in weld W2 are explicitly modelled in the solid model of the T-piece. This gives the possibility to investigate different weldment constituent combinations of creep deformation rate properties. Table 5-8 shows investigated creep property combinations and main results. The base material characteristics are kept constant in all simulations. This in order to maintain the elastic follow-up phenomenon. An increase of the deformation rate of the base material would reduce system forces and moments as an enhanced relaxation of stresses caused by thermal expansion would occur in the whole system.

For combination 1 to 6, the creep exponent is kept constant for all constituents, i.e. equal to that of the base material. Combination 1 is the reference case where all materials in weld W2 have the same deformation rate characteristics. Results from this combination can be compared with that of the piping analysis performed in section 5.4.2. For combination 2 to 6, different combinations of creep constants B for the weld and the HAZ material are investigated. An increase factor of 10-40 is used. For combination 7, the creep exponent for the weld and HAZ material is increased to 10. B is then chosen in such a way that the uniaxial creep strain rate at a stress level of 80 MPa equals that of the base material at the same stress. The stress 80 MPa corresponds the stress in circumferential direction caused by internal pressure at weld W3, see Figure 5-6. It also corresponds the maximum axial stress at the start of the plant, see Figure 5-5. For combination 8, B is further increased so that the uniaxial creep strain rate at 50 MPa is equal for the three materials.

Table 5-8: Constants in Norton's law for weldment constituents and maximum of equivalent creep strain in weld W2.

Combination	Weldment Constituent	Creep constant B $[\mathrm{h \cdot MPa^n}]^{-1}$	Creep exponent n [-]	Creep strain max ε_{eq}^{c} [%]
1	Base	$5.46 \cdot 10^{-26}$	8.17	0.061
	Weld	$5.46 \cdot 10^{-26}$	8.17	0.079
	HAZ	$5.46 \cdot 10^{-26}$	8.17	0.059
2	Base	$5.46 \cdot 10^{-26}$	8.17	0.065
	Weld	$5.46 \cdot 10^{-25}$	8.17	0.126
	HAZ	$5.46 \cdot 10^{-26}$	8.17	0.064
3	Base	$5.46 \cdot 10^{-26}$	8.17	0.063
	Weld	$5.46 \cdot 10^{-26}$	8.17	0.091
	HAZ	$5.46 \cdot 10^{-25}$	8.17	0.075
4	Base	$5.46 \cdot 10^{-26}$	8.17	0.070
	Weld	$10.9 \cdot 10^{-25}$	8.17	0.155
	HAZ	$5.46 \cdot 10^{-25}$	8.17	0.082
5	Base	$5.46 \cdot 10^{-26}$	8.17	0.069
	Weld	$5.46 \cdot 10^{-25}$	8.17	0.149
	HAZ	$10.9 \cdot 10^{-25}$	8.17	0.084
6	Base	$5.46 \cdot 10^{-26}$	8.17	0.073
	Weld	$21.8 \cdot 10^{-25}$	8.17	0.174
	HAZ	$10.9 \cdot 10^{-25}$	8.17	0.089
7	Base	$5.46 \cdot 10^{-26}$	8.17	0.062
	Weld	$1.80 \cdot 10^{-29}$	10	0.089
	HAZ	$1.80 \cdot 10^{-29}$	10	0.061
8	Base	$5.46 \cdot 10^{-26}$	8.17	0.064
	Weld	$4.25 \cdot 10^{-29}$	10	0.108
	HAZ	$4.25 \cdot 10^{-29}$	10	0.068
9	Base	$5.46 \cdot 10^{-26}$	8.17	0.064
	Weld	$5.46 \cdot 10^{-24}$	8.17	0.210
	HAZ	$5.46 \cdot 10^{-24}$	8.17	0.119

Figure 5-13 shows equivalent creep strain at the upper part of weld W2 after 327600 hours of operation for combination 1, see Table 5-8. Maximum is found in the weld material and calculated as $\varepsilon_{eq}^{c} = 0.079$ %, i.e. almost 17 times higher value than for weld W3. This difference is explained by the local bending stress that develops in the junction between the run pipe and the branch pipe.

An increase of the creep rate for the weld material is expected to increase the amount of creep strain in the weld. Figure 5-14 shows the results for combination 2, see Table 5-8. As seen, the accumulated creep strain in the weld is only increased by a factor of 1.6 even though the B constant in Norton's law is increased a factor of 10. The reason is that the stress state in the weld is not uniaxial but multiaxial and the weld is constrained by surrounding material. Figures 5-15 and 5-16 show ε_{eq}^{c} for combination 3 and 4.

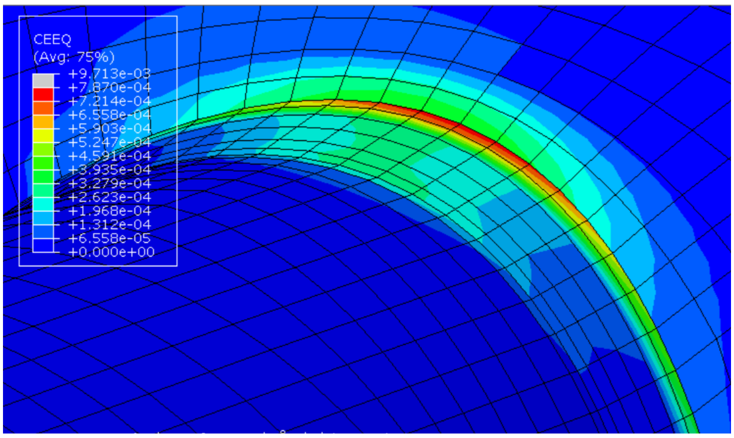

Figure 5-13: Maximum equivalent creep strain $\varepsilon_{eq}^{c} = 0.0787$ % at the upper part of weld W2 after 327600 hours of operation. Material combination 1 in Table 5-8 is used in the simulation.

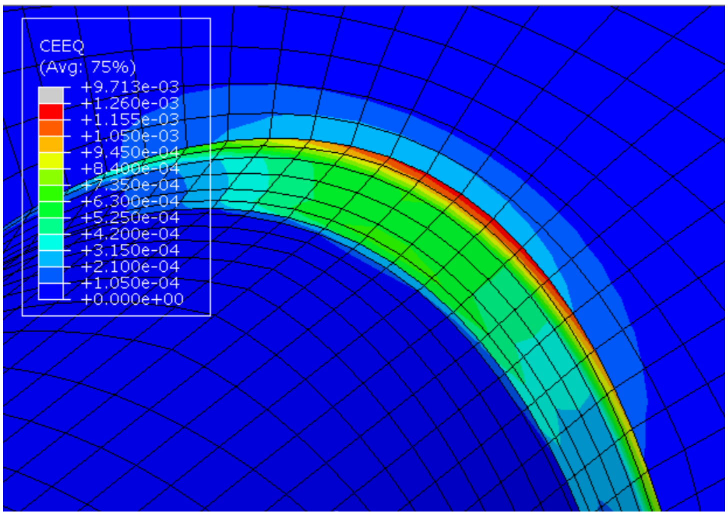

Figure 5-14: Maximum equivalent creep strain $\varepsilon_{eq}^{c} = 0.126$ % at the upper part of weld W2 after 327600 hours of operation. Material combination 2 in Table 5-8 is used in the simulation.

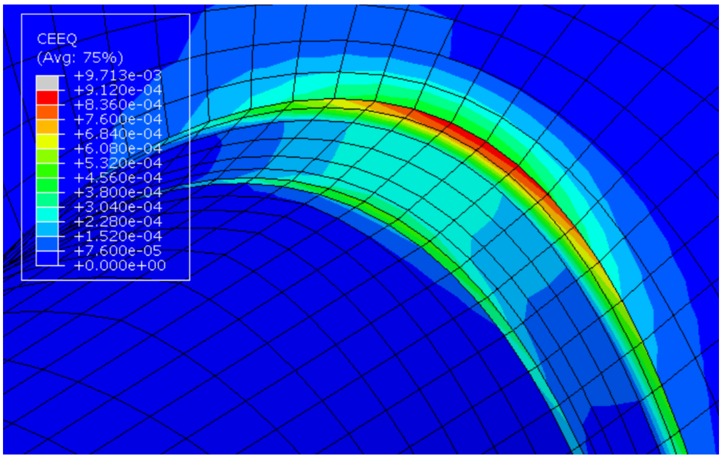

Figure 5-15: Maximum equivalent creep strain $\varepsilon_{eq}^{c} = 0.0912$ % at the upper part of weld W2 after 327600 hours of operation. Material combination 3 in Table 5-8 is used in the simulation.

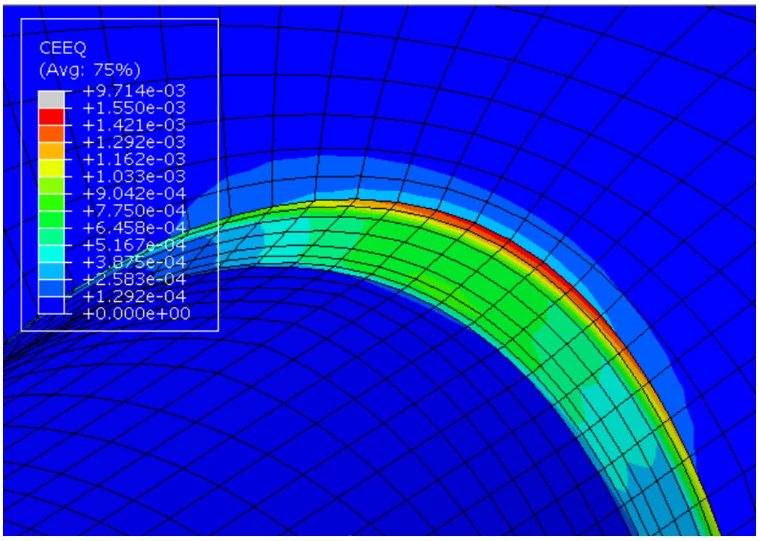

Figure 5-16: Maximum equivalent creep strain $\varepsilon_{eq}^{c} = 0.155$ % at the upper part of weld W2 after 327600 hours of operation. Material combination 4 in Table 5-8 is used in the simulation.

Table 5-9 gives maximum of ε_{eq}^{c} in the weld and in the HAZ for the respective weldment constituent combination in Table 5-8. The creep strain components are shown also for the position where ε_{eq}^{c} has its maximum. In general, most creep strains are developed in the weld. Combination 4 results in $\varepsilon_{eq}^{c} = 0.155$ % in the weld.

For combination 5 and 6, the creep rate of the weld material and HAZ is further increased by increasing the B constant. As expected, accumulated creep strain increases somewhat as seen in Table 5-9.

For combination 7 and 8, the creep exponent is increased from 8.17 to 10 for the weld material and HAZ. B is chosen so that the uniaxial creep rate for the weld material and HAZ equals that of the base material at 80 and 50 MPa, respectively. The results for combination 7 and 8 correspond rather well with that of combination 3 and 2, see Table 5-9.

Finally, combination 9 uses a B constant for the weld material and HAZ that is 100 times higher than that of the base material. This combination gives the highest equivalent creep strains of all combination. In the weld $\varepsilon_{eq}^{c} = 0.210$ %.

As seen in Table 5-9, creep simulations with realistic combinations of creep deformation properties for the weldment constituent show less than 0.20 % equivalent creep strain in weld W2. Thus, only additional loads or low creep ductility at local regions can explain why severe creep damage was found in weld W2.

Table 5-9: Developed creep strains in the weld and HAZ material in weld W2 after 327600 hours of operation. *ax*, φ and *r* denote axial, circumferential and radial direction of the branch pipe. Creep strain components are shown for the position where ε_{eq}^{c} has its maximum. The combination is described in Table 5-8.

Combination	Weldment constituent	Max ε_{eq}^{c} [%]	ε_{ax}^{c} [%]	$\varepsilon_{\varphi}^{c}$ [%]	ε_{r}^{c} [%]
1	Weld	0.079	0.054	0.013	-0.064
	HAZ	0.059	-0.023	0.055	-0.033
2	Weld	0.126	0.087	0.020	-0.102
	HAZ	0.064	-0.026	0.060	-0.038
3	Weld	0.091	0.063	0.011	-0.071
	HAZ	0.075	-0.032	0.071	-0.042
4	Weld	0.155	0.107	0.022	-0.124
	HAZ	0.082	-0.038	0.078	-0.044
5	Weld	0.149	0.103	0.026	-0.117
	HAZ	0.084	-0.038	0.080	-0.053
6	Weld	0.174	0.120	0.033	-0.139
	HAZ	0.089	-0.041	0.084	-0.056
7	Weld	0.089	0.062	0.015	-0.071
	HAZ	0.061	-0.024	0.058	-0.038
8	Weld	0.108	0.075	0.019	-0.087
	HAZ	0.068	-0.028	0.064	-0.042
9	Weld	0.210	0.144	0.038	-0.164
	HAZ	0.119	-0.050	0.096	-0.065

5.5.3 Effect of non-functioning supports

As the analyses in the previous section could not directly explain the creep damage detected in weld W2, the impact of non-functioning supports is investigated. Figure 5-17 shows the supports that might influence creep damage evolution in weld W2. The supports are denoted with their respective node number. Table 5-10 gives details about investigated supports. Material combination 2 in Table 5-8 is used for all simulations with non-functioning supports. Results are shown at time 327600 hours.

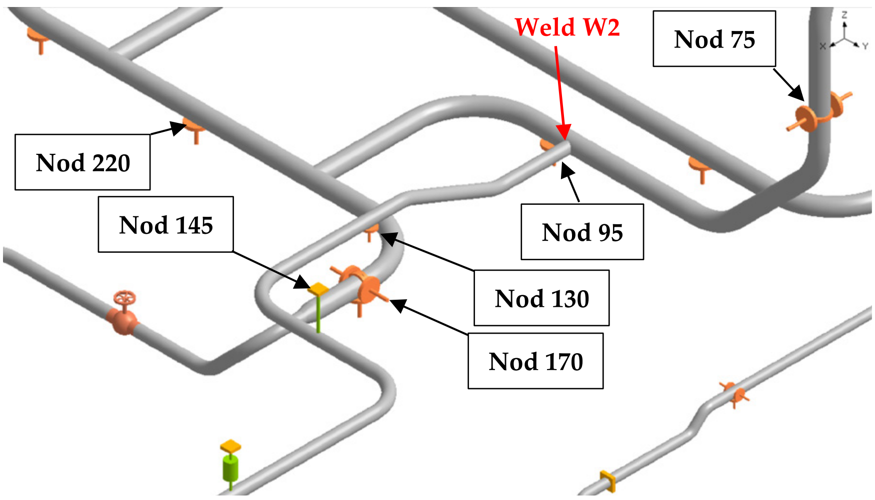

Figure 5-17: Supports that might influence creep damage evolution in weld W2. Supports are denoted by their node number.

Table 5-10: Supports considered in investigation of non-functioning supports.

Node in CAEPIPE and ABAQUS model	Type of support	Active direction
75	Limit stops	X, Z
95	Limit stop	Z
130	Limit stop	Z
145	Rod hanger	Z
170	Limit stops	Y, Z
220	Limit stop	Z

Figure 5-18 shows maximum creep damage at the lower part of weld W2 when the limit stops at node 75 are not functioning. This location of maximum creep damage does not correspond to that detected in the weld. Thus, non-functioning limit stops at node 75 do not explain the creep damage found in weld W2.

Figure 5-19 shows maximum creep damage at the upper part of weld W2 when the limit stop at node 95 is not functioning. The location coincides with that where most creep damage was detected. However, the level is relatively low and has decreased compared to that when all supports were functioning, compare Figures 5-19 with Figure 5-14.

A non-functioning limit stop at node 130 increases the creep damage with 34 % compared to that in Figure 5-14. Figure 5-20 shows maximum equivalent creep strain $\varepsilon_{eq}^{c} = 0.169$ % at the upper part of weld W2. The level is however still rather low.

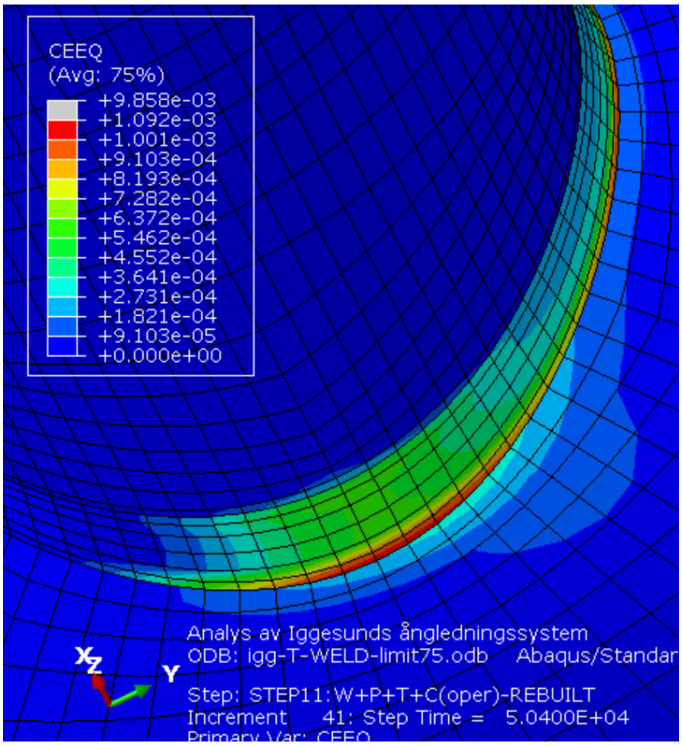

Figure 5-18: Maximum equivalent creep strain $\varepsilon_{eq}^{c} = 0.109$ % at the lower part of weld W2 after 327600 hours of operation. Non-functioning limit stop at node 75 in CAEPIPE and ABAQUS model. Material combination 2 in Table 5-8 is used in the simulation.

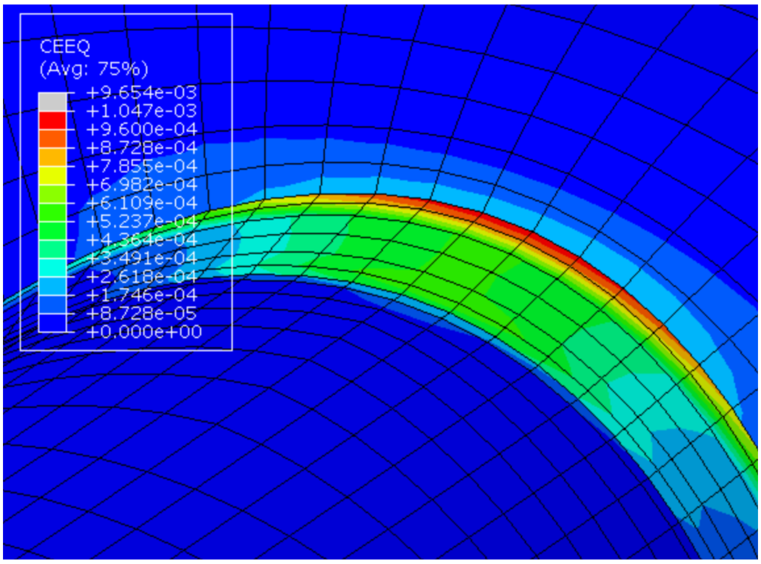

Figure 5-19: Maximum equivalent creep strain $\varepsilon_{eq}^{c} = 0.105$ % at the upper part of weld W2 after 327600 hours of operation. Non-functioning limit stop at node 95 in CAEPIPE and ABAQUS model. Material combination 2 in Table 5-8 is used in the simulation.

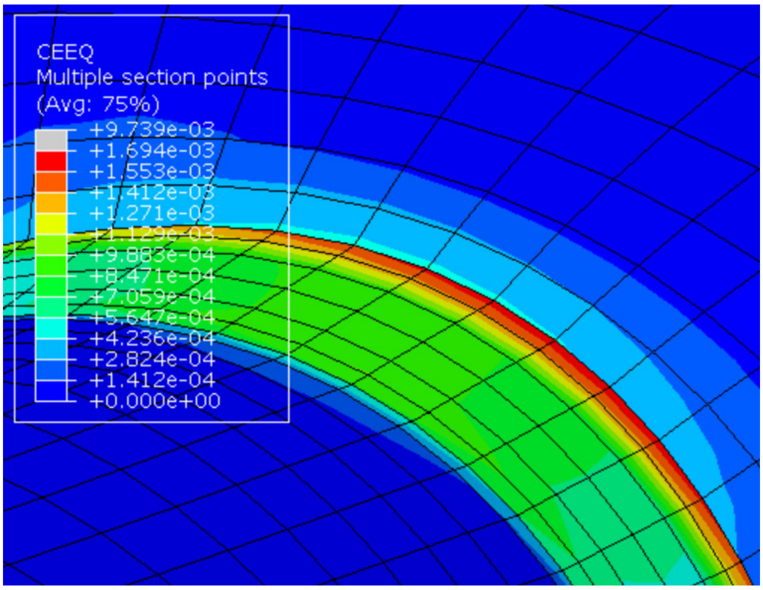

Figure 5-20: Maximum equivalent creep strain $\varepsilon_{eq}^{c} = 0.169$ % at the upper part of weld W2 after 327600 hours of operation. Non-functioning limit stop at node 130 in CAEPIPE and ABAQUS model. Material combination 2 in Table 5-8 is used in the simulation.

A non-functioning rod hanger at node 145 also results in maximum creep damage at the upper part of weld W2, see Figure 5-21. Again, the level is lower than that with all supports functioning.

Equivalent creep strain in weld W2 is shown in Figure 5-22 for the case with non-functioning limit stops at node 170. Maximum creep damage is found at the upper part of weld W2. Maximum $\varepsilon_{eq}^{c} = 0.142$ % which is lower than that for the case with non-functioning limit stop at node 130.

Figure 5-23 shows equivalent creep strain in weld W2 for the case with non-functioning limit stop at node 220. Maximum is found at the upper part of the weld. The level of creep damage is lower than that with all supports functioning, compare with Figure 5-14.

Equivalent creep strain in weld W2 is shown in Figure 5-24 for the case with non-functioning limit stop at node 130 and non-functioning rod hanger at node 145. Maximum creep damage is found at the upper part of weld W2. Maximum ε_{eq}^{c} is lower than that for the case with all supports functioning.

Figure 5-25 shows equivalent creep strain in weld W2 for the case with non-functioning limit stops at node 130 and 170. Maximum is found at the upper part of the weld. Maximum $\varepsilon_{eq}^{c} = 0.181$ % which is 44 % higher than that for combination 2, see Figure 5-14.

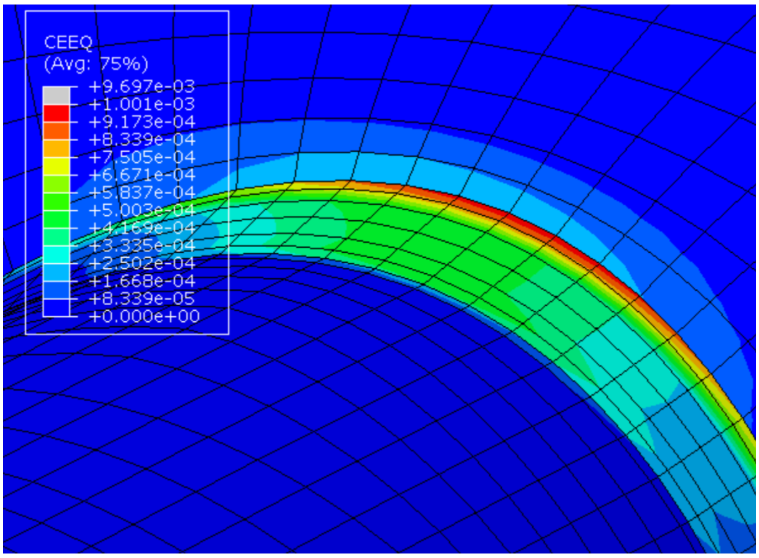

Figure 5-21: Maximum equivalent creep strain $\varepsilon_{eq}^{c} = 0.100$ % at the upper part of weld W2 after 327600 hours of operation. Non-functioning rod hanger at node 145 in CAEPIPE and ABAQUS model. Material combination 2 in Table 5-8 is used in the simulation.

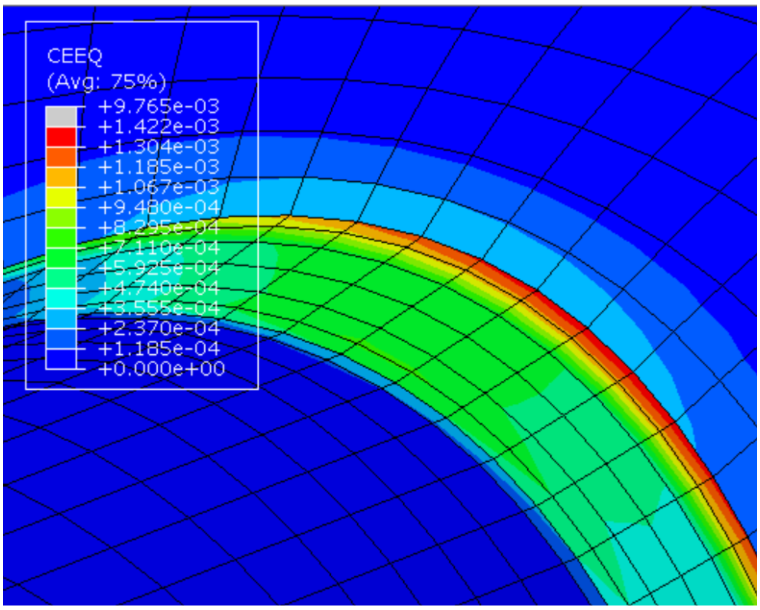

Figure 5-22: Maximum equivalent creep strain $\varepsilon_{eq}^{c} = 0.142$ % at the upper part of weld W2 after 327600 hours of operation. Non-functioning limit stop at node 170 in CAEPIPE and ABAQUS model. Material combination 2 in Table 5-8 is used in the simulation.

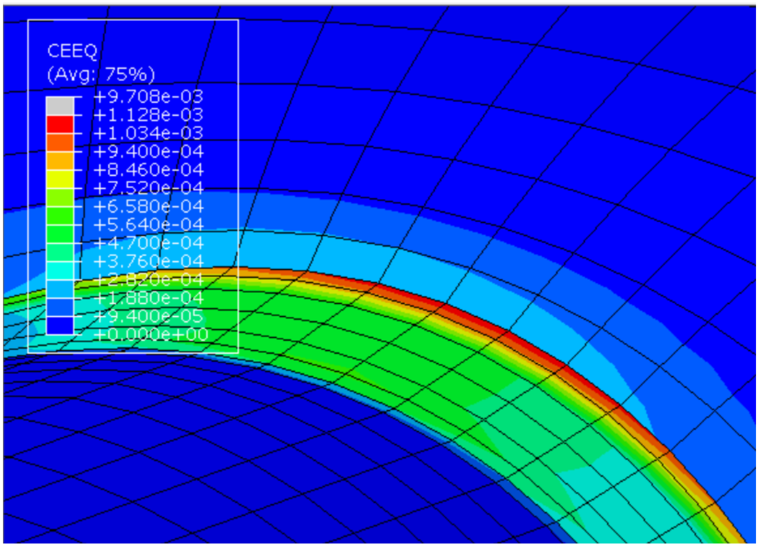

Figure 5-23: Maximum equivalent creep strain $\varepsilon_{eq}^{c} = 0.113$ % at the upper part of weld W2 after 327600 hours of operation. Non-functioning limit stop at node 220 in CAEPIPE and ABAQUS model. Material combination 2 in Table 5-8 is used in the simulation.

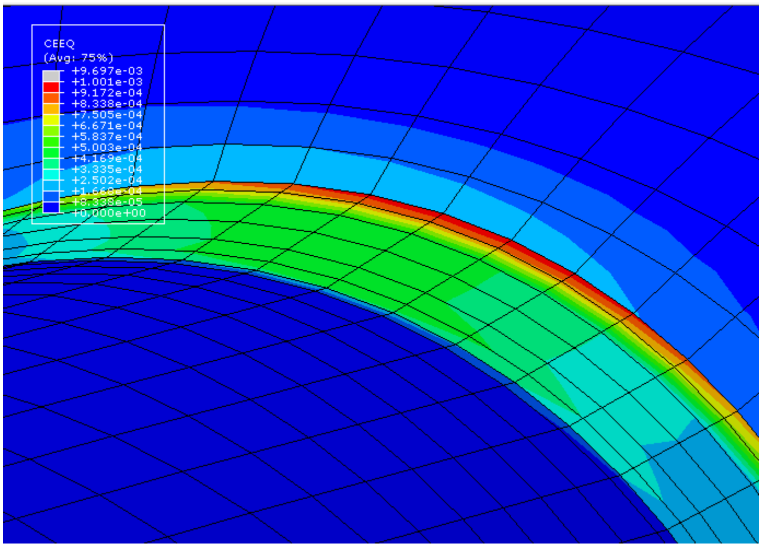

Figure 5-24: Maximum equivalent creep strain $\varepsilon_{eq}^{c} = 0.10$ % at the upper part of weld W2 after 327600 hours of operation. Non-functioning limit stop at node 130 and non-functioning rod hanger at node 145 in CAEPIPE and ABAQUS model. Material combination 2 in Table 5-8 is used in the simulation.

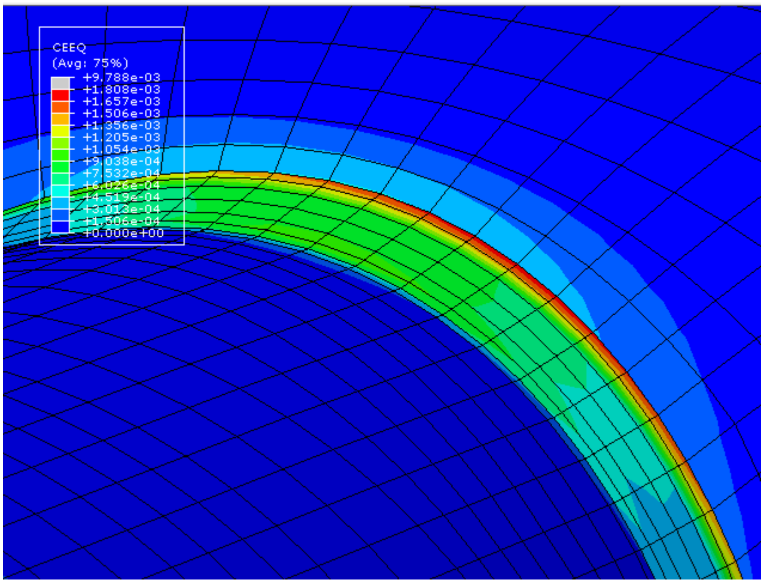

Figure 5-25: Maximum equivalent creep strain $\varepsilon_{eq}^{c} = 0.181$ % at the upper part of weld W2 after 327600 hours of operation. Non-functioning limit stops at node 130 and 170 in CAEPIPE and ABAQUS model. Material combination 2 in Table 5-8 is used in the simulation.

Table 5-11 summarises simulation results for cases with non-functioning supports. About 70 % of the cases show less equivalent creep strain in weld W2 compared to that for the case with all supports functioning. The case where the limit stops at node 130 and node 170 are non-functioning, shows the largest amount of creep damage. Still however, this amount of equivalent creep strain is rather low to explain detected creep damage at the upper part of weld W2.

Table 5-11: Maximum equivalent creep strain ε_{eq}^{c} in weld W2 for cases with non-functioning supports.

Node in CAEPIPE and ABAQUS model	Non-functioning support	Location in weld W2 with maximum	ε_{eq}^{c} [%]
-	All supports are functioning	Upper	0.126
75	Limit stops	Lower	0.109
95	Limit stop	Upper	0.105
130	Limit stop	Upper	0.169
145	Rod hanger	Upper	0.100
170	Limit stops	Upper	0.142
220	Limit stops	Upper	0.113
130+145	Limit stop and rod hanger	Upper	0.100
130+170	Limit stops	Upper	0.181

5.5.4 Effect of temporary temperature rise

During a short period of time in December 2006, the steam temperature was raised to 620 °C, see Figure 5-26. How large part of the piping system that was subjected to this temperature and under how long time is uncertain.

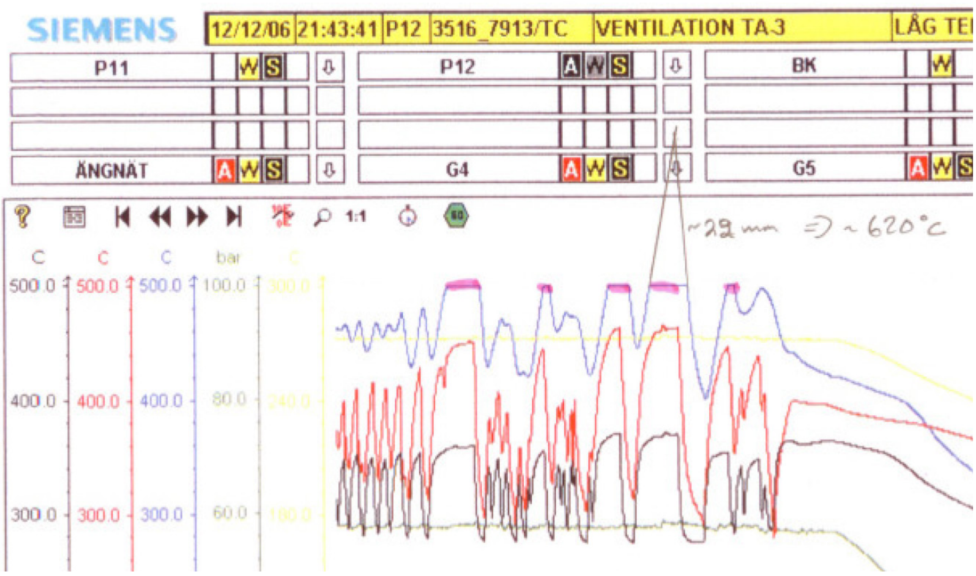

Figure 5-26: Protocol from operation of the plant where the blue curve gives the steam temperature as a function of time.

In order get a feeling for how an increase in temperature under a short period of time influences the accumulation of creep strain in the system, the effect of one hour of operation at 550 °C is investigated. At this temperature creep data is available, see Table 5-6. In order to maintain the effect of elastic follow-up it is assumed that the temporary temperature rise occurred at start of the plant. Furthermore, only the creep properties of the weld and the HAZ is changed to that for 550 °C, i.e.

$$\frac{d\varepsilon}{dt} = \frac{1}{160000} \cdot \frac{d\sigma}{dt} + 1.6 \cdot 10^{-12} \cdot \sigma^{3.08} \qquad (5\text{-}5)$$

For the base material, the constitutive model given in equation (5-4) is used.

The simulation shows that the amount of creep strain accumulated in the weld and HAZ during one hour creep at 550 °C is negligible, $7.49 \cdot 10^{-4}$ % in the weld and $7.16 \cdot 10^{-4}$ % in the HAZ. At 620 °C, part of the piping system will deform plastically before it starts to creep. Without knowing the temperature distribution in the piping system, the accumulation of inelastic strain (plastic+creep) in the weld W2 during the temporary temperature rise cannot be determined. However, it might be that this incident is part of the explanation for the creep damage found in weld W2.

5.5.5 Effect of weld residual stress relaxation

Contribution of creep strains caused by relaxation of weld residual stresses has not been considered in these creep analyses. This can be done in a simplistic way by considering an estimate of weld residual stresses at start of the plant. At room temperature the yield stress and Young's modulus for 13CrMo4-5 is 270 MPa and 210000 MPa, respectively. If a weld residual stress of 270 MPa completely relaxes by creep the creep strain would be $270/210000 = 0.129$ %, assuming uniaxial stress state.

In a welded pressure component, stresses caused by dead weight, internal pressure and thermal expansion are superimposed on the weld residual stresses. Relaxation of the stresses in the weldment region is thus very difficult to simulate. Practically, it can be assumed that not more than half of the weld residual stress can be relaxed and contribute to accumulated creep strain. This means that weld residual stresses in this case can contribute with 0.064 % at the most.

5.5.6 Effect of primary creep

Primary creep will contribute to the accumulation of creep strain. With an operation time of more than 300000 hours, however, it is judged that creep strains caused by primary creep can be neglected in relation to that caused by secondary creep.

5.6 PREDICTION OF CREEP STRAIN AT WELD W3 WITH SOLID T-PIECE MODEL

In section 5.4, maximum equivalent creep strain at the location of weld W3 was calculated as $\varepsilon_{eq}^{c} = 0.0069$ % after 327600 hours of operation. It is of interest to compare this result with that calculated at the same position with the T-piece solid model connected to the piping model. As weld W3 is not explicitly modelled in the T-piece solid model (base material properties are used), a direct comparison of calculated creep strains can be done.

Figure 5-27 shows ε_{eq}^{c} at the position of weld W3 in the T-piece solid model after 327600 hours of operation. Maximum equivalent creep strain is calculated as ε_{eq}^{c} = 0.0064 % and located at almost the same position as in the piping analysis, compare with location of maximum axial stress in Figure 5-5. The amount of creep strain calculated in the solid T-piece model is somewhat lower. The reason for this discrepancy is most probably that the stiffness of the connection between the run pipe and the branch pipe is lower for the solid T-piece model than for the piping model. This difference influences the bending moment at the position of weld W3 which is lower for the solid T-piece model than for the piping model, see Table 5-12.

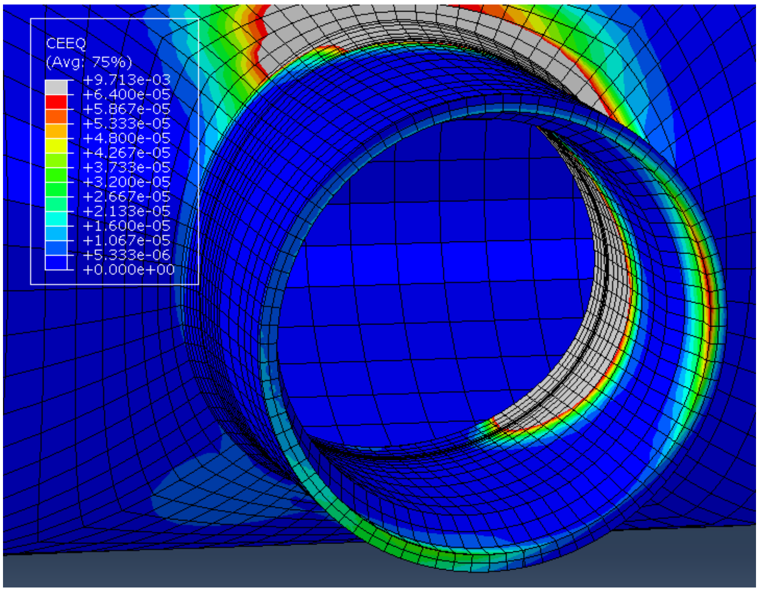

Figure 5-27: Equivalent creep strain ε_{eq}^{c} at the position of weld W3 in the T-piece solid model after 327600 hours of operation. Base material creep properties are used for the whole solid model.

Table 5-12: Section forces and moments in the branch pipe close to weld W3. *SF1* equals the axial force, *SM1* equals bending moment about local 1-axis, *SM2* equals bending moment about local 2-axis and *SM3* equals twisting moment. Base material properties are used for the whole solid T-piece model.

Case	Time [h]	*SF1* [N]	*SM1* [Nmm]	*SM2* [Nmm]	*SM3* [Nmm]
Pipe model	0	1.94E+05	-3.45E+06	8.30E+06	5.04E+06
	327600	1.99E+05	-3.30E+06	5.40E+06	3.50E+06
Pipe model with solid T-piece model	0	1.92E+05	-3.28E+06	6.26E+06	5.06E+06
	327600	1.99E+05	-2.95E+06	2.55E+06	3.11E+06

Based on the results in section 5.5, the weldment with base, weld and HAZ material properties is not explicitly modelled at the location of W3. Compared to weld W2, creep damage is less in weld W3 and the effect of varying creep properties across the weldment is better reflected by the analysis of weld W2.

6 Experimental

6.1 GENERAL

The studied T-piece was cut out after 327600 hours of operation in November 2017. The experimental part of the project consists of

- Metallographic investigations of the positions of the welds W1-W3 where creep damages were observed at replica tests 2014, see section 4.2.
- Creep testing of weld W3. It is a butt weld with very limited amount of creep damage observed at the replica tests and was chosen for two reasons:
    - × It was possible to extract creep test specimens (in contrast to the branch pipe weld).
    - × Creep testing of significantly creep damaged material can give results that are difficult to interpret.
- Metallographic investigations of post-test creep test specimens. The purpose is to study possible creep cavitation and its relationship to uniaxial creep strain.

6.2 METALLOGRAPHIC INVESTIGATION OF SERVICE EXPOSED MATERIAL

Metallographic investigation was conducted on the cut-out T-piece welds by replica testing. Pieces across the welds W1, W2 and W3 were cut and examined at the 3, 6, 9 and 12 o´clock positions of W2 and the 3 and 12 o´clock positions of W1 and W3, see Figure 4.2. The testing was performed on both outer surfaces and at corresponding cross-sections.

At each position an area across the weld was ground stepwise to a high fineness (400 mesh). The electropolishing was performed in adjacent base metals and HAZs on both sides of the weld as well as in the weld metal. After etching, replicas were extracted and examined in light optical microscope. Observed creep damage was classified according to NT TR 302 [11]. It is basically the same as NT NDT 010 [12] but the definitions are stricter and the sub-classes are denoted *a* (low) and *b* (high) instead 1 (low), 2 (medium), and 3 (high). The examined areas are denoted with reference to the steam flow direction: 1 (base metal 1), 2 (HAZ 1), 3 (weld metal), 4 (HAZ 2) and 5 (base metal 2).

The replica test results of the surface of W1, W2 and W3 are shown in Table 6-1. The highest creep damage, class 3b, was observed in weld W2 at the HAZ of the 12 o´clock position. Class 2a was observed in weld W1 and W3.

Table 6-1: Positions with damage rating on the surface of the welds.

Weld	Clock position	Damage rating					Comment
		1	2	3	4	5	
		BM1	HAZ2	WM	HAZ4	BM2	
W1	3	1	1	1	1	1	
	12	1	1	1	1	2a	Highest damage class was the same in 2014.
W2	3	1	1	1	1	1	
	6	1	1	1	1	1	
	9	1	1	1	1	1	
	12	2b	3b*	2a	1	1	*up to 3000 cavities/mm^2 in fg haz
W3	3	1	2a	2a	2a	1	The number of positions with cavities are more observed at the replica testing 2014
	12	1	1	1	1	1	

* wm = weld metal, cg haz = coarse grained haz and fg haz = fine grained haz

Some damage development has occurred between 2014 and 2017. At weld W1 the highest damage classes were 2a and 2b in 2014 and 2017, respectively.

The creep cavity density in HAZ 2 was measured to 1800 cavities/mm^2 and 3000 cavities/mm^2 in 2014 and 2017, respectively.

At the 3 o´clock position the areas with damage class 2a was observed in both HAZs in 2014 but also in the weld metal after further service to 2017.

Table 6-2 shows the cavity evaluations of the cross-sections of the welds.

Table 6-2: Positions with damage rating on the cross sections of the welds.

Weld	Clock position	Damage rating					Comment
		1	2	3	4	5	
		BM1	HAZ2	WM	HAZ4	BM2	
W1	3	2a	1	1	1	1	
	12	1	1	1	1	1	Cavity class 2a was observed on the surface
W2	3	1	1	1	1	1	
	6	1	1	1	1	1	
	9	1	1	1	1	1	
	12	2b	2b	1	1	1	
W3	3	1	1	1	1	1	
	12	1	1	1	1	1	

The results can be summarised as follows:

- Creep cavities were observed through cross sections and almost through the entire wall thickness in some of them.
- Replication testing of the surface represents the creep damage in the rest of the material. Figures 6-1 to 6-8 show the creep damage distribution in all the metal pieces that were investigated with respect to creep damages. Figures 6-1 to 6-4 show outside surfaces while Figures 6-5 to 6-8 show sections through the thickness.

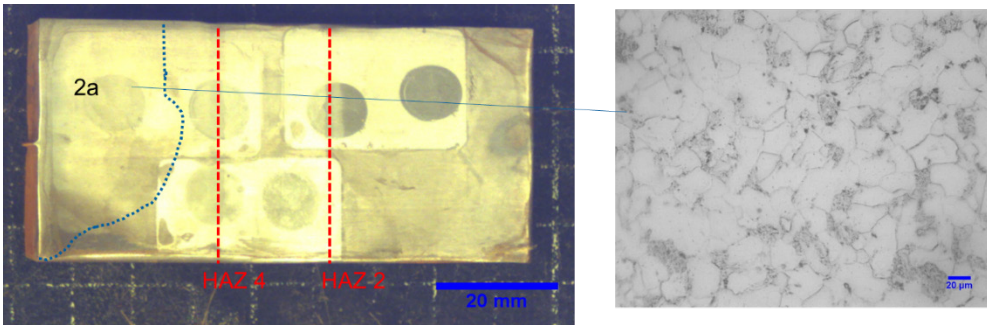

Figure 6-1: Areas with different creep damage classes according to NT TR 302 on the surface of weld W1, clock 12. The surface is etched and the HAZs are marked with red dashed lines on both sides of the weld metal. The blue dashed line shows the creep damage class 2a on the surface.

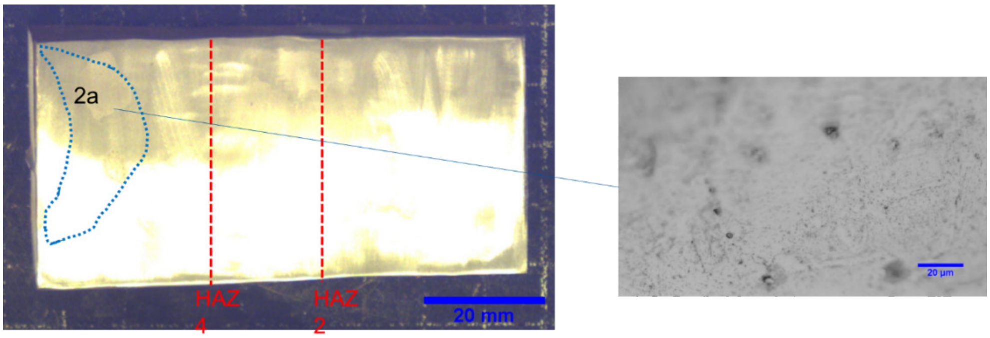

Figure 6-2: Areas with different creep damage classes according to NT TR 302 on the surface of weld W1, clock 6. The surface is etched and the HAZs are marked with red dashed lines on both sides of the weld metal. The blue dashed line shows the creep damage class 2a on the surface.

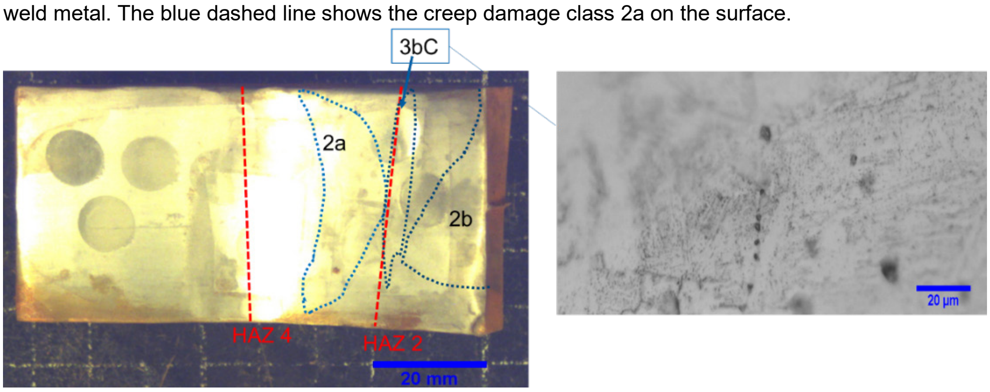

Figure 6-3: Areas with different creep damage classes according to NT TR 302 on the surface of weld W2, clock 12. The surface is etched and the HAZs are marked with red dashed lines on both sides of the weld metal. The blue dashed lines show the creep damage classes. Maximum cavity 3b is observed on the HAZ2.

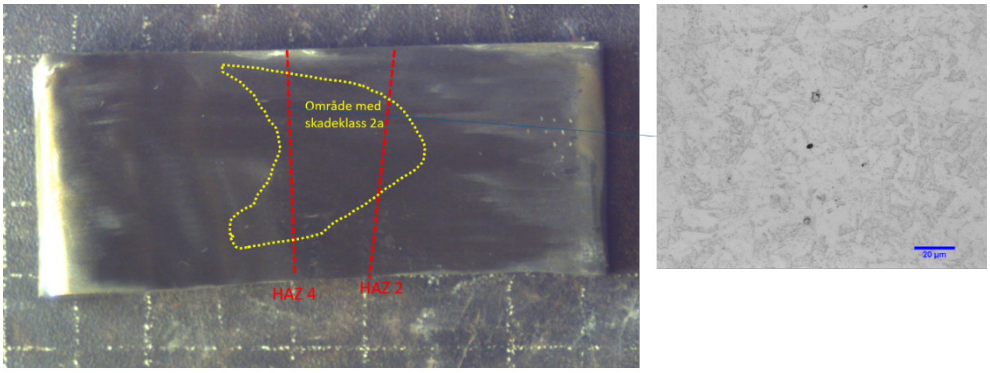

Figure 6-4: Areas with different creep damage classes according to NT TR 302 on the surface of weld W3, clock 3. The surface is etched and the HAZs are marked with red dashed lines on both sides of the weld metal. The yellow dashed line shows the creep damage class 2a on the surface.

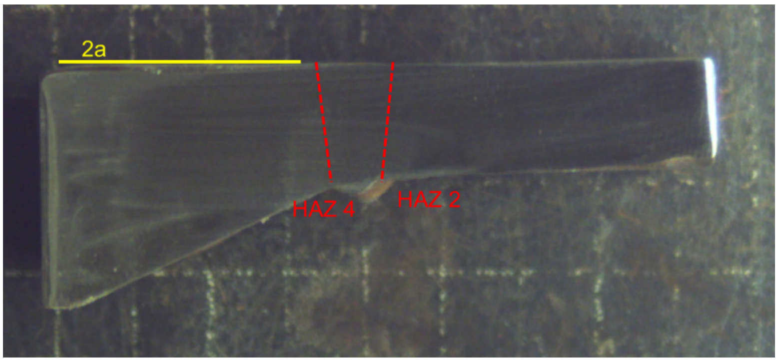

Figure 6-5: Areas with different creep damage classes according to NT TR 302 on the section of weld W1, clock 12. The section is etched and the HAZs are marked with red dashed lines on both sides of the weld metal. The yellow line shows the creep damage classes on the surface. The highest cavity class on the surface is 2a.

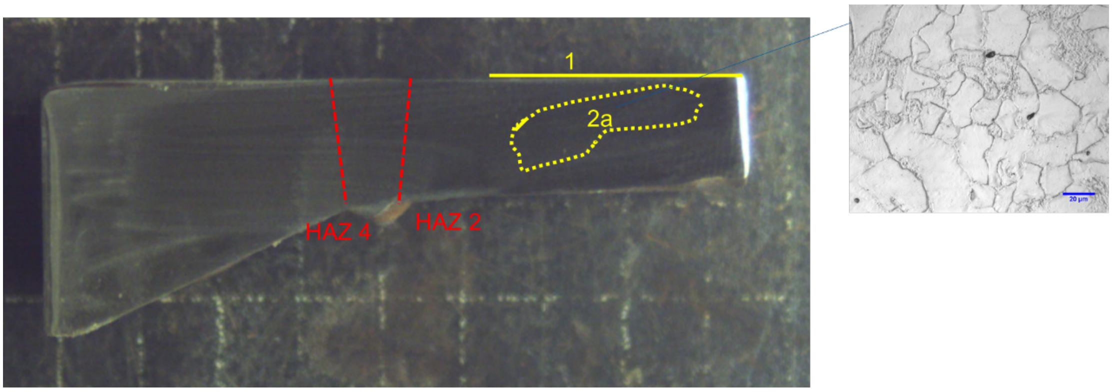

Figure 6-6: Areas with different creep damage classes according to NT TR 302 on the section of weld W1, clock 3. The section is etched and the HAZs are marked with red dashed lines on both sides of the weld metal. The yellow line shows the creep damage classes on the surface and the yellow dashed line shows cavity classes on the section. No cavities were observed on the surface, while the cavity class on the section was 2a.

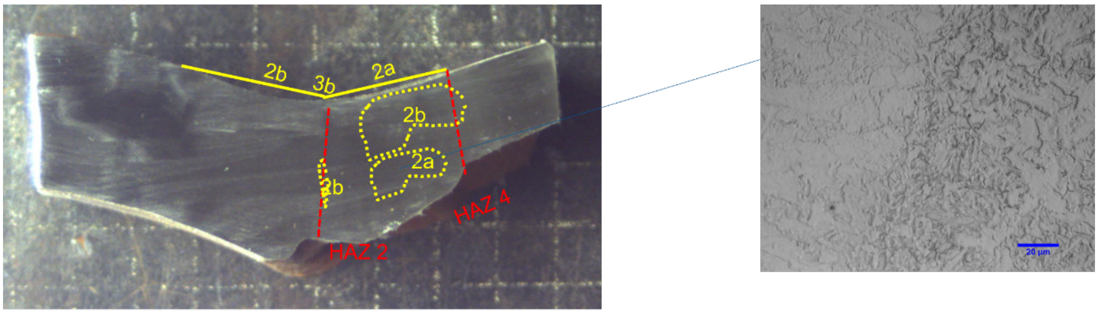

Figure 6-7: Areas with different creep damage classes according to NT TR 302 on the section of weld W2, clock 12. The section is etched and the HAZs are marked with red dashed lines on both sides of the weld metal. The yellow line shows the creep damage classes on the surface and the yellow dashed lines show the cavities on the section. Cavity class was 3b and 2b on the surface and section respectively.

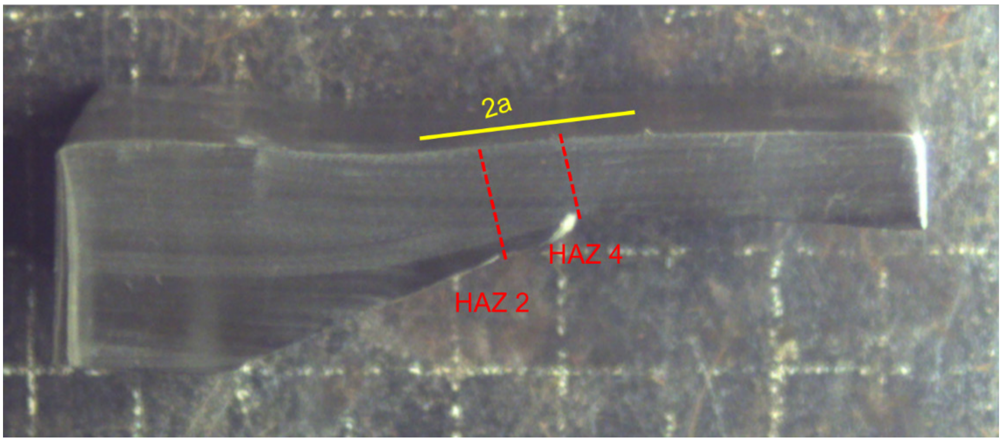

Figure 6-8: Areas with different creep damage classes according to NT TR 302 on the section of weld W3, clock 3. The section is etched and the HAZs are marked with red dashed lines on both sides of the weld metal. The yellow line shows the creep damage classes on the surface. No cavities were observed on the section, while the cavity class on the surface was 2a.

Figure 6-9 shows the equivalent creep strain ε_{eq}^{c} distribution across the weld W2 after 327600 h. Enhanced strains are formed between the 10.30 and 12.00 o´clock positions where the highest strains appear at and near the outside surface. The strains decline to a minimum at about one third of the wall thickness. In comparison, the actual creep damage in the HAZ and the weld metal of this position, Figure 6-7, also declines but can be observed as deep as two thirds of the wall.

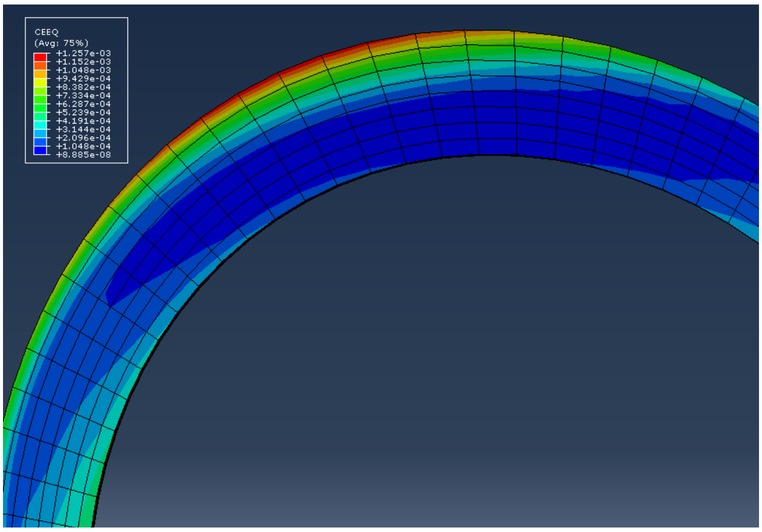

Figure 6-9: Equivalent creep strain ε_{eq}^{c} across weld W2 after 327600 hours of operation. The weld is seen in the flow direction and top of structure corresponds to 12 o'clock. Red colour corresponds to $\varepsilon_{eq}^{c} = 0.126$ %. Material combination 2 in Table 5-8 is used in the simulation.

6.3 CREEP TESTING OF SERVICE EXPOSED MATERIAL

6.3.1 Introduction

The impact of the combination of presence of weldment and elastic follow-up on the useful life of piping systems subjected to low temperature creep (460 °C or lower) is investigated. The work starts out from the power plant in Iggesund where unexpected creep damage has been found in a T-piece weldment. Results from numerical simulations of the whole system and the local weldment, investigation of the microstructure in the damaged T-piece and creep testing of parent and weld metal specimens taken out from the T-piece, form basis for an enhanced understanding.

6.3.2 Material

The pipe from Iggesund was received at the institute after being removed from the plant, see Figure 6-10. Blanks for testing came from the saddle weld, and from the base metal in the smaller connecting pipe. Blanks for specimen manufacture were cut using water jet cutting. Other pieces were at the same time cut from the cardinal point in the weld for creep damage assessment in another part of the project. These positions are marked in Figure 6-11.

Figure 6-10: The material received for the testing. The saddle weld in the T-piece is where the weld specimens came from and the end of the connecting (smaller) pipe is where the base metal specimens came from. The clock positions for the weld specimens is visible on beside the saddle weld, 12 at the top and 9 closest to the camera.

Figure 6-11: The weld in preparation for cutting by water jet. The ellipses are the positions for metallographic studies.

6.3.3 Experimental

Creep testing was conducted in an active creep test rig where the load is measured continuously by a load cell and fed back to the step motor controlling the load. This setup can conduct testing at an accuracy of +/- 3 N. The testing was performed according to SS-EN ISO 204:2018 [13]. Temperature was measured using three type S thermocouples along the gauge length of the specimen. The middle thermocouple was used to control the furnace and the two outer ones were used to keep the axial thermal gradient less than +/- 1 °C.

The base metal specimens were named as they were started (Insp2-R1 to Insp2-R5). The weld specimens were named after the clock position they were taken from. Insp2-3 was taken from the material between clock position 12 and 3. Insp2-3x between clock positions 3 and 6. Insp2-6 was taken from the material between clock positions 9 and 6. Finally Insp2-9 was taken from the material between clock positions 9 and 12.

6.3.4 Results

Creep testing

The results from the creep testing are given in Table 6-3. The same information is given in graphical form in Figure 6-12 and Figure 6-13. One of the base metal specimens failed during loading. Of the other four, one was still running at the end of the project and it was interrupted. Two of the four weld metal specimens ruptured and two were interrupted. For all the interrupted specimens the minimum creep rate was estimated at the time of interruption.

The Norton exponent in equation (5-1) has been calculated for both material conditions. The results have been included in Figure 6-14 and Table 6-3. The high Norton exponents, 31 and 49 respectively, show that the materials at these stresses and this temperature are well within the power-law breakdown area. The creep curves for all specimens are given in Figures 6-15 and 6-16.

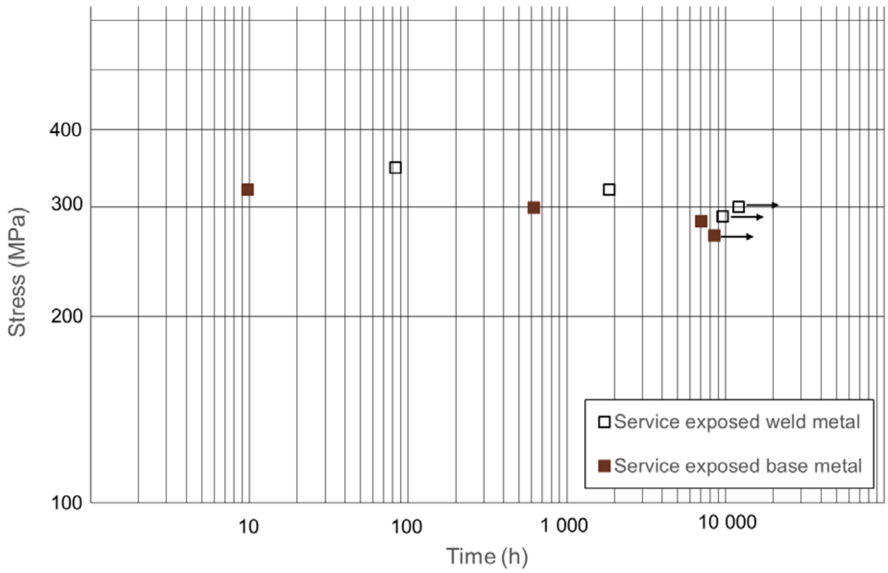

Figure 6-12: Time to rupture given against applied stress. Arrows denote interrupted specimens.

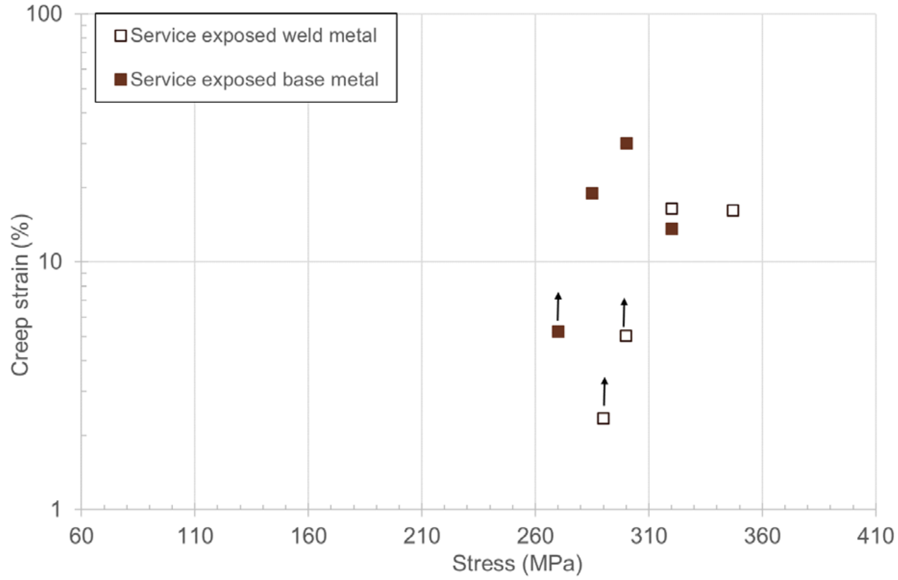

Figure 6-13: Creep elongation given against applied stress.

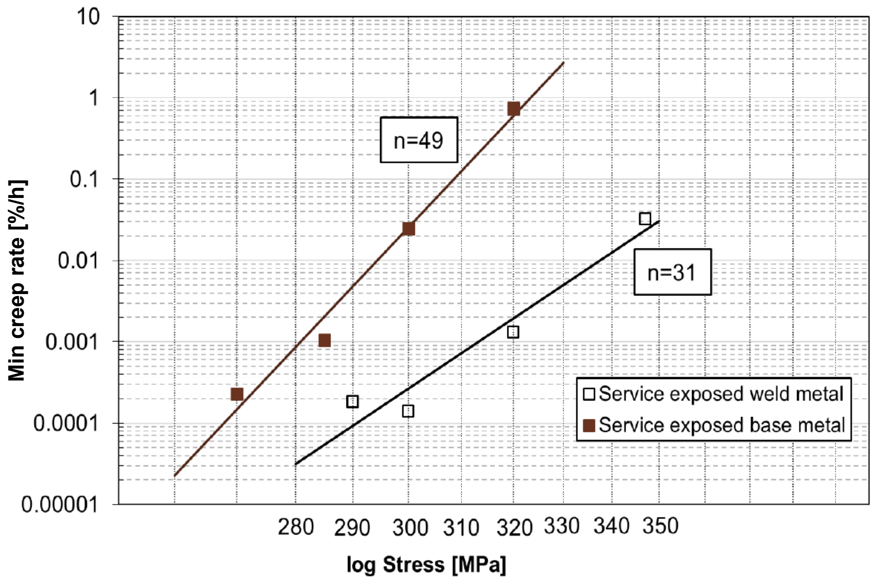

Figure 6-14: Minimum creep strain rate versus stress.

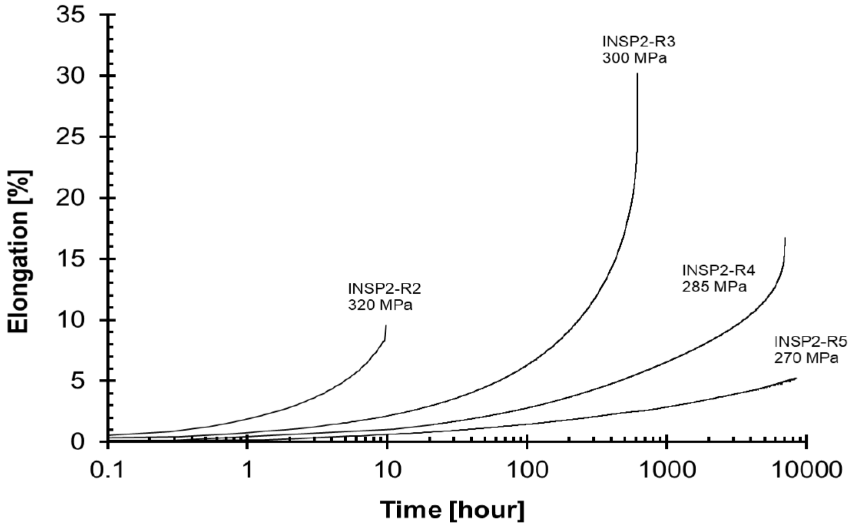

Figure 6-15: Creep curves for the service exposed base metal.

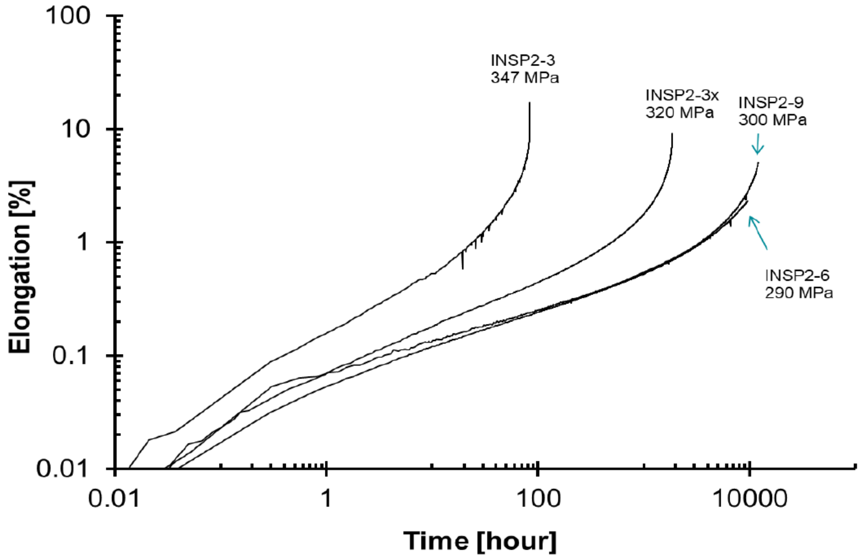

Figure 6-16: Creep curves for service exposed weld metal.

Table 6-3: Test matrix and results. Test temperature is 460 °C.

ID nr	Material	Temp (°C)	Stress (MPa)	Creep time (h)	Loading strain (%)	Creep elongation (%)	Area red (%)	Total strain (%)	Min creep rate* (%/h)	Norton exponent	Ruptured
INSP2-3	Service exposed weld metal	460	347	83	1.21	16.1	69.7	17.3	0.03242	31	Ruptured
INSP2-3x		460	320	1 846	1.24	16.4	67.1	17.6	0.00132		Ruptured
INSP2-9		460	300	12 087	1.43	5.0		6.5	0.00014		Interrupted
INSP2-6		460	290	9 594	0.48	2.3		2.8	0.00018		Interrupted
INSP2-R1	Service exposed base metal	460	347	0	16.80	-		-	-	49	Ruptured
INSP2-R2		460	320	10	3.90	13.6	77.9	17.5	0.74400		Ruptured
INSP2-R3		460	300	619	2.06	30.2	69	32.3	0.02465		Ruptured
INSP2-R4		460	285	7 016	1.14	19.0	33.5	20.1	0.00106		Ruptured
INSP2-R5		460	270	8 489	1.40	5.3	69.7	6.7	0.00023		Interrupted

* Minimum creep rate estimated for the interrupted specimens.

Minimum creep strain rate as a function of stress is shown in Figure 6-17 for service exposed base and weld metal. Data according to DIN EN 100028-2 is included for comparison. The minimum creep strain rate for the base metal is higher than that of the weld metal. The Norton creep exponent for the two materials is 49 and 31, respectively. This can be compared to the creep exponent for virgin base metal which is 8.17 according to DIN EN 100028-2. The magnitude of the creep exponents indicates that power law break-down prevails. One important result is however that the base metal shows a more creep soft characteristics (higher minimum creep rate) than the weld metal. However, at lower stresses the opposite can prevail, see further in the discussion section below.

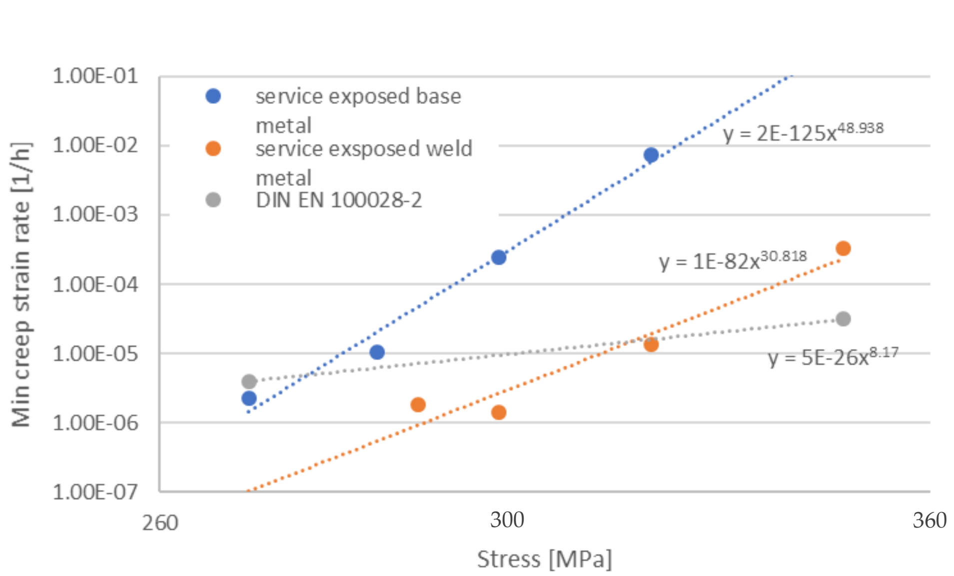

Figure 6-17: Minimum creep strain rate of service exposed base and weld metal. Virgin base metal data according to DIN EN 100028-2 is included for comparison.

Post-test metallography

After the testing was completed selected specimens were cut up and mounted to facilitate the metallographic studies. The selected specimens were all weld specimens and one of the base metal specimens with the longest creep test time. For the ruptured specimens three areas were studied. An area directly adjacent to the rupture, an area far from the rupture but still inside the gauge length and an area of unstressed material in the threaded head of the specimens were investigated. For the unbroken specimens only an area in the middle of the gauge length was studied.

The creep damage was classified according to the guidelines in Nordtest NT TR 302 [11]. The assessment of the studied specimens can be found in Table 6-4. All observed damage was of the classes 2a or 2b. No damage was assessed to classes 3, 4 or 5 (strings of cavities, microcracks and macrocracks, respectively).

As can be seen in Table 6-4, all weld specimens contain cavities to class 2a or 2b with a predominance for the latter. It is also evident that this creep damage was present in the material before testing since the same amount of damage is present in the unstressed head of the specimens. The service exposed base metal does not contain any visible creep damage, either before or after testing. Micrographs of the test specimen microstructures and creep damages are shown in Appendix 2.

Table 6-4: Assessed creep damage in the studied specimens according to Nordtest NT TR 302 [11].

Specimen	Position in component	Head of specimen	Middle of gauge length	Gauge length close to fracture
INSP2-3	Service exposed weld metal between positions 12 and 3	2b	*	2b
INSP2-3x	Service exposed weld metal between positions 3 and 6	2b	*	2b
INSP2-6	Service exposed weld metal between positions 6 and 9	*	*	2a or 2b
INSP2-9	Service exposed weld metal between positions 9 and 12	*	*	2b
INSP2-R4	Service exposed base	0 or 1	0 or 1	0 or 1

* Position not studied or not available

7 Discussion

The aim with this project is to investigate if a combination of elastic follow-up and varying creep properties across a weldment can explain creep damage found in a specific piping system operating at 460 °C. After 300000 hours of operation both the weld metal and HAZ in a T-piece junction weldment unexpectedly showed severe creep damage. The stresses in the investigated piping system is in the range of 60-80 MPa and the material used in the system is 13CrMo4-5 or equivalent. With this material and a uniaxial stress state at 80 MPa not more than 0.0019 % creep strain should develop after 100000 hours. Thus, problems with creep damage should not be expected.

The reason why elastic follow-up is of interest here is the relatively low operating temperature of 460 °C. At this temperature, relaxation of the piping system goes slow and deformation-controlled system forces and moments can be maintained over long periods. In combination with a weak cross section, creep damage can be accumulated locally.

In general, weldments are weak sections in piping systems subjected to creep. This emanates from creep properties, i.e. deformation rates and creep rupture data, that vary across the weldment. Varying deformation rates between weldment constituents result in local stress concentrations in the weldment. In addition, variation in deformation rate results in varying degree of constraint in the multiaxial stress space which in turn influences creep ductility of the material. The higher the degree of constraint, the higher the triaxiality and the lower the creep ductility. Finally, creep rupture data varies across the weldment. The complexity of the weldment system is obvious. Now, a bad combination of these parameters might result in low creep strength and early development of creep damage within the weldment.

Creep testing of a steel material is normally conducted under uniaxial stress state conditions. The elongation at rupture gives the creep ductility of the material. In general, creep ductility is reduced with decreasing stress level and increasing creep rupture time. For a multiaxial stress state, the degree of constraint increases. This also reduces creep ductility. Thus, how much creep strain that is developed at rupture for a specific material and temperature depends on stress level and degree of constraint. Creep rupture strain at lower stresses (i.e. longer creep rupture times) in combination with higher degree of constraint can be well below 1 % [14].

Numerical simulations can be used for a better understanding of how creep develops in a piping system over time. The FE-model used in this project is built by special pipe element in ABAQUS called ELBOW31. This element is very powerful and gives the possibility to capture creep deformation properly, both in straight pipes and bends. In order to predict the effect of mis-match of creep deformation properties in weld W2, a solid model of the T-piece with the weld W2 is implemented into the piping model. In the simulation, a visco-elastic material model is applied, and calculated creep strains are used to evaluate the degree of creep damage. No rupture criterion is implemented into the FE-code. Dead weight, internal pressure and thermal expansion are considered loads in the analysis.

Modelling the piping system with ABAQUS ELBOW31 element and solid modelling of the T-piece is time consuming. A specific pre-processor for modelling piping systems with ELBOW31 element would have been beneficial.

Creep simulations of the investigated piping system show that the elastic follow-up phenomenon is present. Relaxation of deformation-controlled system forces and moments takes a considerable amount of time. After 100000, 200000 and 327600 hours of operation the relaxation is about 19 %, 26 % and 29 %, respectively.

The combination of creep deformation properties across the weld W2 influences accumulation of creep damage in the weldment. Nine different combinations of base material, weld material and HAZ are investigated. The base material properties are kept the same in all simulations. Reference case is that where base material is used for all weldment constituents. For the reference case, maximum equivalent creep strain accumulated in weld W2 after 327600 hours of operation is 0.079 %. Increased creep deformation rates for the weld material and HAZ increase the creep strain developed in the weldment. With hundred times higher creep strain rate for the weld material and HAZ, accumulated equivalent creep strain in the weldment increases to 0.210 %. The triaxial stress state and increased degree of constraint in the weld region explains why not more creep strain develops.

Non-functioning supports can locally increase accumulation of creep strain in a piping system. This effect is investigated where different combinations of supports, in the vicinity of weld W2, are removed from the piping model. For the eight cases analysed, equivalent creep strain in weld W2 increased with about 44 % at the most compared to that for the case with functioning hangers. In these simulations, creep deformation rate for the weld material was ten times higher than that of the base material.

It is unclear what happened in the piping system during the temporary temperature rise to 620 ^{o}C. At this temperature, plastic deformation also can take place besides creep. In combination with the elastic follow-up phenomenon with maintained system forces and moments, one result might be that inelastic strains (plastic+creep) were particularly accumulated in weld W2. The lack of information from the incident, however, makes it impossible to predict the piping system response during this temperature rise.

A combination of the effects of elastic follow-up, varying creep deformation properties across weld W2, a non-functioning support and the temporary temperature rise to 620 ^{o}C could result in an accumulated creep strain of about 0.3 % in weld W2. Considering an operation time of more than 300000 hours and a high degree of constraint in certain parts of the weldment, it is concluded that 0.3 % creep strain may be enough to cause severe creep damage to develop.

Part of the project has been experimental. The microstructure of welds W1, W2 and W3 has been investigated. Service-exposed material from the base and weld metal from weld W3 have been creep tested.

The observed creep damage at on-site replica testing was verified by the metallographic studies. The amount of damage observed at the outer surface agreed well with previous replica test results and a slight damage development occurred between 2014 and 2017.

Comparisons between strain distributions in the T-piece welds and the simulated distributions by the analyses can be done for W2 and W3. In the weld metal and in HAZ2, the creep damage declines from the outside towards the inside at 12 o´clock. This agrees with the numerical result. The depth of creep damage is deeper than for the analysis and the amount of creep damage typically corresponds to higher strain levels than a few tenths of a percent. However, as described above, the creep ductility at the present stress state and very long service time, although unknown, can be significantly lower than a few percent. A stress concentration is typically associated with ductility reduction, as observed in the W2 at 12 o´clock where a HAZ and a saddle point position, both considered as stress concentrations, coincide. On the other hand, creep cavitation was also observed over relatively large volumes in the base metal at some positions. The elastic follow-up phenomenon can be associated with such creep damage in a weaker part as observed in the thinner section W1, 6 o´clock, Figure 6-6. However, the opposite was observed at W1 at 12 o´clock with quite significant creep damage in the thicker part of the section, Figure 6-6.

Creep test results show different characteristics for the service-exposed base and weld material. At the stresses tested, the creep strength of the weld material is higher than that of the base material. However, at stresses corresponding to piping system stresses, i.e. 60-80 MPa, the creep strength of the base material might be the highest. The creep tests also show higher creep rates for the base material than for the weld material. The opposite might prevail at lower stresses. The creep exponent is high for both materials, 49 for the base material and 31 for the weld material. In summary, input to the numerical simulations is that creep deformation properties of the base material and the weld material differ.

8 Conclusions

8.1 NUMERICAL SIMULATIONS

Numerical simulations show the possibility for severe creep damage to develop in the T-piece junction weld W2. The reasons are as follows:

- The effect of elastic follow-up maintains the deformation-controlled system forces and moments for a longer period during operation.
- An operation time of more than 300000 hours is considered as long. One effect of long creep duration is that creep ductility is reduced.
- Differences in creep deformation properties across the weldment result locally in both stress concentrations and a higher degree of constraint. The latter reduces creep ductility.
- Non-functioning supports in the vicinity of weld W2 might have increased the stresses in the T-piece junction weld.
- The temporary temperature rise to 620 ^{o}C might have increased the development of inelastic strain (plastic+creep) in the weldment region of weld W2.

Considering all these factors, it should be possible for sever creep damage to develop in weld W2 even though predicted creep strains do not exceed 0.3 %.

8.2 EXPERIMENTAL

From the metallographic investigation of selected positions of the T-piece welds the following conclusions can be drawn:

- The observed creep damage at on-site replica testing was verified by the metallographic studies. The amount of damage observed at the outer surface agreed well with previous replica test results and a slight damage development occurred between 2014 and 2017.
- At some positions significant creep damage was formed through the wall and creep cavities were observed almost through the entire wall thickness.
- The creep damage distributions agreed fairly well with analysis results at the 12 o´clock position of W2.

Creep tests of base and weld material from the studied T-piece were conducted with purpose to reach the secondary creep region within 100-10 000 hours for material. The results showed that:

- Relatively high stresses compared to service stresses were required to get into the secondary creep, not only for the short term but also for the long-term testing.
- Higher creep rates were obtained for the base metal than for the weld metal. However, the results indicate the opposite relationship at service stress.
- The creep tested weld metal from W2 contained creep cavities before the tests. The amount of cavitation did not increase during the tests.

9 Recommendations

In order to avoid unexpected creep damage to develop in power plants subjected to low-temperature creep, the following is recommended:

- Avoid placing welds in high-stressed regions of the piping system, e.g. in T-piece junctions between run pipe and branch pipe.
- Use weld deposit material with creep characteristics which match that of the base material.
- Regularly perform in-service inspections of high-stressed weldments and bends with replica testing. At start of operation, elastic stress analyses should be used to determine locations to inspect. When the piping system has started to relax, creep analyses should be used instead. The time interval between inspections should decrease with time of operation.
- Regularly inspect the function of hangers and supports.
- Continuously monitor operating temperature of the power plant at different locations. A position close to the boiler should be one of the locations.

10 References

[1] J. Storesund et.al. Oväntade krypskador och/eller haverier orsakade av krypning under gränstemperaturen. Värmeforsk rapport 978, Stockholm Juli 2006.

[2] R. Wu, J. Storesund and T. Bolinder. Creep crack growth in service-exposed 13 CrMo 4 4 weld joints below
limit temperature for creep , Värmeforsk rapport 1207, Stockholm, januari 2012.

[3] British Energy Generation Ltd., Assessment Procedure for the High Temperature Response of Structures,
R5, Issue 3, (2003)

[4] R.A. Ainsworth. Consideration of elastic follow-up in the treatment of combined primary and secondary
stresses in fracture assessments. Engineering Fracture Mechanics, Vol. 96, 2012, pp. 558–569.

[5] SS-EN 13480-3:17, Metallic industrial piping. Part 3: Design and calculation.

[6] Dassault Systémes, 2014. Abaqus Analysis User's Manual Volume I-V, Version 6.14, Abaqus INC.

[7] CAEPIPE, Pipe Stress Analysis Software, Version 7.30.

[8] 1002239-1, rev 1. Replikprovning 2014 - Iggesund Paperboard AB. Inspecta Technology, 2014-07-01.

[9] 1007565-104-1, rev 0. Replikprovning 2015 - Iggesund Paperboard AB. Inspecta Technology, 2016-01-26.

[10] DIN EN 100028-2, Flacherzeugnisse aus Druckbehälterstählen,
Teil 2: Unlegierte und legierte Stähle mit festgelegten Eigenschaften bei erhöhten Temperaturen.

[11] P Auerkari et al. Nordtest Report TR 302, Espoo 1996.

[12] Nordtest method NT NDT 010.

[13] SS-EN ISO 204:2018.

[14] S Holdsworth. Crepp-Ductility of High Temperature Steels: A Review; Metals, March 2019.

Appendix 1: ABAQUS piping model

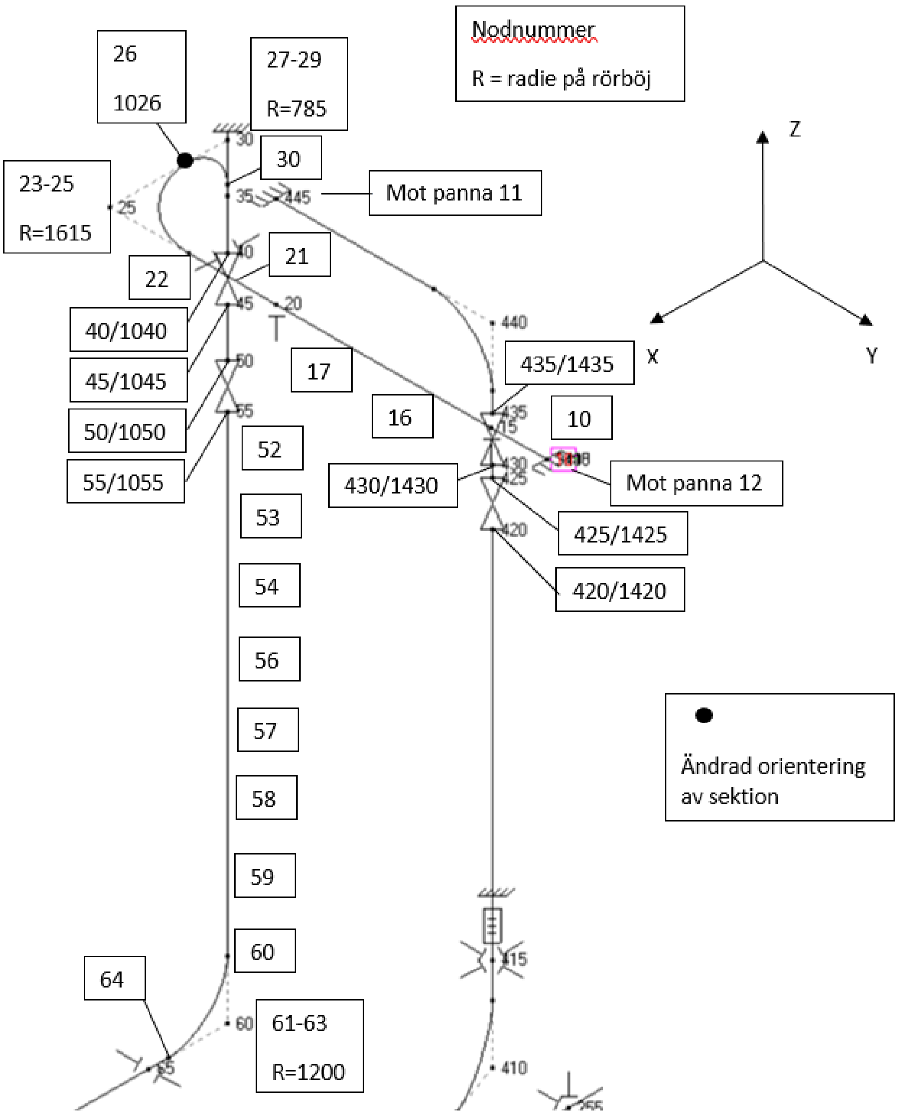

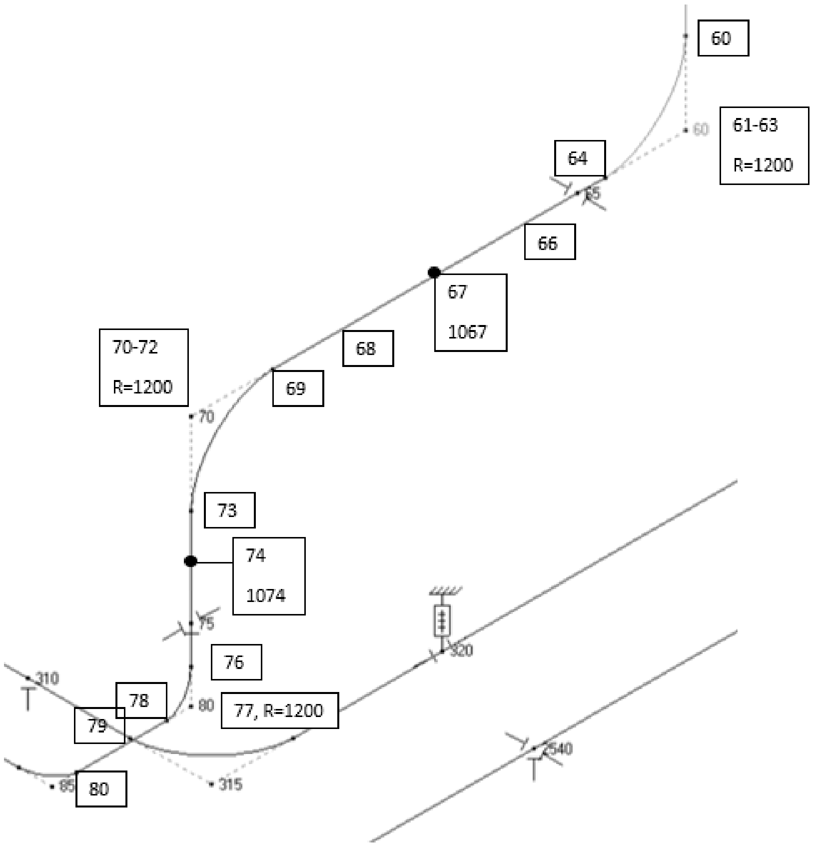
60
61-63
R=1200
64
66
67
1067
68
69
70-72
R=1200
73
74
1074
76
78
79
77, R=1200
80

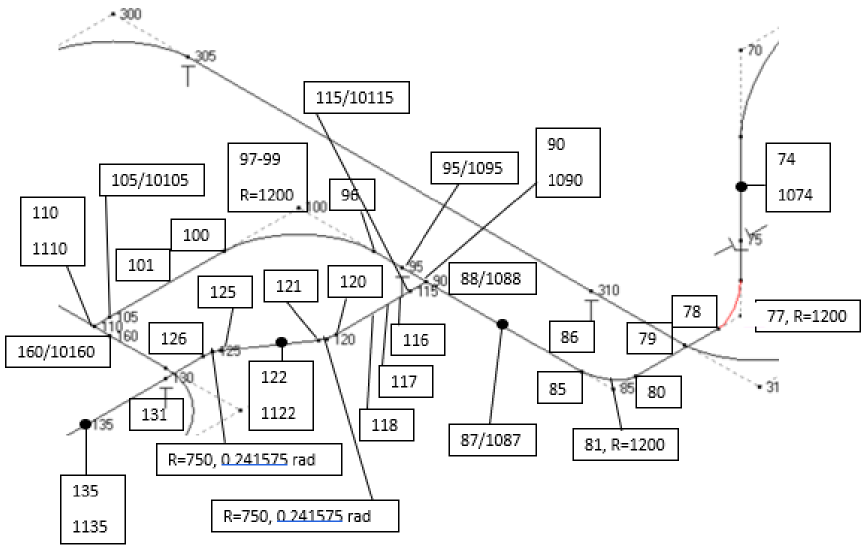
115/10115
90
1090
95/1095
97-99
R=1200
98
105/10105
110
1110
100
101
74
1074
125
121
120
88/1088
78
77, R=1200
160/10160
126
116
86
79
122
1122
117
85
80
131
118
87/1087
81, R=1200
R=750, 0.241575 rad
135
1135
R=750, 0.241575 rad

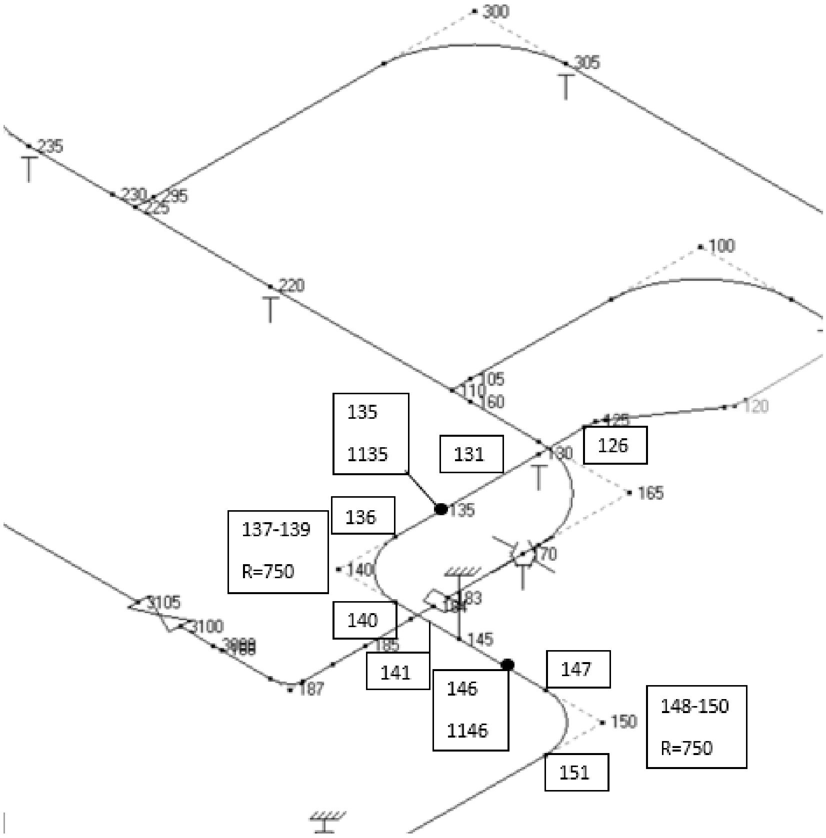
300
305
235
230
295
225
220
100
105
110
160
120
125
135
1135
131
126
130
165
135
136
137-139
R=750
140
170
183
184
3105
3100
140
185
145
141
146
1146
147
148-150
R=750
150
187
151

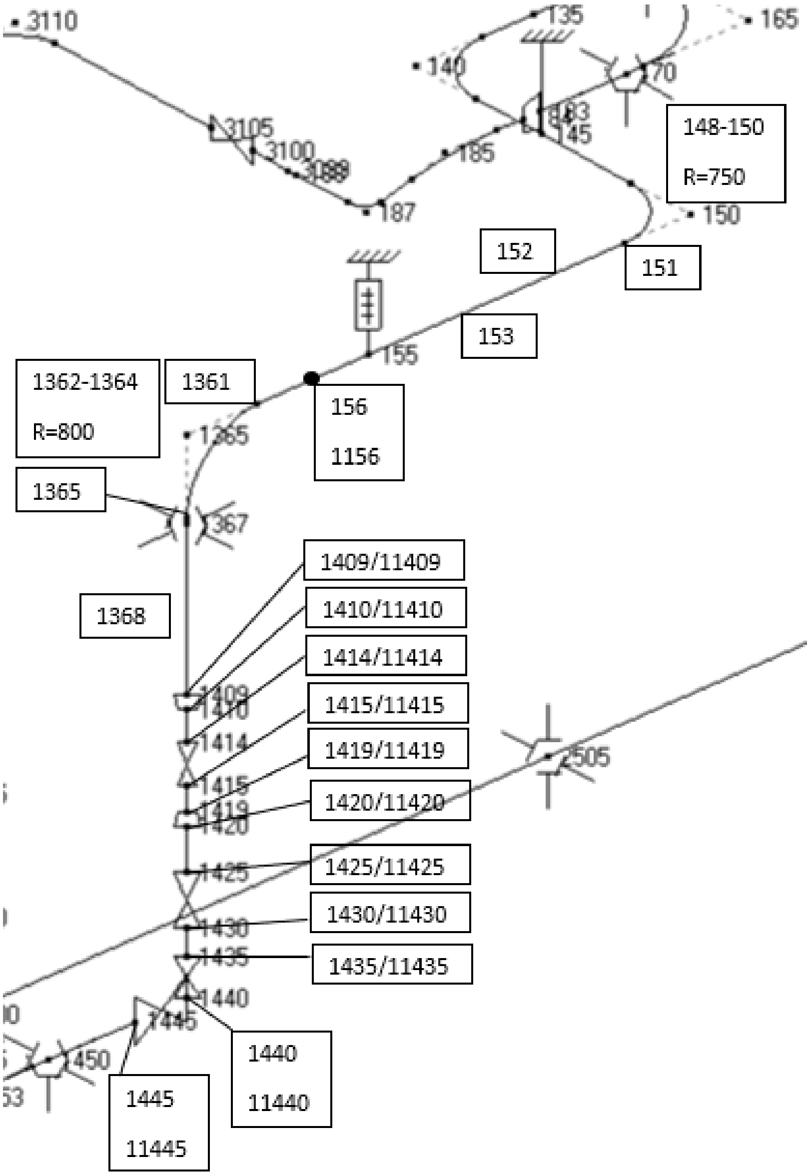
3110
135
165
140
170
3105
3100
3088
185
183
145
148-150
R=750
187
150
152
151
153
155
1362-1364
R=800
1361
156
1156
1365
1365
1367
1409/11409
1410/11410
1368
1414/11414
1415/11415
1419/11419
505
1420/11420
1425/11425
1430/11430
1435/11435
1440
1445
1450
1440
11440
1445
11445

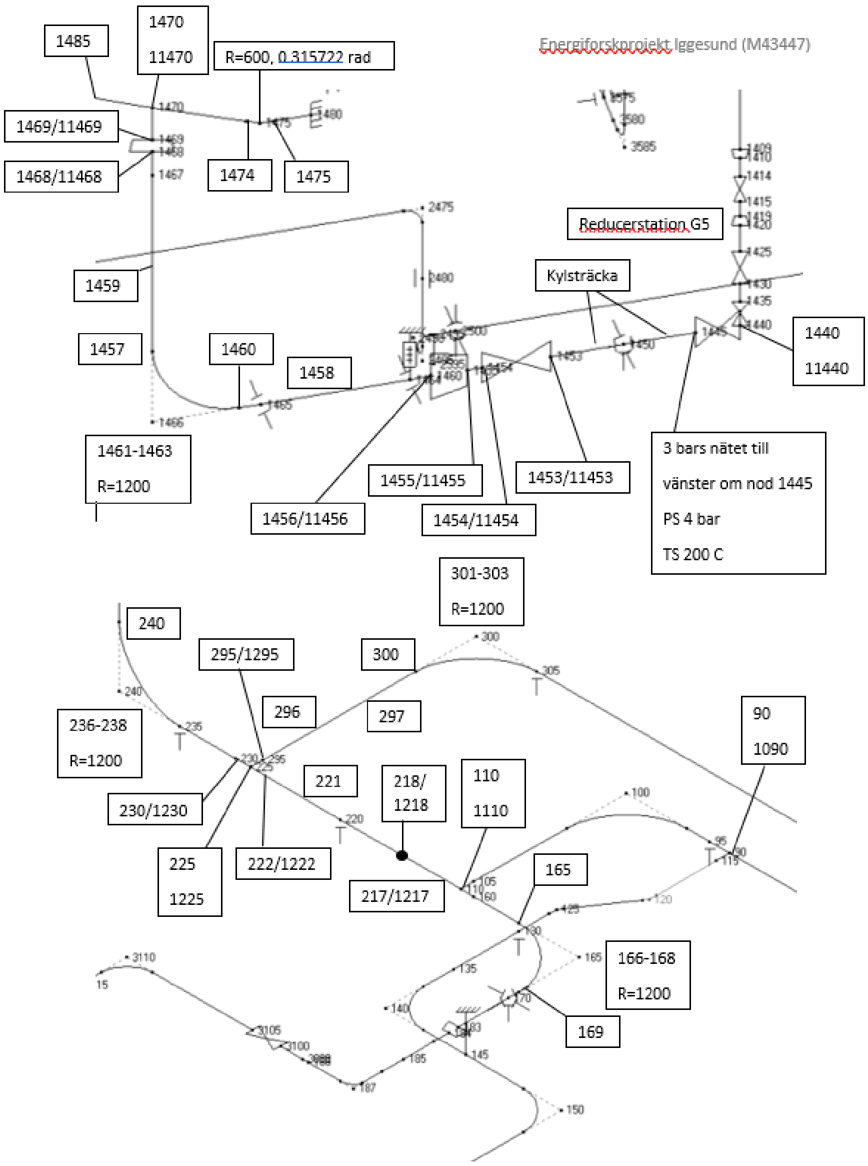

Energiforsk

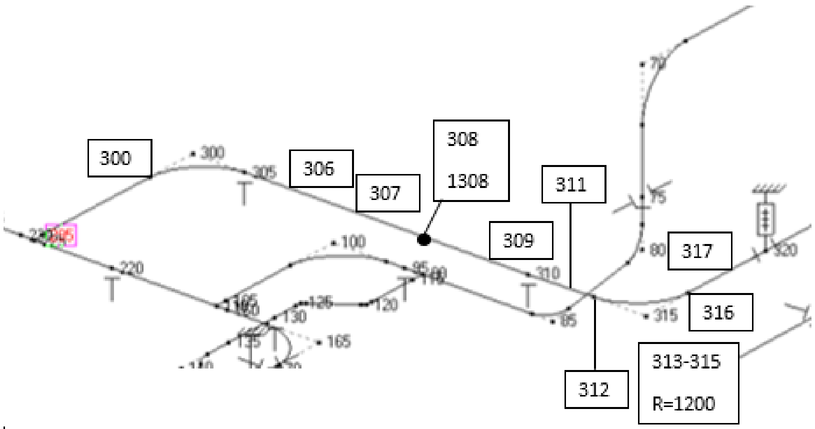
300
306
307
308
1308
311
309
317
316
313-315
R=1200
312

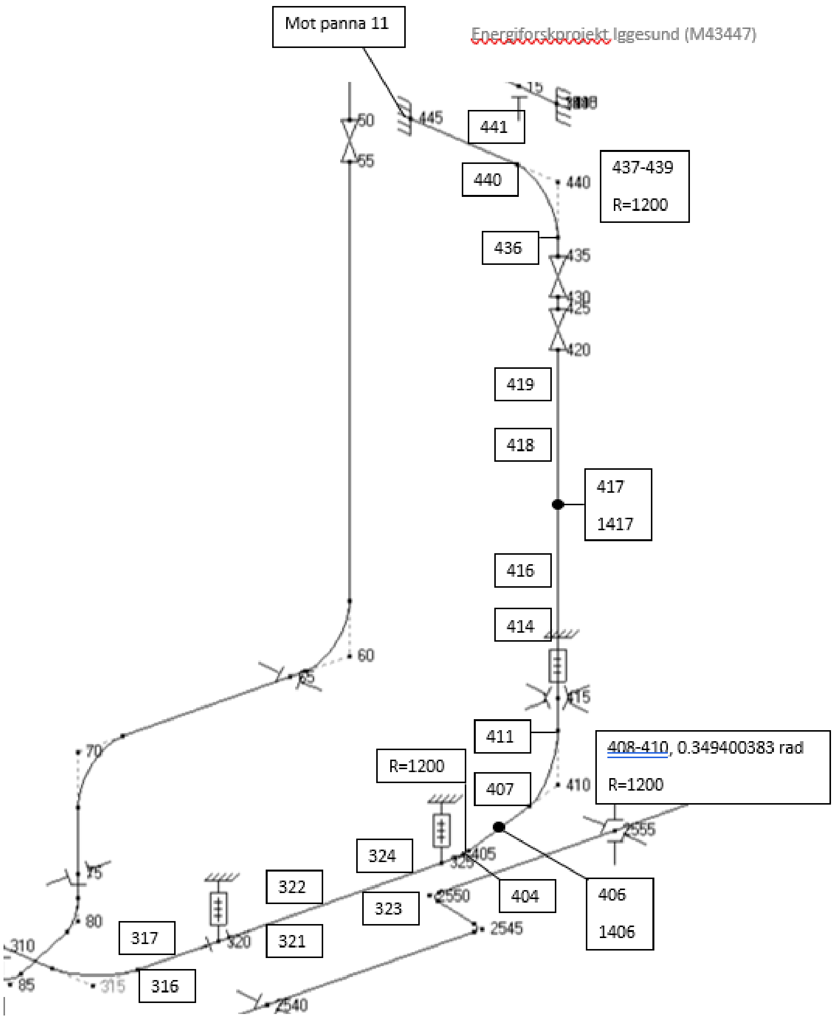
Mot panna 11
Energiforskprojekt Iggesund (M43447)
441
440
437-439
R=1200
436
419
418
417
1417
416
414
411
R=1200
407
408-410, 0.349400383 rad
R=1200
324
322
323
404
406
1406
321
317
316

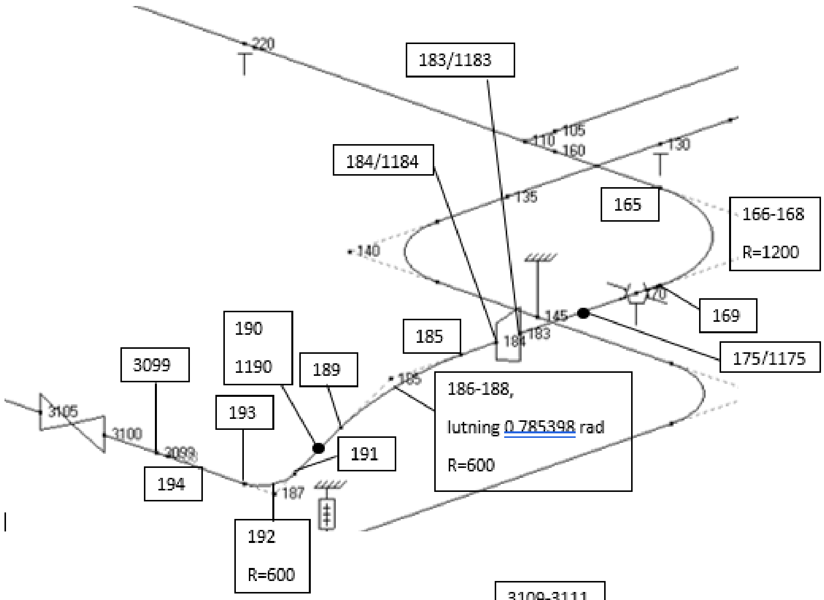
183/1183
184/1184
165
166-168
R=1200
169
175/1175
185
186-188,
lutning 0.785398 rad
R=600
190
1190
189
3099
193
191
194
192
R=600

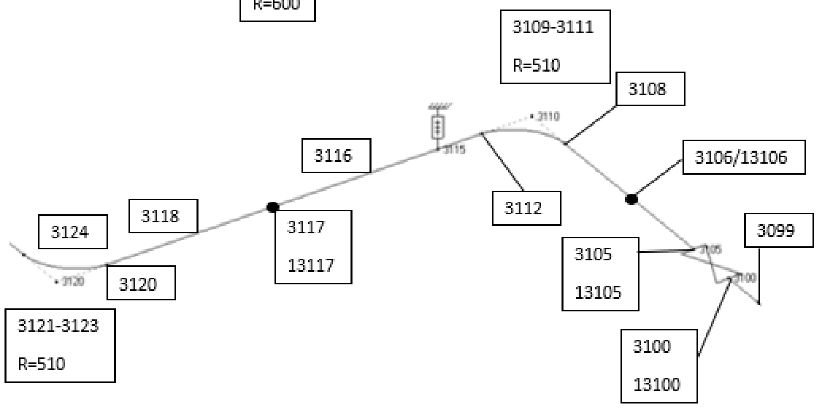
3109-3111
R=510
3108
3116
3106/13106
3112
3118
3124
3117
13117
3099
3105
13105
3120
3121-3123
R=510
3100
13100

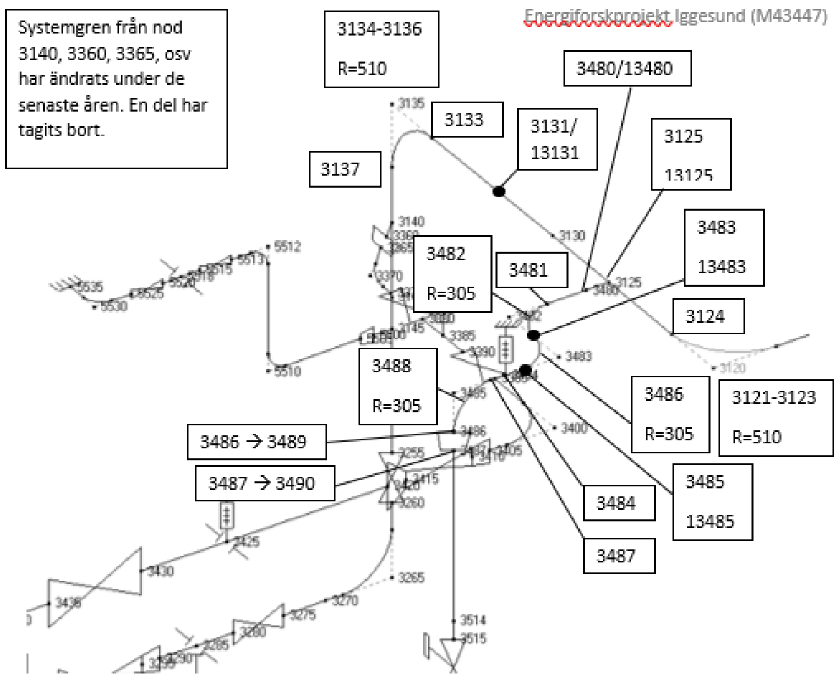
Systemgren från nod 3140, 3360, 3365, osv har ändrats under de senaste åren. En del har tagits bort.
3134-3136
R=510
Energiforskprojekt Iggesund (M43447)
3480/13480
3133
3131/
13131
3125
13125
3137
3483
13483
3482
R=305
3481
3124
3488
R=305
3486
R=305
3121-3123
R=510
3486 → 3489
3487 → 3490
3485
13485
3484
3487

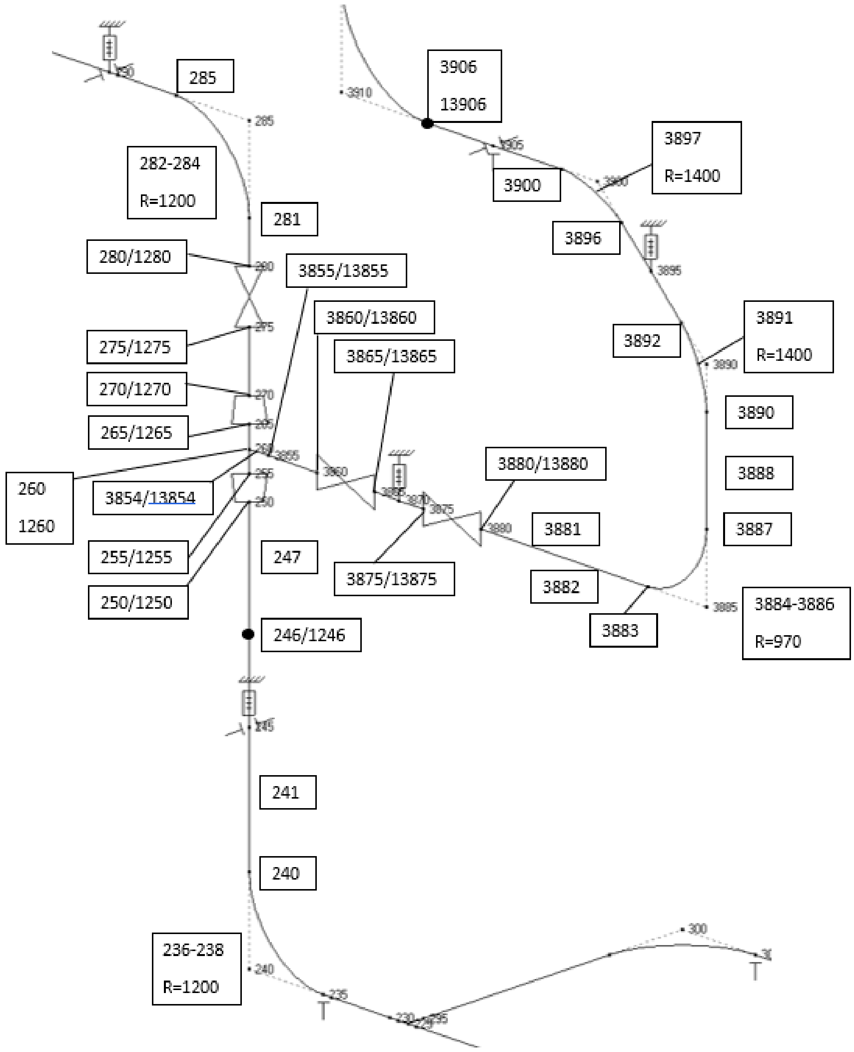
285
282-284
R=1200
281
280/1280
275/1275
270/1270
265/1265
260
1260
3854/13854
255/1255
250/1250
247
246/1246
241
240
236-238
R=1200
3855/13855
3860/13860
3865/13865
3875/13875
3880/13880
3881
3882
3883
3906
13906
3900
3897
R=1400
3896
3892
3891
R=1400
3890
3888
3887
3884-3886
R=970

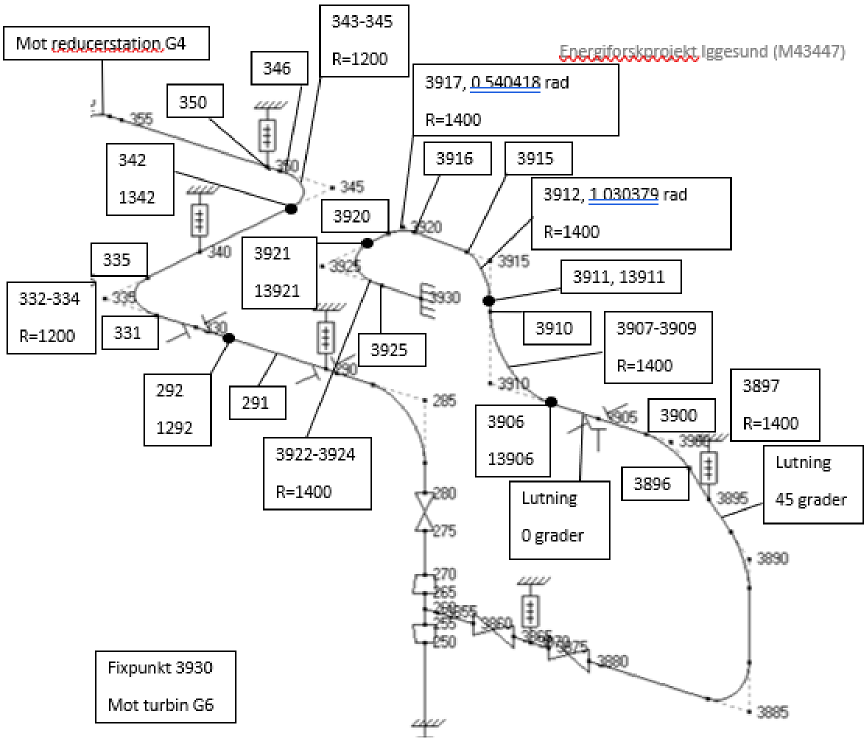

Systemgrenen mot turbin G6 mellan nod 260 och nod 3930 installerades 2011.

Hängarna i det ursprungliga systemet ändrades inte vid installationen.

Appendix 2 Micrographs of creep tested specimens

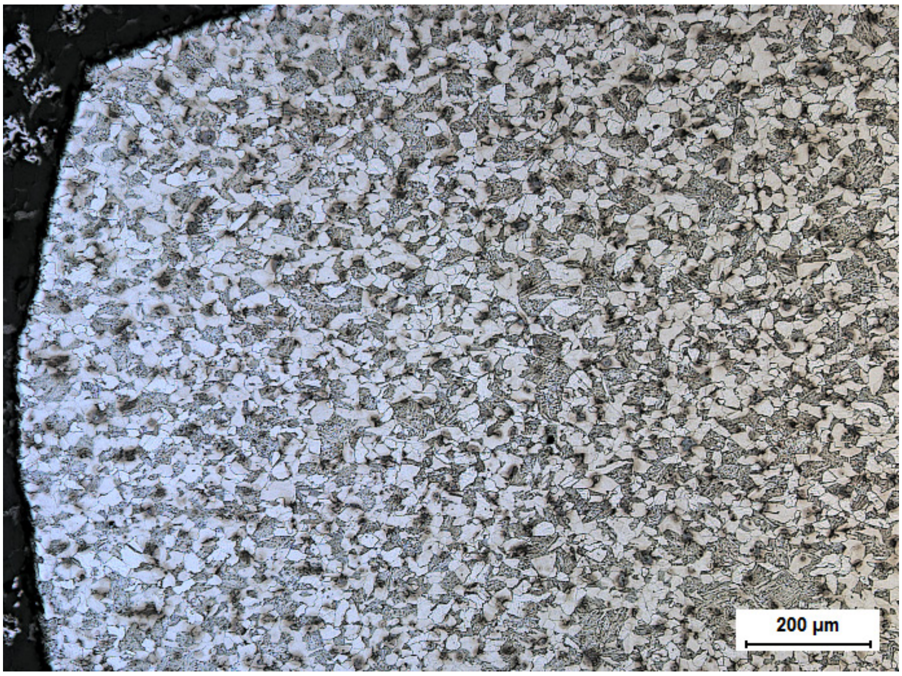

INSP2-R4 close to fracture. 50x.

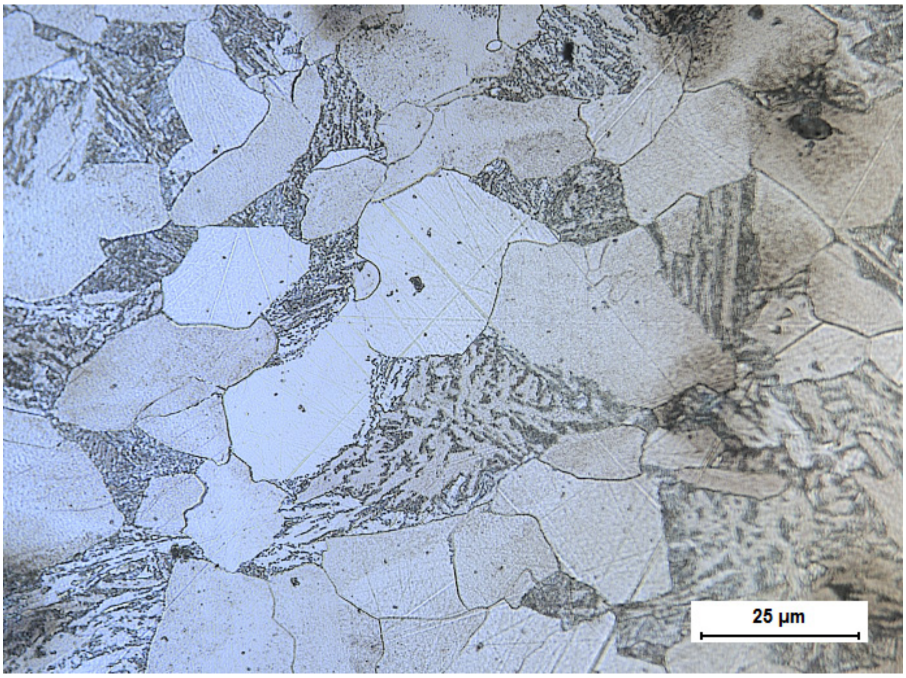

INSP2-R4 close to fracture. No visible cavitation. 500x.

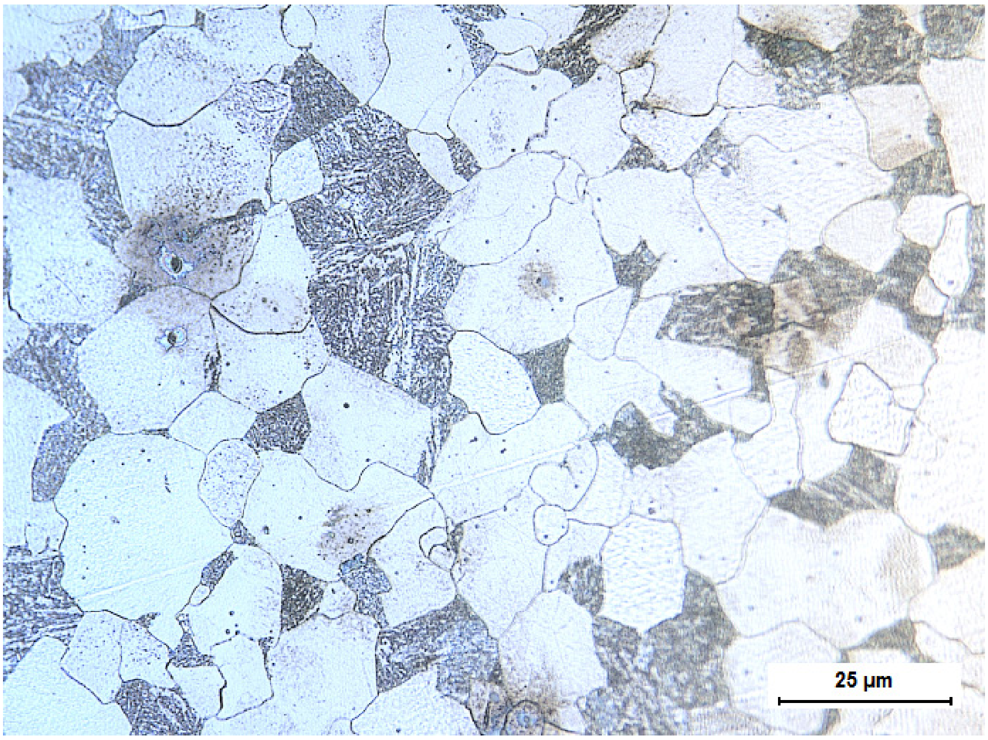

INSP2-R4 head of specimen. No visible cavitation. 500x.

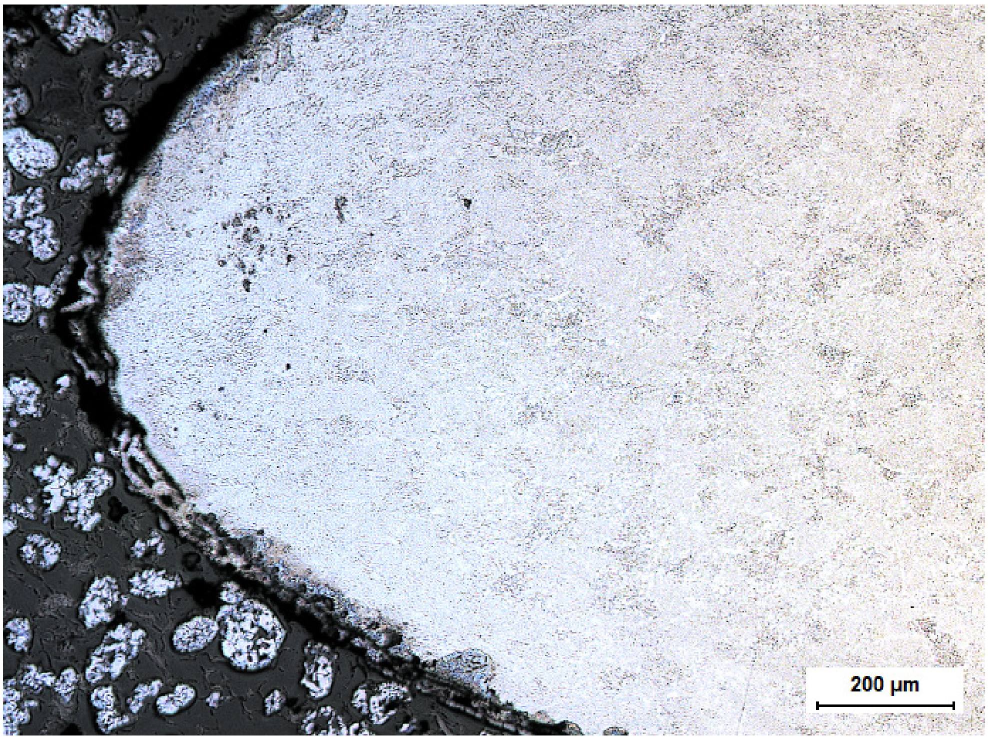

INSP2-3x close to fracture 50x.

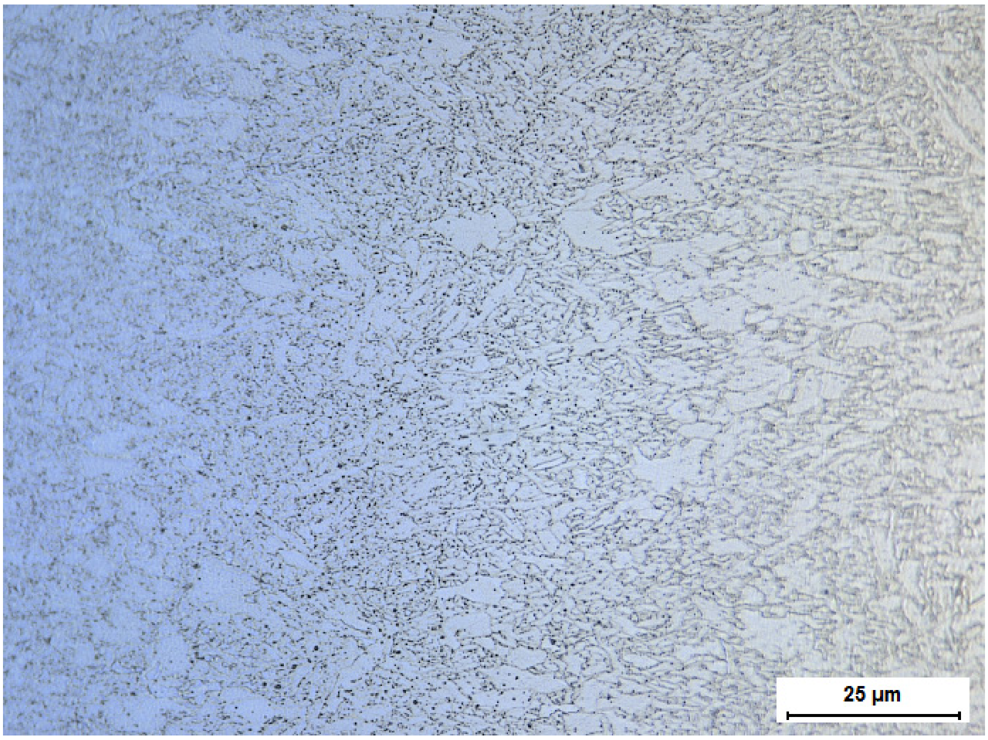

INSP2-3x close to fracture 500x. Damage class 2b.

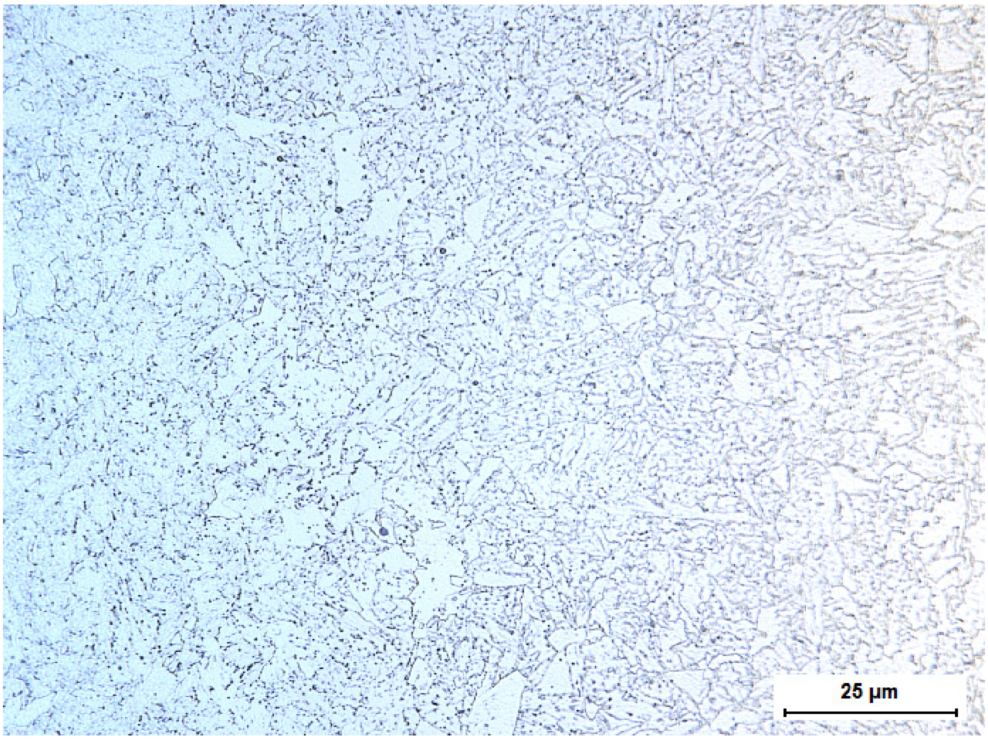

INSP2-3x head of specimen 500x. Damage class 2b.

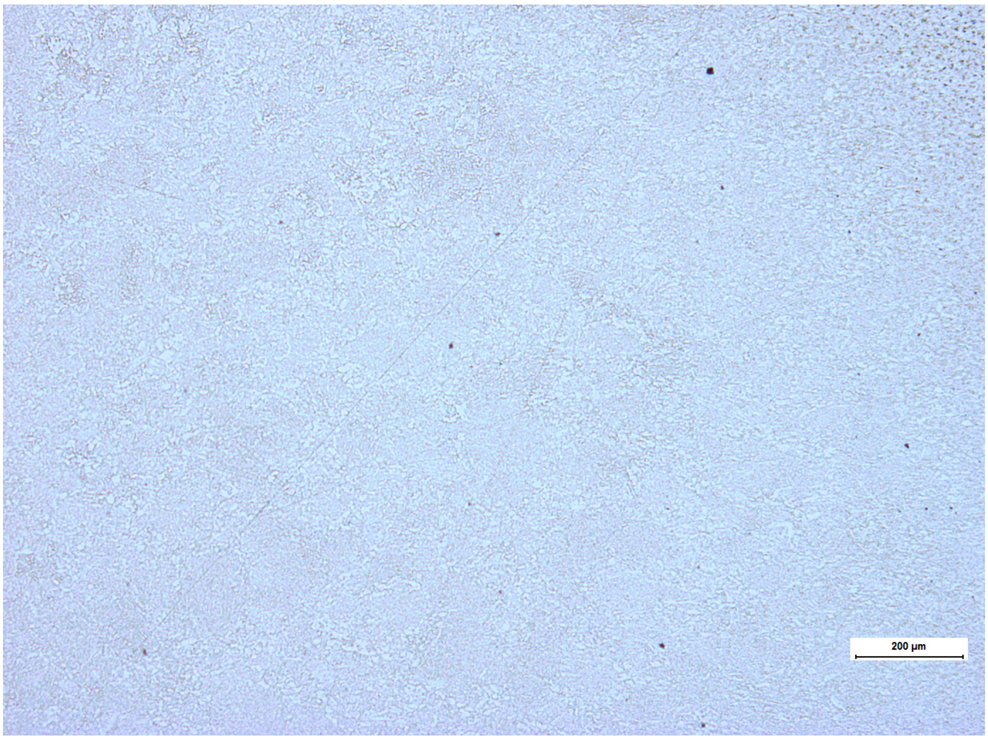

INSP2-3 close to fracture 50x.

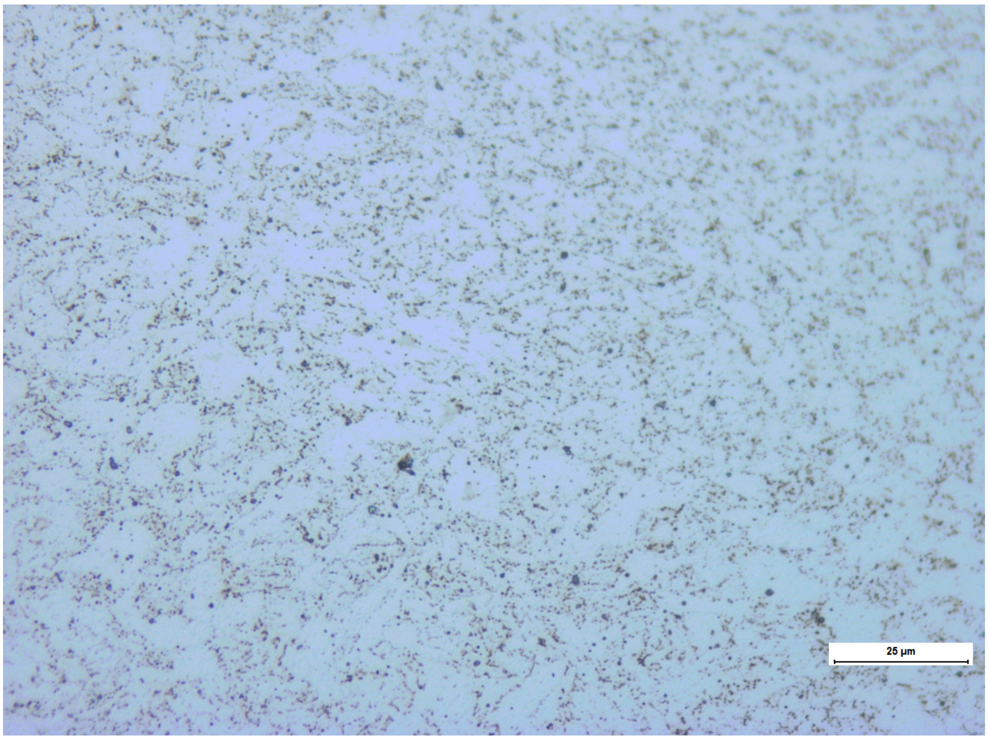

INSP2-3 close to fracture 500x. Damage class 2b.

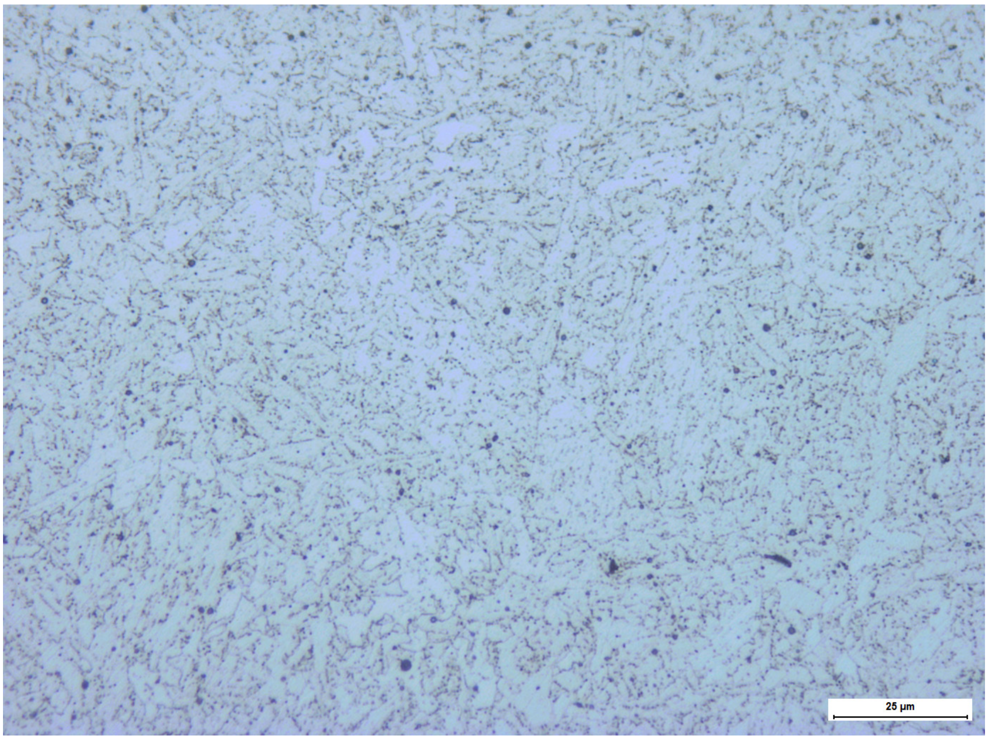

INSP2-3 head of specimen 500x. Damage class 2b.

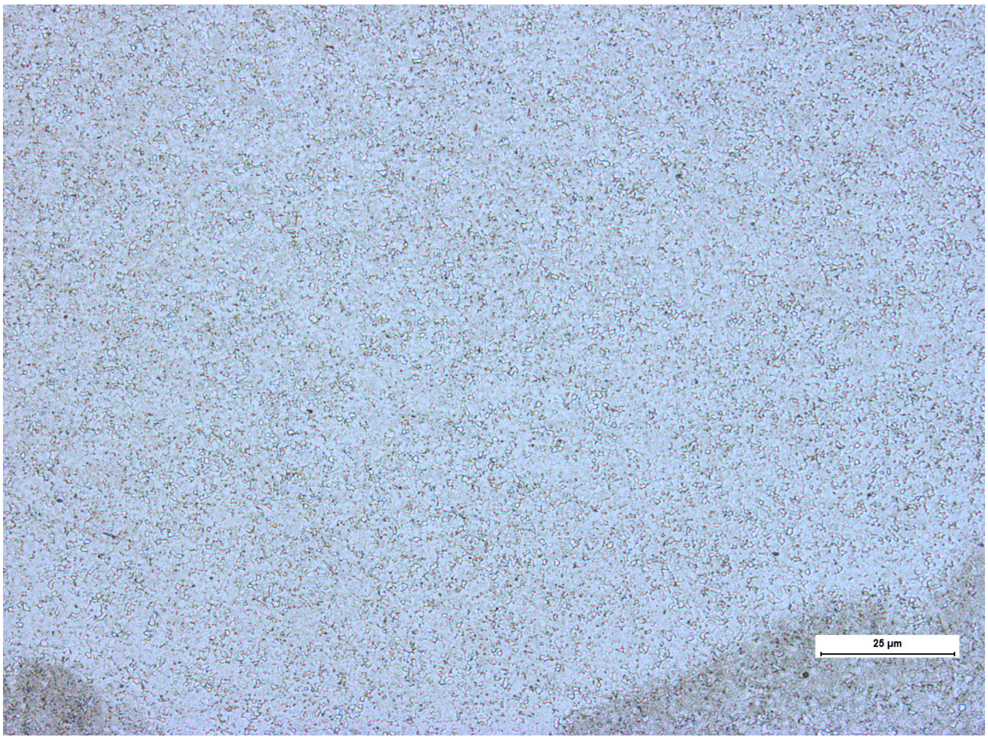

INSP2-6 middle of gauge length 50x.

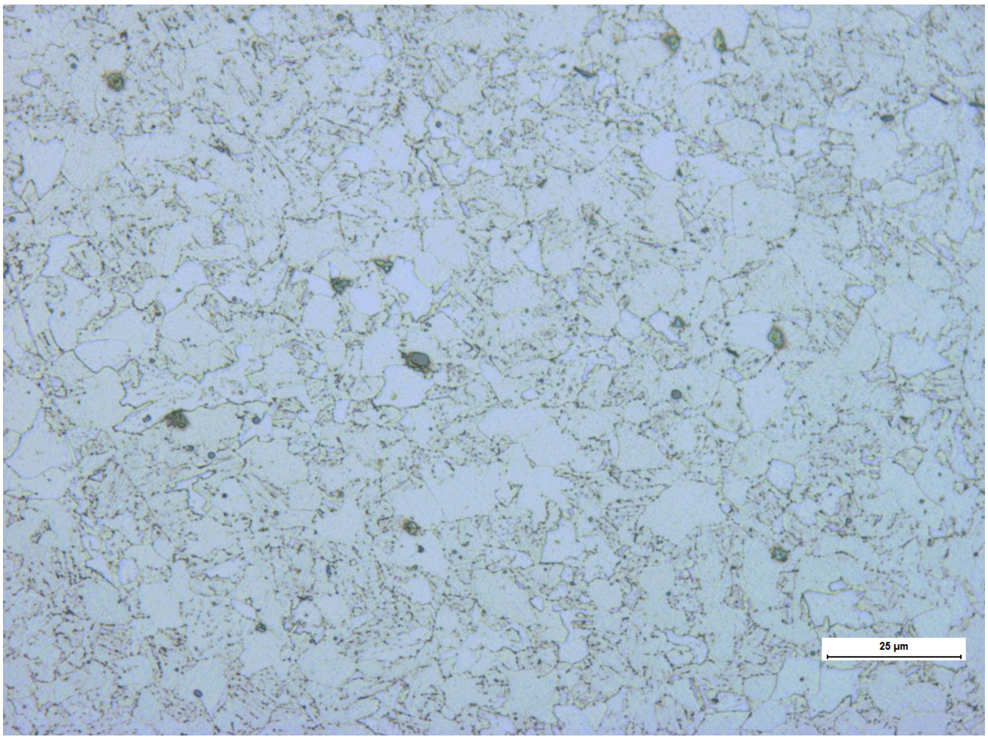

INSP2-6 middle of gauge length 50x. Damage class 2a or 2b.

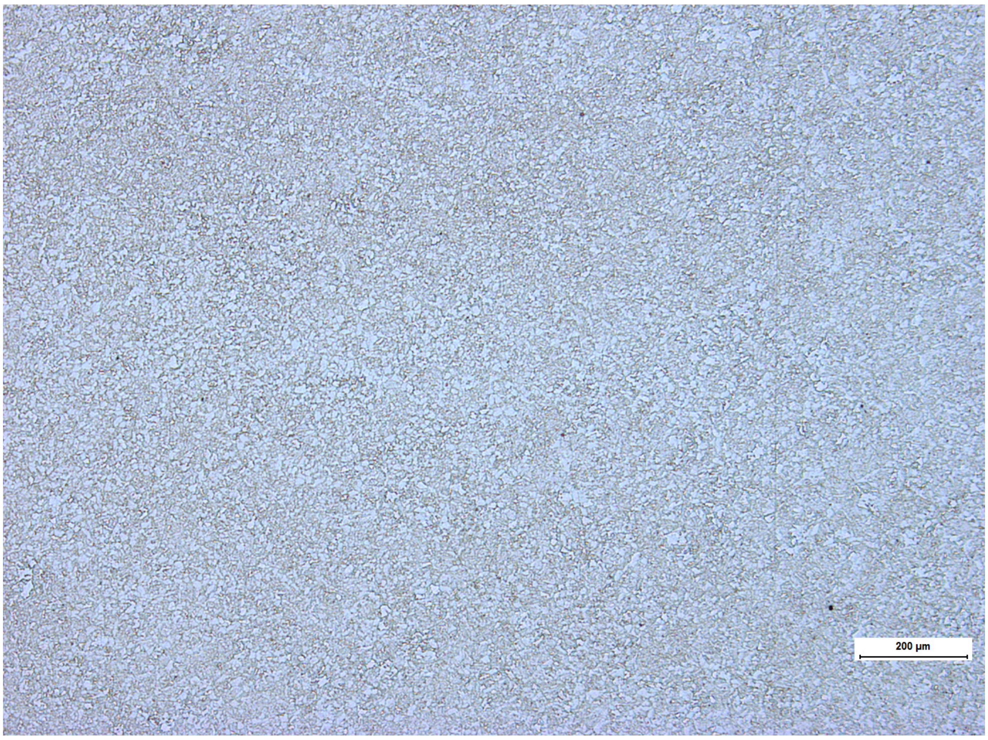

INSP2-9 middle of gauge length 50x.

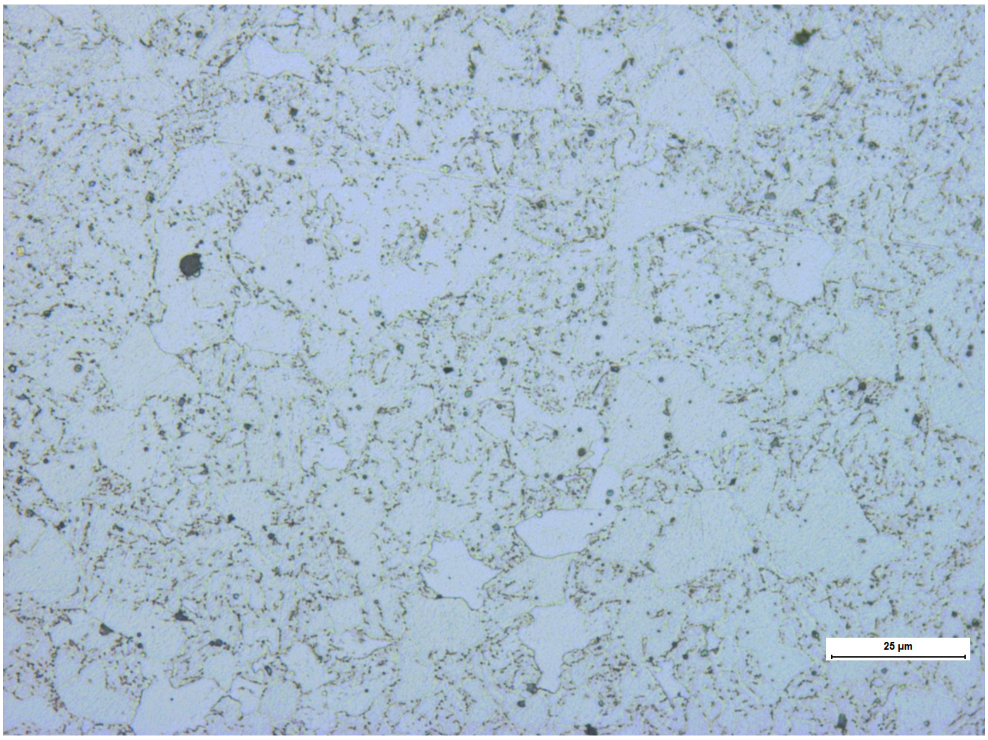

INSP2-9 middle of gauge length 50x. Damage class 2b.

RISK WITH THE COMBINATION WELDMENT AND ELASTIC FOLLOW-UP AT LOW TEMPERATURE CREEP

I kraftvärmeverk som arbetar vid temperaturer kring 460°C eller lägre förväntas inga större krypskador, alltså skador på materialet orsakade av krypning.

Trots det uppvisar exempelvis T-stycken ofta betydande krypskador vid övergången mellan huvudledning och avstickare normalt efter 25–30 års drift vilket begränsar livslängden. För att bättre förstå fenomenet ”elastic follow-up” i kombination med svetsförband, de skador de leder till och hur sådana skador kan motverkas både i befintliga anläggningar och vid design av nya har denna studie genomförts.

Här har ett T-stycke som uppvisar oväntade krypskador studerats och rapporten ger ett antal rekommendationer för ökad livslängd av systemet.

Energiforsk is the Swedish Energy Research Centre – an industrially owned body dedicated to meeting the common energy challenges faced by industries, authorities and society. Our vision is to be hub of Swedish energy research and our mission is to make the world of energy smarter!